Metallomics of Mercury: The Role of Selenium

By

Mohammad Abdul Kader Khan

A Thesis submitted to the Faculty of Graduate Studies of

The University of Manitoba

in partial fulfillment of the requirements of the degree of

DOCTOR OF PHILOSOPHY

Department of Chemistry

University of Manitoba

Winnipeg, Manitoba, Canada

Permission to Use

In presenting this thesis, in partial fulfillment to the requirements of the degree of Doctor of Philosophy from the University of Manitoba, I agree that the libraries of this University may make it freely available for inspection. I further agree that permission for copying of this thesis in any manner, in whole or in part, for scholarly purposes may be granted by the professors who supervised my thesis work or, in their absence, by the Head of the Department of Chemistry, or the Dean of the Faculty of Graduate Studies. It is understood that any copying or publication or use of this thesis or parts thereof, for financial gain shall not be allowed without my written permission. It is also understood that due recognition shall be given to me and to the University of Manitoba in any scholarly use which may be made of any material in this thesis.

Request for permission to copy or to make other use of material in this thesis in whole or in part should be addressed to:

Head of the Department of Chemistry

University Of Manitoba

Winnipeg, Manitoba

R3T 2N2

Abstract

Mercury-selenium (Hg-Se) interaction is perhaps the most documented bioantagonism. Since its discovery in the 1960s, extensive studies have been carried out on the wide occurrence, chemical mechanisms, and toxicological significance of this bioantagonism. However, major knowledge gaps exist in the underlying mechanism at the molecular level which is the objective of this thesis research. The molecular level mechanism of Hg-Se bioantagonism was studied from three interrelated aspects: 1) synthesis and characterization of four important methylmercury (MeHg) – selenoamino acid complexes that are of biological relevance; 2) the pathway of the formation of HgSe, the end product of Hg-Se antagonism, from the interaction between inorganic Hg and Se; and 3) the pathway of the formation of HgSe from the interaction between MeHg and Se.

The four new MeHg-selenoamino acid compounds synthesized are methylmercury-$_{D,L}$-selenopenicillaminate, methylmercury-$_{L}$-selenoglutathionate, and two methylmercury-$_{L}$-selenomethioninate complexes (one via a Hg-Se bond formed at pH < 2 and the other via a Hg-N bond at pH > 8). The complexes were characterized by NMR, FT-IR and mass spectra. Their structural and electronic properties were further studied by X-ray crystallography and quantum mechanical calculations. Crystallography and spectroscopic studies reveal that all four complexes chemically and structurally resemble their sulfur analogues. Chemical coupling values from NMR suggest that $MeHg^{+}$ has a stronger affinity for Se than for S. These results are in agreement with those of MeHg-selenocysteine complex, the only MeHg selenoamino acid complex that was

characterized in the literature prior to the present study, suggesting that chemical and structural mimicry could play a role in MeHg-Se antagonism in biological systems.

It has long been proposed and analytically proven that mercury selenide, HgSe(s), is the end metabolic product of the Hg-Se bioantagonism. However, the pathway of its formation in biological systems was poorly known. Experiments carried out in this study suggested that HgSe(s) could be formed from both inorganic Hg and MeHg in the presence of Se.

In the case of MeHg, we found that its binding with selenoamino acids could result in the demethylation of MeHg and formation of HgSe nanoparticles. NMR and gas chromatography – mass spectrometry (GC-MS) studies confirmed the presence of bis(methylmercury) selenide (BMSe) and dimethylmercury as reaction intermediates based on which a demethylation pathway was proposed. To our knowledge, this is the second chemical demethylation pathway of MeHg under natural or physiological conditions.

In the case of inorganic Hg, we found that its interaction with selenite in the presence of glutathione (GSH) could lead to the formation of $HgSe_{1-x}S_x$ ($0 < x < 1$) nanoparticles via a black solution or precipitate as the formation of the intermediate depends on the pH of the medium. When the pH is less than 2.0, the intermediate is a black precipitation which readily dissolves at higher pH (pH > 7.4). The dissolution/precipitation is reversible upon adjustment of the pH. UV-visible spectra, TEM (transmission electron microscopy) and XPS (X-ray photoelectron spectroscopy) analyses revealed that the black solution is due to $HgSe_{1-x}S_x$ nanoparticles (diameter < 5 nm) which at high pH and upon separation becomes sparingly soluble $HgSe_xS_{1-x}$. This

pH-reversible dissolution-precipitation of $HgSe_xS_{1-x}$ offers a new plausible explanation of tissue distribution patterns of $HgSe_xS_{1-x}$ in biological systems.

Acknowledgements

All praises are due to Allah, the Most-Beneficent and the Most-Merciful. With Him, the glory and the success – and He bestow these to whomever He wants. I thank Him for all those He gave me and bring me up to this.

I would like to thank my supervisor, Dr. Feiyue Wang, for giving me the opportunity to complete my Doctor of Philosophy degree with him. I learnt a lot from him, not only in the area of chemistry but also in many other aspects. He shared his vast knowledge with us in a very friendly manner and always encouraged me to think critically. I also want to thank my committee members Dr. H. Georg Schreckenbach, Dr. Jörg Stetefeld and Dr. Gary Stern for their advice, criticism and support during my research.

I would like to acknowledge the help from all the past and present Wang group members. I am grateful to Dr. Abu Md. Asaduzzaman for carrying out all the quantum chemical calculations. I would like to thank Dr. Kirk Marat and Terry Wolowiec for helping collecting all the NMR spectra. I would also like to thank Neil Ball for collecting the XRD data, Mark Cooper for the X-ray crystallography and Panseok Yang in the microbeam analysis, Sergei Rudenja and Dr. Michael Freund in the XPS and FTIR analysis, and John Van Dorp in the TEM analysis.

I am grateful to NSERC for providing me a PGS-D fellowship for this project.

Finally, I want to express my gratitude to my family. Without their encouragement and support, it would not have been possible for me to come up to this level. My love is for my two little angels (Samaah and Adiba) who came to this world during my PhD and bring all the joy in my life.

Dedication

This work is dedicated to those who spent their lives for the sake of truth, right path and guidance – who are our everlasting source of hope and inspiration to strive for the best.

Contents of the Thesis

This dissertation comprises of the following manuscripts published in peer-reviewed scientific journals. The list below is provided as it is arranged in this dissertation:

I. **Khan, M. A. K.**; Wang, F., Mercury-Selenium Compounds and Their Toxicological Significance: Toward a Molecular Understanding of the Mercury-Selenium Antagonism. *Environ. Toxicol. Chem*. **2009**, 28(8), 1567-1577.

Contribution: I wrote the first draft of the manuscript. Dr. Wang initiated the project, and provided guidance and revisions to the manuscript.

II. **Khan, M. A. K.**; Asaduzzaman, A. M.; Schreckenbach, G.; Wang, F. Methylmercury Complexes with Selenoamino Acids: A Synthetic and Theoretical Study. *Dalton Transac.* **2009**, 5766-5772.

Contribution: I carried out all the experimental works and wrote the first draft of the manuscript. Drs. Asaduzzaman and Schreckenbach did the computational work. Dr. Wang initiated the project, and provided guidance and revisions to the manuscript.

III. **Khan, M. A. K.**; Wang, F. Chemical Demethylation of Methylmercury by Selenoamino Acids. *Chem. Res. Toxicol.* **2010**, 23, 1202–1206.

Contribution: I did all the experimental works and wrote the first draft of the manuscript. Dr. Wang initiated the project, and provided guidance and revisions to the manuscript.

IV. **Khan, M. A. K.**; Wang, F. Reversible Dissolution of Glutathione-Mediated $HgSe_xS_{1-x}$ Nanoparticles and Possible Significance in Hg-Se antagonism. *Chem. Res. Toxicol.* **2009**, 22 (11), 1827–1832.

Contribution: I did all the experimental works and wrote the first draft of the manuscript. Dr. Wang initiated the project, and provided guidance and revisions to the manuscript.

Table of Contents

List of Tables

List of Figures

List of Schemes

List of Abbreviations

BBB	blood-brain barrier
BMSe	bis(methylmercury)selenide
CNS	central nervous systems
CPCM	conductor polarizable continuum model
CSeH	$_{L}$-selenocysteine
Cys	cysteine
DMHg	dimethylmercury
DPPD	N,N'-diphenyl-p-phenylenediamine
ESI	electrospray ionization
EXAFS	extended x-ray absorption fine structure
FT-IR	fourier transform infrared
FWHM	full width at half maximum
G-6-PDH	glucose-6-phosphate dehydrogenase
GC	gas chromatography
G.I.	gastrointestinal
GPx	glutathione peroxidase
GSeH	$_{L}$-selenoglutathione
GSH	glutathione
GSSeSG	selenodiglutathione
GSSG	oxidized glutathione; diglutathione
Hb	hemoglobin

$[Hg]_t$	the toxicity threshold concentration (molar) of mercury
HPLC	high performance liquid chromatography
Hz	hertz
ICP	inductively coupled plasma
IRB	iron-reducing bacteria
LAT	L-type neutral amino acid transporters
MeHgSeAA	methylmercury selenoamino acids
MeHgSeR	methylmercury selenol compounds
MeHgSR	methylmercury sulphur compounds
MS	mass spectrometry
MSEM	microbeam scanning electron microscopy
ORTEP	oak ridge thermal ellipsoid plot
ppm	parts per million
SDD	Stuttgart-Dresden basis set
$[Se]_d$	deficiency threshold concentrations of selenium
$[Se]_t$	the toxicity threshold concentrations of selenium
-SeH	selenohydryl group
SelP	Selenoprotein P
SEM	scanning electron microscopy
SeMet	$_L$-selenomethionine
SePen	$_{D,L}$-selenopenicillamine
-SH	sulfhydryl group
SRB	sulfate-reducing bacteria

RBC	red blood cell
RSeH	selenols
TEM	transmission Electron Microscopy
UV-vis	ultra violet-visible
XANES	x-ray absorption near-edge structure
XPS	x-ray photoelectron spectroscopy
XRD	X-ray powder diffraction

Chapter 1: Introduction

1.1. Mercury as a Global Contaminant

Mercury (Hg) is a global contaminant due to its long range atmospheric transport, bioaccumulation in aquatic ecosystems, and neurotoxicity to humans (*1, 2*). Mercury occurs naturally and can be released to the surface environment by weathering of geological materials, volcanic eruptions, and natural forest fires (*3*). However, human activities have greatly increased Hg emission to the environment since the industrialization. Major anthropogenic Hg sources include coal combustion, gold and non-ferrous metals production, and biomass burning (*4*).

Mercury exists in the environment in two major oxidations states: Hg(0) and Hg(II) The volatility and low reactivity of Hg(0) is primarily responsible for the long range transport via the atmosphere, accounting for its wide-spread distribution even in remote regions that are far away from localized Hg sources.

Once in the aquatic or terrestrial systems, inorganic Hg(II) may undergo methylation to form monomethylmercury (MeHg). Methylmercury in the aquatic environment is thought to be produced primarily by microbial methylators such as sulphate-reducing bacteria (SRB) (*5*) and also by iron-reducing bacteria (IRB) (*6*). SRB which thrive in the aerobic- anaerobic transition environment utilize methylcobalamin to convert inorganic Hg into MeHg. Intracellular methylcobalamin is proposed to catalyze the methyl group transfer (*7, 8*). SRB such as *Desulfovibrio desulfuricans* and other closely related organisms were shown to utilize an acetylcoenzyme A pathway, with methyl group transfer from methyltetrahydrofolate (*7, 9*). Chemical methylation of

inorganic Hg(II) is also possible in the aquatic environment. Chemical reagents such as methyl iodide, dimethylsulfide, and dissolved organic matter such as fulvic and humic acids are thought to be able to methylate Hg (*10-12*). Where present, organometallic complexes such as methylcobalamin, methyllead or methyltin in the aquatic environment, are known to methylate Hg via transmethylation reactions. Transmethylation reactions can proceed by transferring carbocationic Me^+, carbanionic Me^- or radical Me•, depending on the chemical properties of the metal component of the methylating agent (*10*).

While both inorganic Hg(II) and MeHg can bioaccumulate in the aquatic ecosystems, only MeHg biomagnifies, meaning increasing MeHg concentrations are found at higher trophic levels in the aquatic ecosystems due to the process of retaining MeHg more than excretion in the subsequent level of the food chain (*13*). As a result, MeHg concentrations in top predators such as sharks can be as high as 4 mg/kg, which exceeds MeHg concentrations in seawater (*14*) (typically < 0.1 ng/L) by a factor of 10^6 (*15*).

1.2. Metallomics of Mercury

1.2.1 Introduction to metallomics

Biological systems take up and utilize many metal ions for various purposes and via many routes. While some of the metals are essential for biochemical functions and thus for the health of biota, others cause diseases or exert toxic effects. For example, some metalloenzymes contain a specific number of metal ion(s) (such as Fe, Mo, Cu, Se) at the active sites in specific proteins (*16*) where they act as biocatalysts to

regulate the biochemical reactions and physiological functions including gene (DNA, RNA) synthesis, metabolism, antioxidation. Genes and proteins cannot be synthesized without the assistance of metalloenzymes containing zinc and other metals like Cu (*17*). Whereas the absence of these essential metals results in adverse effects, exposure to elevated concentrations of non-essential metals may cause carcinogenic effects (e.g., As, Cr, Pt), nephrotoxicity (e.g., Cd, U), or neurotoxicity (e.g., Al, Hg) (*18*). Therefore, to better understand how a cell functions, one needs to characterize the cell not only by its genome in the nucleus and by protein content (proteome) but also by the nature, distribution and speciation of the metals and metalloids in various cell compartments. Williams (*19*) first termed these biometals and biometal species as metallomes by analogy with proteome. To distinguish from other fields of studies and promote this area of research, Haraguchi (*17*) later coined the term “metallomics” and proposed it as a separate branch of -omics study complementary to proteomics and genomics.

In this thesis research we are specifically interested in the metallmoics of Hg, i.e., the interactions of Hg and MeHg with biomolecules, with an emphasis on how the presence of Se affects the speciation and metabolic pathways of Hg and MeHg under physiologically or environmentally relevant conditions.

1.2.2 Exposure pathways of mercury

The bioavailability and toxicity of Hg depend on its concentration and chemical form (species), the co-existence of other chemicals (e.g., organic matter, selenium (Se)), the pathway and length of the exposure, and the sensitivity and age of the organism. The primary source for Hg in marine mammals, predatory birds and humans is via the dietary

consumption of fish which takes up Hg and MeHg either through food or directly from water. Whereas MeHg is almost completely absorbed from the gastrointestinal (G.I.) tract and incorporated into erythrocytes (red blood cells or RBC) in the blood, inorganic Hg(II) is absorbed at the microvilli interface which results in a very low uptake rate (*20*). The absorption of inorganic Hg salts from the G.I. tract is one order less than that of MeHg (*21*). Laboratory experiments showed that the transfer of MeHg from diatom to copepod is four times more efficient than that of inorganic Hg (*22*). This is due to the fact that inorganic Hg, being more hydrophilic in nature, tends to be excreted more readily than being absorbed. In contrast, the more lipophilic MeHg tends to be more readily associated with the soluble fraction of the diatom cell which allows it to be accumulated in the fatty tissue of copepod (*22*). As a result, the average proportion of MeHg over total Hg increases rapidly from phytoplankton to fish (15% to 95%) (*23*).

1.2.3 Tissue distribution of mercury

For a given species, the total Hg content is known to vary among the different organs (e.g., brain, liver, kidneys, and spleen). Wagemann et al. (*24*) found that more than 90% total Hg in muscle tissues in marine mammals is present as MeHg, while in liver inorganic Hg(II) dominates. Mercury content has also been shown to vary across the species exposed to same source depending on their food intake. MeHg was found to be in seabirds like black-footed albatross, herring gull and arctic tern in 35%, 36% and 66% in liver, kidneys and muscle, respectively (*25*). This is due to the complicated metabolic processes involved.

Once in marine mammals and humans, MeHg readily transfers into the blood, with the largest portion binding to haemoglobin (Hb) in RBC (*26, 27*) and the rest in

plasma (*28*). RBC acts as a carrier for the MeHg to various organs including the brain (Figure 1). When binding with $_{L}$-cysteine, MeHg is thought to easily cross the blood-brain barrier (BBB) and affect the central nervous systems (CNS), giving rise to its neurotoxicity (*29*). Elemental Hg can also cross the BBB and be oxidized to Hg(II) and damage CNS (*30*).

Methylmercury can be gradually demethylated to inorganic Hg in animal tissues (*31, 32*). In fact, inorganic Hg in the liver and kidneys or other tissues including the brain is mainly due to biotransformation of MeHg (*33, 34*). Fang et al. (*35*) reported that the C-Hg bond can be cleavaged by dietary Se which accounted for the inorganic Hg species in rat liver and kidneys. Hirayama and Yasutake (*36*) showed that reactive oxygen species actively participate in the MeHg demethylation in the liver. Rowland et al. (*37*) demonstrated the involvement of gut flora in the MeHg demethylation in mice.

Methylmercury is excreted out mainly through the bile and through urine to some extent (*38-40*). Methylmercury complexes excreted in bile are mostly associated with small molecular weight forms which can be reabsorbed from the intestine. This circulation is one of the major reasons responsible for the long half-life of MeHg in animals (*39*). Inorganic Hg is mostly excreted (in general 50%) by feces in rats which most probably is related to the biotransformation of MeHg in liver followed by the biliary excretion, or to metabolic transformation in the intestinal lumen (*31*).

Figure 1.1 is a simplified diagram showing the dynamics of mercurials in animals. Details of the metallobolic pathways remain poorly understood.

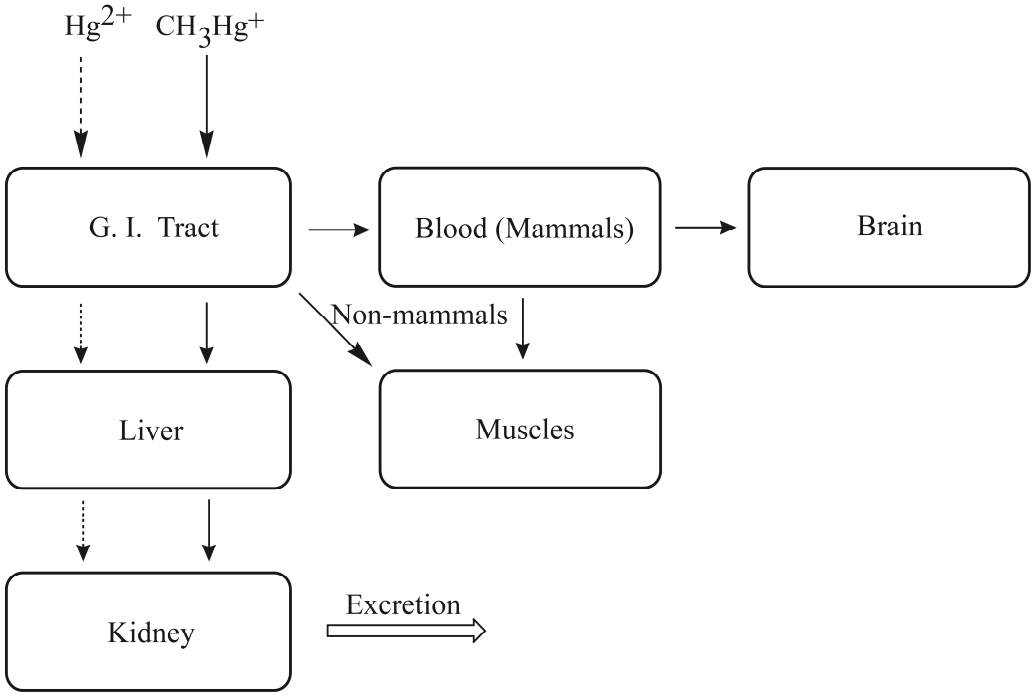

Figure 1.1. A schematic diagram showing the general transport of inorganic Hg(II) and MeHg in different organs of a mammal.

1.2.4 The role of thiols

Both inorganic and MeHg speciation in the intracellular environment is dominated by MeHg-SR complexes (-SR = amino acids contain sulphur where R is the rest part) (*13*), due to the abundance of S-containing proteins and their strong affinity to Hg^{2+} or $MeHg^+$. Despite the very high formation constants (10^{15}-10^{17} range (*41*)) of MeHg complexes with thiols, the MeHg-SR bonding is extremely labile, and can undergo rapid ligand exchange reactions in aqueous solutions (*30, 42-44*) and likely in biological systems (*30*). Mercurials are specific in binding with thiols but not selective; thus almost every protein in the biological systems is a potential target for Hg (*45*). Typically MeHg is found to bind with di- and tri-peptides containing cysteine moieties (*46*). It can also

bind with glutathione or methionine. Glutathione binds with MeHg making it portable (*29*) into different organs. This helps MeHg to distribute through all potential organs of a biological system where it can bind with all sulphur-rich amino acid environments in the proteins. Several enzyme systems are inhibited both by inorganic and organic Hg. MeHg disrupts the structure and function of any protein to which it binds. For example, MeHg blocks the assembly of tubulin and ultimately depolymerises microtubules, a component of the cytoskeleton which is essential for cell structure and support, cell division, and cell migration (*47-49*). It also inhibits protein synthesis in general (e.g., selenoprotein P). One most important feature of this extreme mobility is that after intravenous injection of MeHg compounds, it appears in the brain within 5 min (*50, 51*). It was shown by Kerper et al. (*29*) that MeHg can form complex with cysteine or glutathione (act as a source for MeHg-cysteine) and cross the BBB through the L-type large neutral amino acid transporters (LAT 1 and 2). It was assumed that this occurs in part due to the resemblance of MeHg-cysteine complex with methionine which can easily cross the BBB to enter into the brain.

Inorganic Hg, irrespective of its chemical forms, tends to accumulate in the kidneys and little is found in the brain due to its inability to cross the BBB. It is assumed that this may take place through the endocytosis of filtered Hg-albumin complexes as albumin has a free –SH group on a terminal cysteinyl residue (*52, 53*) and inactivate them or form heavy-metal derivatives with crystalline proteins. This inhibition may partly account for the toxicity of mercurials (*54-57*). Other primary sites of action of Hg may be the cell membrane (*58, 59*). Mercury compounds may cause increased membrane permeability and changes in active membrane transport. Inorganic Hg is more effective

than the organic one in disrupting membrane function (*60-62*). Interaction with -SH groups might cause a disturbance stimulation of membrane receptors which in turn may disturb immunoregulation (*63*).

1.3. Role of Selenium in the Metallomics of Mercury

Since Parizek and Ostadalova's (*64*) discovery of the protective effect of Se on kidney intoxication by Hg in laboratory rats, extensive studies have demonstrated that Se can modify the toxicity of both inorganic Hg and MeHg in the laboratory and in nature. While the majority of the studies reported antagonistic interactions between Se and Hg, synergistic interactions have also been documented. A comprehensive review on this subject is provided in Chapter 2 of this dissertation.

As detailed in Chapter 2, the following possible pathways have been suggested for the Hg/MeHg-Se antagonism in biological systems:

(a) *Formation of MeHg-Se compounds*: Several MeHg-Se compounds such as bis(methyl mercuric)selenide (BMSe) (*65, 66*) and MeHg-selenoamino acid complexes are suggested to form in vivo, which could reduce the toxicity of MeHg. However, the presence of BMSe has never been analytically verified in vivo. Even though MeHg is believed to bind with any selenoamino acid present in biological systems, so far only one MeHg selenoamino acid complex, MeHg selenocysteinate, has been synthesized and characterized.

(b) *Selenium-aided demethylation of MeHg*: Se is suggested to be involved in the demethylation process, but the mechanism remains unknown.

(c) *Formation of inorganic Hg-Se compounds*: Similar to the case with MeHg, binding between Se and inorganic Hg could also reduce the bioavailability and toxicity of inorganic Hg. The sparingly soluble HgSe(s) is likely to be the ultimate detoxification product. Although its in vivo presence has been confirmed analytically, the mechanism leading to its formation remains poorly characterized.

(d) *Redistribution of inorganic Hg in the presence of Se*: It has been observed that Hg may redistribute itself in the presence of Se in biological systems. However, it is not clear how at molecular level Se induce redistribution of MeHg in different organs.

(e) *Selenium inhibition of methyl radicals from MeHg*: According to this hypothesis, oxygen-dependant metabolic reactions at the close proximity of lipids of the target tissues (e.g., the brain) break down MeHg and form methyl radical which results in the toxicity of MeHg (*67*). This proposed mechanism can explain the protective effect of the anti-oxidants such as glutathione peroxidase (GPx) (Se in GPx decomposing peroxides which otherwise would initiate the MeHg breakdown) and vitamin E in the biological systems (*67, 68*). However, no direct evidence has been reported to support this hypothesis (*69*).

(f) *Mercury-induced Se deficiency*: Since MeHg has been shown to bind with Se very strongly, therefore it is possible that MeHg may make Se less bioavailable and cause Se deficiency in biological systems.

1.4. Objectives of the Research

The goal of this study was to a gain molecular-level understanding of the interaction between Se and Hg under conditions similar to in vivo physiological

conditions to fill up some major knowledge gaps in the Se-Hg(MeHg) antagonism. Specifically, the objectives were to –

(a) Synthesize and characterize MeHg complexes with several important Se-containing biomolecules and to compare their properties with their sulfur analogs.
(b) Investigate the mechanisms of the interaction between Se and inorganic Hg leading to the formation of HgSe(s); and,
(c) Investigate the mechanisms of the interaction between Se and MeHg leading to the formation of HgSe(s).

1.5. NMR, XRD, and Computational Approaches in the Study of Hg-Se Interactions

As shown in Chapters 3-5, the major techniques used in this thesis for the study of the Hg-Se interaction included nuclear magnetic resonance (NMR) spectroscopy, X-ray diffraction (XRD) and computational approaches. While the details are given in the corresponding chapters, here is a brief overview of each approach.

1.5.1 NMR

NMR utilizes the characteristic frequency of active nuclei (such as ^{1}H or ^{13}C) to resonate when placed in a magnetic field. The resonant frequency, energy of the absorption and the intensity of the signal are proportional to the strength of the magnetic field. As the NMR spectrum of a particular element in a molecule is sensitive to its chemical environment, the characteristic peaks at particular positions in a spectrum can be used for identifying the molecule. Therefore, NMR is a very versatile technique for characterizing molecules chemically and structurally. ^{1}H NMR has been routinely used to study MeHg complexes with sulfur-containing biomolecules (*46*, *70*). However,

Rabenstein et al. (*71*) concluded that since amino acids act as unidentates toward $MeHg^{+}$ in aqueous solution, ^{1}H NMR only gives an average signal for the methyl group. On the other hand, as ^{199}Hg NMR gives rise to separate peaks for individual Hg atoms in the molecule, it can be used as an alternative method of detection for the MeHg binding environment. Carty et al. (*72*) were the first to used ^{1}H and ^{199}Hg NMR to characterize the MeHg selenocysteinate complex. In this dissertation, both ^{1}H and ^{199}Hg NMR are used as a primary NMR technique, while ^{77}Se NMR is used as a complementary technique to support the evidence translated from the previous ones.

1.5.2 XRD

XRD is based on the observation of the scattered intensity of an X-ray beam hitting a sample as a function of incident and scattered angle, polarization, and wavelength or energy. XRD is commonly used to characterize the crystallographic structure, crystallite size (grain size), and preferred orientation in polycrystalline or powdered solid samples. Since the end product of the Hg(MeHg)-Se antagonism, HgSe(s), is highly crystalline in nature, XRD study can reveal its size, and the preferred orientation in the crystals by recording its characteristic diffraction pattern (*73*). In the research of this dissertation, XRD is used to confirm and characterize the highly crystalline compound HgSe(s) as the final end product of the Hg(MeHg)-Se antagonism.

1.5.3 Theoretical study

Computer aided quantum mechanical calculations are very helpful to determine the electronic and structural features, stabilities, and properties of chemical compounds by optimizing structures. Theoretical study is most useful to provide insight into a

chemical structure especially in the absence of a crystal structure. In this dissertation, quantum mechanical calculations of the MeHg-selenoamino acid complexes are carried out to investigate the element specific binding sequence of MeHg, bond properties and their thermodynamic stability. Specialized software Gaussian-03 (*74*) was used with the B3LYP hybrid functional (*75, 76*). The Stuttgart–Dresden basis set (SDD) (*77*) for the Hg atom was used with the respective effective core potential to treat the (scalar) relativistic effects for the heavier atom and 6-31+G(p) basis for all other atoms.

1.6. Organization of This Dissertation

This dissertation is written in a "sandwich" style; i.e., it is essentially composed of four published manuscripts in peer-reviewed scientific journals. The linkage between these chapters is illustrated in Figure 1.2.

Chapter 1 (this chapter) is a brief introduction of the thesis describing the general outline of Hg toxicity and the role of selenium in biological systems.

Chapter 2 is entitled "*Mercury-Selenium Compounds and Their Toxicological Significance: Toward a Molecular Understanding of the Mercury-Selenium Antagonism*" which has been published in "*Environmental Toxicology and Chemistry*". It provides a critical review of our current (i.e., at the beginning of this thesis research) understanding of the Hg-Se antagonism, with a focus on the roles of potentially important Hg-Se compounds including bis(methylmercuric)selenide, MeHg selenocysteinate, selenoprotein P-bound HgSe clusters, and the ultimate biominerals $HgSe_xS_{1-x}$. Major knowledge gaps are identified in the need of direct analytical techniques, thermodynamic

databases, and linkage between laboratory spiking studies and real world exposure scenarios.

Chapter 3 is entitled "*Synthesis, Characterization and Structures of Methylmercury Complexes with Selenoamino Acids*", which has been published in "*Dalton Transactions*". It reports the synthesis of four new MeHg-selenoamino acid complexes, including MeHg-$_{L}$-selenoglutathionate, MeHg-$_{D,L}$-selenopenicillaminate, and two MeHg-$_{L}$-selenomethioninate complexes (one via a Hg-Se bonding and the other Hg-N bonding). NMR characterization was provided and molecular structures were studied. Quantum mechanical calculations were used to find chemical and structural similarity between these complexes and their sulfur analogues. All four complexes were found to chemically and structurally resemble their sulfur analogues, with a slightly stronger binding affinity of Hg to Se than to S, suggesting chemical and structural mimicry might play a role in MeHg-Seantagonism in biological systems.

Chapter 4 is entitled "*Chemical Demethylation of Methylmercury by Selenoamino Acids*" which has been published in "*Chemical Research in Toxicology*". It reports a new chemical demethylation pathway for MeHg by reacting with selenoamino acids. The demethylation occurs through the formation of bis(methylmercury) selenide (BMSe) as an intermediate, eventually forming HgSe(s). The presence of BMSe was confirmed by NMR.

Chapter 5 is entitled "*Reversible Dissolution of Glutathione-Mediated $HgSe_xS_{1-x}$ Nanoparticles and Possible Significance in Hg-Se Antagonism"* which has been published in "*Chemical Research in Toxicology*". It proposes a new pathway for the in

vivo biomineralization of inorganic Hg. The pathway involves the reaction of Hg(II) with selenite in the presence of glutathione (GSH) which eventually form HgSe(s) which is thought to be the ultimate metabolic product responsible for the Hg-Se antagonism in biological systems.

Chapter 6 concludes the dissertation by stating the main findings from the study, how they can help us better understand the Hg-Se antagonism, as well as future perspectives.

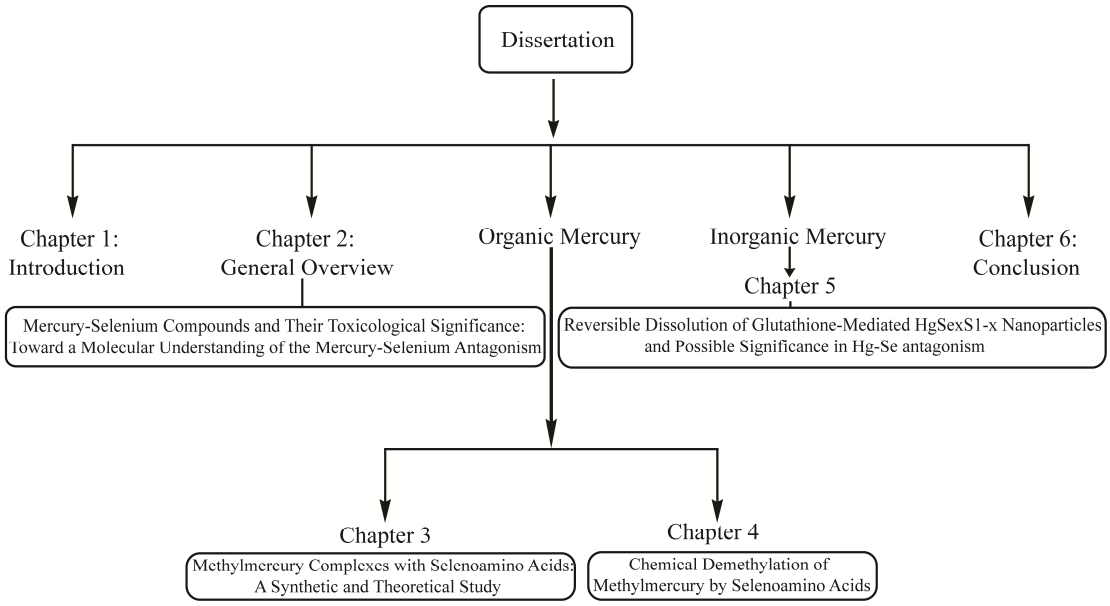

Figure 1.2. Flow chart to show the overall organization of the dissertation

1.6. References

(1) Mergler, D., Anderson, H. A., Chan, L. H. M., Mahaffey, K. R., Murray, M., Sakamoto, M. and Stern, A. H. (2007) Methylmercury exposure and health effects in humans: a worldwide concern. *Ambio 36*, 3-11.

(2) WHO. (1990) Methylmercury, International programme on chemical safety, World Health Organization, Geneva.

(3) Nriagu, J. O. (1989) A global assessment of natural sources of atmospheric trace metals. *Nature 338*, 47-49.

(4) Pacyna, E. G., Pacyna, J. M., Steenhuisen, F. and Wilson, S. (2006) Global anthropogenic mercury emission inventory for 2000. *Atmos. Environ. 40*, 4048-4063.

(5) Wood, J. M., Kennedy, F. S. and Rossen, C. G. (1968) Synthesis of methylmercury compounds by extracts of a methanogenic bacterium. *Nature 220*, 173-174.

(6) Kerin, E. J., Gilmour, C. C., Roden, E., Suzuki, M. T., Coates, J. D. and Mason, R. P. (2006) Mercury methylation by dissimilatory iron-reducing bacteria. *Appl. Environ. Microbiol. 72*, 7919–7921.

(7) Choi, S.-C., Chase, T. and Bartha, R. (1994) Enzymatic catalysis of mercury methylation by *Desulfovibrio desulfuricans*. *Appl. Environ. Microbiol. 60*, 1342-1344.

(8) Choi, S.-C. and Bartha, R. (1993) Cobalamin-mediated mercury methylation by *Desulfovibrio desulfuricans*. *Appl. Environ. Microbiol. 59*, 290-295.

(9) Choi, S.-C., Chase, T. and Bartha, R. (1994) Metabolic pathways leading to mercury methylation in *Desulfovibrio desulfuricans LS*. *Appl. Environ. Microbiol. 60*, 4072-4077.

(10) Krishnamurthy, S. (1992) Biomethylation and environmental transport of metals. *Chem. Environ. 69*, 347-350.

(11) Craig, P. J. and Rapsomanikis, S. (1985) Methylation of tin and lead in the environment: oxidative methyl transfer as a model for environmental reactions. *Environ. Sci. Technol. 19*, 726-730.

(12) Falter, R. and Wilken, R.-D. (1998) Isotope experiments for the determination of the abiotic mercury methylation potential of a River Rhine sediment. *Vom Wasser 90*, 217-231.

(13) Haris, H. H., Pickering, I. J. and George, G. N. (2003) The chemical form of mercury in fish. *Science 201*, 1203.

(14) Pongratz, R. and Heumann, K. G. (1998) Determination of concentration profiles of methyl mercury compounds in surface waters of polar and other remote oceans by GC-AFD *Intl. J. Environ. Anal. Chem. 71*, 41-56.

(15) Strasdeit, H. (2008) Mercury-alkyl bond cleavage based on organomercury lyase. *Angew. Chem. Int. Ed. 47,* 828-830.

(16) Lippard, S. J. and Berg, J. M. (1994) *Principles of bioinorganic chemistry*, University Science Book, Princeton, NJ, USA.

(17) Haraguchi, H. (2004) Metallomics as integrated biometal science. *J. Anal. At. Spectrom. 19*, 5-14.

(18) Szpunar, J. (2004) Metallomcs: a new frontier in analytical chemistry. *Anal. Bioanal. Chem. 378*, 54-56.

(19) Williams, R. J. P. (2001) Chemical selection of elements by cells. *Coord. Chem. Rev. 216*, 583-595.

(20) Boudou, A. and Ribeyre, F. (1997) Mercury in the food web: accumulation and transfer mechanisms. *Metal Ions Biol. Syst. 34*, 289-319.

(21) Magos, L. and Webb, M. (1980) The interactions of selenium with cadmium and mercury. *Crit. Rev. Toxicol. 8*, 1-42.

(22) Mason, R. P., Reinfelder, J. R. and Morel, F. M. M. (1996) Uptake, toxicity and trophic transfer of mercury in a coastal diatom. *Environ. Sci. Technol. 30*, 1835-1845.

(23) Watras, C. J. and Bloom, N. S. (1992) Mercury and methylmercury in individual zooplankton:implication of bioaccumulation. *Limnol. Oceanogr. 37*, 1313-1318.

(24) Wagemann, R., Trebacz, E., Boila, G. and Lockhart, W. L. (1998) Methylmercury and total mercury in tissues of arctic marine mammals. *Sci. Total Environ. 218*, 19-31.

(25) Kim, E. Y., Murakami, T., Saeki, K. and Tatsukawa, R. (1996) Mercury levels and its chemical form in tissues and organs of seabirds. *Arch. Environ. Contam. Toxicol. 30*, 259-266.

(26) Chen, R. W., Lacey, V. L. and Whanger, P. D. (1975) Effect of selenium on methylmercury binding to subcellular and soluble proteins in rat tissues. *Res. Comm. Chem. Pathol. Pharmacol. 12*, 297-308.

(27) Garcia, J. D., Yang, M. G., Wang, J. H. C. and Belo, P. S. (1974) Carbon-mercury bond cleavage in blood of rats fed methyl mercuric chloride. *Proc. Soc. Exp. Biol. Med. 146*, 66-70.

(28) Nordberg, G. F. and Skerfving, S. (1972) Metabolism, In *Mercury in the environment* (Friberg, L. T. and Vostal, J. J., Eds.) pp 29-91, CRC Press, Cleaveland, Ohio.

(29) Kerper, L. E., Ballatori, N. and Clarkson, T. W. (1992) Methylmercury transport across the blood-brain barrier by an amino acid carrier. *Am. J. Physiol. 262*, R761-R765.

(30) Rabenstein, D. L. (1978) The chemistry of methylmercury toxicology. *J. Chem. Edu. 55*, 292-296.

(31) Norseth, T. and Clarkson, T. W. (1970) Studies on the biotransformation of ^{203}Hg-labelled methyl mercury chloride in rats. *Arch. Environ. Health 21*, 717-727.

(32) Mehra, M. and Choi, B. H. (1981) Distribution and biotransformation of methyl mercuric chloride in different tissues of mice. *Acta Pharmacol. Toxicol. 49*, 28-37.

(33) Hansen, J. C., Reske-Nielsen, E., Thorlacius-Ussing, O., Rungby, J. and Dansher, G. (1989) Distribution of dietary mercury in a dog. Quantification and localization of total mercury in organs and central nervous system. *Sci. Total Environ. 78*, 23-43.

(34) Lind, B., Friberg, L. and Nylander, M. (1988) Primary studies on methylmercury biotransformation and clearance in the brain of primates II. Demethylation of mercury in brain. *J. Trace Elem. Exp. Med. 1*, 49-56.

(35) Fang, S. C. (1974) Induction of carbon-mercury cleavage enzymes in rat liver by dietary selenite. *Res. Comm. Chem. Pathol. Pharmacol. 9*, 579-582.

(36) Hirayama, K. and Yasutake, A. (1999) Effects of reactive oxygen modulators on in vivo demethylation of methylmercury. *J. Health Sci. 45*, 24-27.

(37) Rowland, I. R., Robinson, R. D. and Doherty, R. A. (1984) Effects of diet on mercury metabolism and excretion in mice given methylmercury: role of gut flora. *Arc. Environ. Health 39*, 401-408.

(38) Norseth, T. and Clarkson, T. W. (1971) Intestinal transport of ^{203}Hg-labelled methylmercury cysteine. *Arch. Environ. Health 22*, 568-577.

(39) Hirata, E. and Takahashi, H. (1981) Degradation of methyl mercury glutathione by pancreatic enzymes in bile. *Toxicol. App. Pharmacol. 58*, 483-491.

(40) Refsvik, T. and Norseth, T. (1975) Methylmercuric compounds in the bile. *Acta Pharmacol. Toxicol. 36*, 67-78.

(41) Reid, R. S. and Rabenstein, D. L. (1981) Nuclear magnetic resonance studies of the solution chemistry of metal complexes. XVII. Formation constants for the complexation of methylmercury by sufhydryl-containing amino acids and related molecules. *Can. J. Chem. 59*, 1505-1514.

(42) Rabenstein, D. L. and Evans, C. A. (1978) The mobility of methylmercury in biological systems. *Bioinorg. Chem. 8*, 107-114.

(43) Rabenstein, D. L., Isab, A. A. and Reid, R. S. (1982) A proton nuclear magnetic resonance study of the binding of methylmercury in human erythrocytes. *Biochim. Biophys. Acta 720*, 53-64.

(44) Rabenstein, D. L. and Reid, R. S. (1984) Nuclear magnetic resonance studies of the solution chemistry of metal complexes. 20. Ligand-exchange kinetics of methylmercury(II)-thiol complexes. *Inorg. Chem. 23*, 1246-1250.

(45) Prokof'ev, A. K. (1981) Chemical forms of mercury, cadmium and zinc in natural waters. *Russ. Chem. Rev. 50*, 32-48.

(46) Rabenstein, D. L. and Fairhurst, M. T. (1975) Nuclear magneic resonance studies of the solution chemistry of metal complexes. XI. The binding of methylmercury by sulfhydryl-containing acids and by glutathione. *J. Am. Chem. Soc. 97*, 2086-2092.

(47) Davis, L. E., Kornfeld, M., Mooney, H. S., Fiedler, K. J., Haaland, K. Y., Orrison, W. W., Cernichiari, E. and Clarkson, T. W. (1994) Methylmercury poisoning: long-term clinical, radiological, toxicological, and pathological studies of an affected family. *Ann. Neurol. 35*, 680-688.

(48) Vogel, D. G., Margolis, R. L. and Mottet, N. K. (1985) The effects of methyl mercury binding to microtubules. *Toxicol. App. Pharmacol. 80*, 473-486.

(49) Abe, T., Haga, T. and Kurokawa, M. (1975) Blockage of axoplasmic transport and depolymerization of reassembled microtubules by methyl mercury. *Brain Res. 86*, 504-508.

(50) Hirayama, K. (1985) Effects of combined administration of thiol compounds and methylmercury chloride on mercury distribution in rats. *Biochem. Pharmacol. 37*, 2030-2032.

(51) Thomas, D. J. and Smith, J. C. (1982) Effects of coadministered low-molecular weight thiol compounds on short-term distribution of methylmercury in the rat. *Toxicol. Appl. Pharmacol. 62*, 104-110.

(52) Madsen, K. M. (1980) Mercury accumulation in kidney lysosomes or proteinuric rats. *Kid. Inter. 18*, 445-453.

(53) Zalups, R. K. and D.W., B. (1993) Intrarenal distribution of inorganic mercury and albumin after coadministration. *J. Toxicol. Environ. Health 40*, 77-103.

(54) Waku, K. and Nakazawa, Y. (1979) Toxic effect of several mercury compounds on SH- and non-SH enzymes. *Toxicol. Lett. 4*, 49-55.

(55) Grundt, I. K., Roux, F., Treich, I., Loriette, C., Raulin, J. and Fournier, E. (1982) Effects of methyl mercury and triethyllead on Na+K~ATPase and pyruvate dehydrogenase activities in Glioma C6 cells. *Acta Pharmacol. Toxicol. 51*, 6-11.

(56) Domanska-Janik, K. and Bourre, J. M. (1987) Effect of mercury on rabbit myelin CNP-ase in vitro. *Neurotoxicol. 8*, 23-32.

(57) Inoue, Y., Saijoh, K. and Sumino, K. (1988) Action of mercurials on activity of partially purified soluble protein kinase C from mice brain. *Pharmacol. Toxicol. 62*, 278-281.

(58) Ribarov, S. R. and Benov, L. C. (1981) Relationship between the hemolytic action of heavy metals and lipid peroxidation. *Biochim. Biophys. Acta 640*, 721-726.

(59) Nakada, S. and Imura, N. (1983) Susceptibility of lipids to mercurials. *J. Appl. Toxicol. 3*, 131-134.

(60) Walum, E. and Marchner, H. (1983) Effects of mercuric chloride on the membrane integrity of cultured cell lines. *Toxicol. Lett. 18*, 89-95.

(61) Ballatori, N., Shi, C. and Boyer, J. L. (1988) Altered plasma membrane ion permeability in mercury induced cell injury: Studies in hepatocytes of Elasmobranch *Raja erinacea*. *Toxicol. Appl. Pharmacol. 95*, 279-291.

(62) Rajanna, B. and Hobson, M. (1985) Influence of mercury on uptake of [^{3}H]dopamine and [^{3}H]norepinephrine by rat brain synaptosomes. *Toxicol. Lett. 27*, 7-14.

(63) Pfeifer, R. W. and Irons, R. D. (1985) Mechanism of sulfhydryl-dependent immunotoxicity, In *Immunotoxicology and Immunopharmacology* (Dean, J. H., Luster, M. I., Munson, A. E. and Amos, H., Eds.) pp 255-262, Raven Press, New York.

(64) Pařízek, J. and Ošádalová, I. (1967) The protective effect of small amounts of selenite in sublimate intoxication. *Experientia 23*, 142-143.

(65) Naganuma, A. and Imura, N. (1980) Bis(methylmercuric) selenide as a reaction product from methylmercury and selenite in rabbit blood. *Res. Comm. Chem. Pathol. Pharmacol. 27*, 163-173.

(66) Magos, L., Webb, M. and Hudson, A. R. (1979) Complex formation between selenium and methylmercury. *Chem. -Biol. Interactions 28*, 359-362.

(67) Ganther, H. E. (1978) Modification of methyl mercury toxicity and metabolism by selenium and vitamin E: Possible mechanisms. . *Environ. Health Perspect. 25*, 71-76.

(68) Beyrouty, P. and Chan, H. M. (2006) Co-consumption of selenium and vitamin E altered the reproductive and developmental toxicity of methylmercury in rats. *Neurotoxicol. Teratol. 28*, 49-58.

(69) Sheline, J. and Schmidt-Nielsen, B. (1977) Methyl mercury-selenium: Interaction in killifish, *Fundulus heteroclitus*, In *Physiological Responses of Marine Biota to Pollutants* (Vemberg, F., Ed.) pp 119-130, Symposium, Milford, CN.

(70) Fairhurst, M. T. and Rabenstein, D. L. (1975) Nuclear magnetic resonance studies of the solution chemistry of metal complexes. XII. Binding of methylmercury by methionine. *Inorg. Chem. 14*, 1413-1415.

(71) Rabenstein, D. L., Ozubko, R., Libich, S., Evans, C. A., Fairhurst, M. T. and Suvanprakorn, C. (1974) Nuclear magnetic resonance studies of the solution chemistry of metal complexes. X. Determination of the formation constants of the methylmercury complexes of selected amines and aminocarboxylic acids. *J. Coord. Chem. 3*, 263-271.

(72) Carty, A. J., Malone, S. F., Taylor, N. J. and Canty, A. J. (1983) Synthesis, spectroscopic and X-ray structural characterization of methylmercury-D,L-selenocysteinate monohydrate, a key model for the methylmercury(II)-selenoprotein interaction. *J. Inorg. Biochem. 18*, 291-300.

(73) Ng, P.-S., Li, H., Matsumoto, K., Yamazaki, S. and Kogure, T. (2001) Striped dolphin detoxificates mercury as insoluble Hg(S, Se) in the liver. *Proc. Japan Acad. 77(B)*, 178-183.

(74) Frisch, M. J., Trucks, G. W., Schlegel, H. B., Scuseria, G. E., Robb, M. A., Cheeseman, J. R., Montgomery, J. A., Vreven, T., Kudin, K. N., Burant, J. C., Millam, J. M., Iyengar, S. S., Tomasi, J., Barone, V., Mennucci, B., Cossi, M., Scalmani, G., Rega, N., Petersson, G. A., Nakatsuji, H., Hada, M., Ehara, M., Toyota, K., Fukuda, R., Hasegawa, J., Ishida, M., Nakajima, T., Honda, Y., Kitao, O., Nakai, H., Klene, M., Li, X., Knox, J. E., Hratchian, H. P., Cross, J. B., Bakken, V., Adamo, C., Jaramillo, J., Gomperts, R., Stratmann, R. E., Yazyev, O., Austin, A. J., Cammi, R., C. Pomelli, C., Ochterski, J. W., Ayala, P. Y., Morokuma, K., Voth, G. A., Salvador, P., Dannenberg, J. J., Zakrzewski, V. G., Dapprich, S., Daniels, A. D., Strain, M. C., Farkas, O., Malick, D. K., Rabuck, A. D., Raghavachari, K., Foresman, J. B., Ortiz, J. V., Cui, Q., Baboul, A. G.,

Clifford, S., Cioslowski, J., Stefanov, B. B., Liu, G., Liashenko, A., Piskorz, P., Komaromi, I., Martin, R. L., Fox, D. J., Keith, T., Al-Laham, M. A., Peng, C. Y., Nanayakkara, A., Challacombe, M., Gill, P. M. W., Johnson, B., Chen, W., Wong, M. W., Gonzalez, C., Pople, J. A. and GAUSSIAN-03, R. C. (2004) GAUSSIAN-03, Gaussian, Inc., Wallingford, CT.

(75) Becke, A. D. (1993) Density-functional thermochemistry. III. The role of exact exchange. *J. Chem. Phys. 98*, 5648-5652.

(76) Lee, C., Yong, W. and Parr, R. G. (1988) Development of the Colle-Salvetti correlation-energy formula into a functional of the electron density. *Phys. Rev. B 37*, 785-789.

(77) Figgen, D., Rauhut, G., Dolg, M. and Stoll, H. (2005) Energy-consistent pseudopotentials for group 11 and 12 atoms: adjustment to multi-configuration Dirac-Hartree-Fock data. *Chem. Phys. 311*, 227-244.

Preface to Chapter 2

This chapter is based on the following manuscript published in the journal "*Environmental Toxicology and Chemistry*". Full citation of the paper is as follows:

> Khan, M. A. K.; Wang, F., Mercury-Selenium Compounds and Their Toxicological Significance: Toward a Molecular Understanding of the Mercury-Selenium Antagonism. *Environ. Toxicol. Chem.* **2009**, 28(8), 1567-1577.

This chapter provides a critical review on the key Hg-Se compounds leading to the Hg-Se antagonism at the molecular level in biological systems. Their role in the antagonism is clearly explained and any ambiguity is identified to guide the researchers in this field for future endeavour. Differences between the outcomes of the laboratory experiments and real biological samples are highlighted. This chapter sets the foundation of the subsequent research carried out in this dissertation.

Chapter 2: Mercury-Selenium Compounds and Their Toxicological Significance: Toward a Molecular Understanding of the Mercury-Selenium Antagonism

Abstract

The interaction between mercury (Hg) and selenium (Se) is one of the best known examples of biological antagonism, yet the underlying mechanism remains unclear. This review focuses on the possible pathways leading to the Hg-Se antagonism, with an emphasis on the potential Hg-Se compounds that are responsible for the antagonism at the molecular level (i.e., bis(methylmercuric)selenide, methylmercury selenocysteinate, selenoprotein P-bound HgSe clusters, and the biominerals $HgSe_xS_{1-x}$). The presence of these compounds in biological systems has been suggested by direct or indirect evidence, and their chemical properties support their potentially key roles in alleviating the toxicity of Hg and Se (at high Hg and Se exposures, respectively) and deficiency of Se (at low Se exposures). Direct analytical evidences are needed, however, to confirm their in vivo presence and metabolic pathways, as well as to identify the roles of other potential Hg-Se compounds. Further studies are also warranted for the determination of thermodynamic properties of these compounds toward a better understanding of the Hg-Se antagonism in biota, particularly under real world exposure scenarios.

Key Words: Mercury; Methylmercury; Selenium; Antagonism; Metallomics

1. Introduction

Mercury (Hg) is a global contaminant (*1, 2*) and has received much scientific attention since the onset of the Minamata disease in Japan in the 1950s (*3, 4*) and following the MeHg poisoning in Iraq in the early 1970s (*5*). Both inorganic and organic forms of Hg are toxic due to their high affinities to thiol-containing enzymes and proteins, but exhibit distinct clinical patterns of toxicity because of their different patterns of uptake and organ distribution (*6*). Inorganic Hg(II) is primarily nephrotoxic (*7-9*), and is thought to enter the proximal tubular cells through the endocytosis of Hg complex with albumin in the plasma (*7, 10*). The nephrotoxicity of inorganic Hg(II) is mainly due to its perturbation of the enzymes responsible for the protection of cells against peroxidation, resulting in mitochondrial oxidative stress in renal tubular damage (*11-13*). Gaseous elemental Hg (Hg^0) can be rapidly oxidized to inorganic Hg(II) in the blood and become a nephrotoxin; the remaining vapour form can also diffuse through the blood-brain barrier and become a neurotoxin following oxidation in the brain (*14, 15*). The most neurotoxic form of Hg that can be found in biological systems is the organic form of Hg(II), monomethylmercury (MeHg) (*2, 3*). It can cross the blood-brain barrier by the L-type neutral amino acid transporters (LAT 1 and 2) (*15-18*), and causes disruptions in various cellular processes including ionic homeostasis, synaptic function, oxidative stress, synthesis of proteins including selenoproteins (*19, 20*), and selenium (Se) deficiency (*21*). Of particular concern is the ability of MeHg to cross the placental barrier (*22, 23*) and affect the nervous system in children prenatally (*3, 24, 25*), making it one of a few known developmental neurotoxins (*1, 26*). There is also evidence that MeHg may be associated

with a range of cardiovascular (*1, 27, 28*) and reproductive (*29, 30*) effects in mammals including humans.

It has long been observed that Se protects animals from the toxicity of both inorganic Hg and MeHg. One of the earliest studies on the protective effect of Se was reported by Pařízek and Oštádalová on the laboratory rats from kidney intoxication by inorganic Hg (*31*). A similar antagonism was reported between Se and MeHg in Japanese quails and rats (*32*). Subsequent studies have confirmed this as a widespread phenomenon in bacteria (*33*), aquatic organisms (bacteria, zooplankton, mayflies, amphipods, perch, walleye) (*34, 35*), quails (*36*), chicks (*36, 37*), ducks (*38*), rats (*39-42*), mice (*21, 43, 44*), and pigs (*45*). Accumulations of total Hg and Se have also been frequently found to co-vary, often following a 1:1 molar ratio, in tissues of marine mammals (*46, 47*), in various organs (kidney, liver and muscle) of Hg mine workers (*48*), and in urine samples from miners and residents in Hg-contaminated areas (*49*).

Although Hg-Se antagonism is generally observed, additive or even synergistic effect of Hg and Se have also been reported in the literature (e.g., (*50-54*)). This is not surprising, as Se, though an essential element for animals and humans, will cause toxic effects when the concentration is elevated above what is considered optimal. The net effect is likely dependent on the relative concentrations of Hg and Se (*52, 53*), their bioavailabilities, and the sensitivity of the animal or the specific organ (*38*). Assuming the formation of a 1:1 molar ratio Hg-Se compound that is biologically inert, Figure 2.1 illustrates the potential biological effects upon exposure to different concentrations of Hg and Se. Whether there is an antagonism or synergistic effect depends on the sensitivity of

the organ/organism (which determines the threshold concentrations $[Hg]_t$, $[Se]_d$, and $[Se]_t$), and the relative concentrations of Hg and Se.

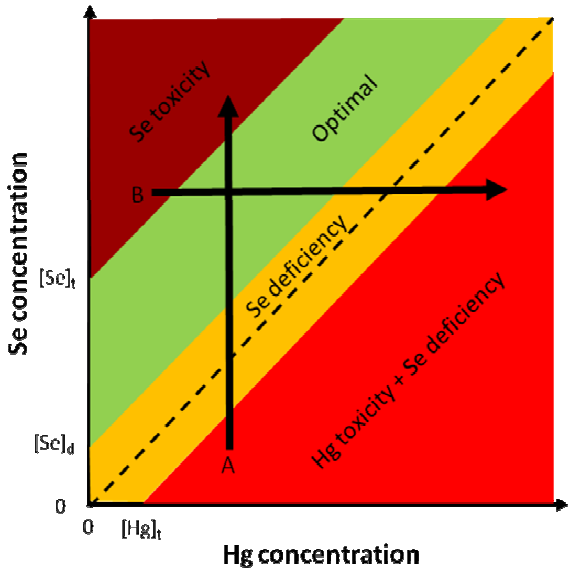

Figure 2.1. Potential biological effects upon exposure to different concentrations of Hg and Se. This is a rather simplified illustration assuming the formation of a 1:1 molar ratio Hg-Se compound that is not bioavailable. $[Hg]_t$: the toxicity threshold concentration (molar) of Hg; $[Se]_d$ and $[Se]_t$: deficiency and toxicity threshold concentrations of Se, respectively. Whether there is an antagonism or synergistic effect depends on the sensitivity of the organ/organism (which determines $[Hg]_t$, $[Se]_d$, and $[Se]_t$), and the relative concentrations of Hg and Se. Arrow A: at a specific [Hg], increasing [Se] will first decrease the toxicity of Hg, then alleviate the Se deficiency, but eventually result in Se toxicity. Arrow B: At a specific [Se], increasing [Hg] will first decrease the toxicity of Se, then induce Se deficiency, and ultimately the toxicity of Hg. The green region denotes the "optimal" condition. Note that the well-observed Se/Hg 1:1 molar ratio (the dashed line) in marine mammals is located in the Se deficiency region as Se would have

been bound to Hg and not bioavailable.

Despite a great deal of study on the toxicity of Hg and on the interaction between Hg and Se, the fundamental mechanism for the Hg-Se antagonism remains elusive (*55, 56*). Here we provide a critical review on possible pathways leading to the Hg-Se antagonism, with an emphasis on a few key Hg-Se compounds that may be responsible for the antagonism at the molecular level. Given the rapid development in high resolution, high sensitive analytical techniques such as liquid chromatography – tandem mass spectrometry and synchrotron-based X-ray absorption spectroscopy, we believe the identification (or lack thereof) and quantification of some of these compounds in vivo will become possible in the foreseeable future, which will provide a mechanistic basis for detoxification and remediation strategies. For a basic understanding of the chemistry and biological uptake of Hg and Se, several recent review papers are available and should be consulted (*57-60*).

2. Possible Pathways Leading to Biological Hg-Se Antagonism

Several earlier reviews have examined possible mechanisms for the antagonistic effect between Hg and Se (*55, 56, 61-63*), which are summarized in the six pathways detailed below (Sections 2.1-2.6): formation of MeHg-Se compounds; Se-aided demethylation of MeHg; formation of inorganic Hg-Se compounds; redistribution of inorganic Hg in the presence of Se; Se inhibition of methyl radicals from MeHg; and Hg-induced Se deficiency. The first four pathways are based on the assumption that the toxicity of Hg and MeHg is caused by the Hg^{2+} or $MeHg^{+}$, whereas the last two attribute

the observed Hg toxicity to, at least in part, the methyl group and Se deficiency, respectively.

2.1 Formation of MeHg-Se Compounds

Due to the abundance of thiol (sulfhydral, -SH) groups in biomolecules and their high affinity toward $MeHg^+$ (*64*), MeHg speciation in the intracellular environment is dominated by MeHg-SR (-SR = amino acids containing S) complexes (*65*, *66*). Despite the very high formation constants (10^{15}-10^{17} range; (*64*)) of MeHg complexes with thiols, the MeHg-SR bonding is extremely labile, and can undergo rapid ligand exchange reactions in aqueous solutions (*67-70*) and likely in biological systems (*67*). Several mechanisms (associative, dissociative, bridging) have been hypothesized for the rapid ligand exchange, but the displacement of complexed thiol by free thiols via an associative mechanism seems to be the dominant pathway (*70*):

$$\mathrm{MeHgSR + R'SH \rightleftharpoons MeHgSR' + RSH} \qquad (1)$$

The rate constant for thiol ligand exchange increases with increasing relative formation constants of the complexes $K_{f,MeHgSR'}/K_{f,MeHgSR}$ (*70*).

Since MeHg-SeR bonding is stronger than that of MeHg-SR (*71-74*), and the formation constants for MeHg-selenol complexes are greater than their thiol analogs (*75*) (e.g., Table 1), ligand exchange between -SR and –SeR can take place rapidly in favour of the formation of MeHg-Se complexes (*75*, *76*) :

$$\mathrm{MeHgSR + RSeH \rightleftharpoons MeHgSeR + RSH} \qquad (2)$$

Several MeHg-Se compounds have been proposed in the literature, including bis(methyl mercuric)selenide and MeHg-selenocysteine, which will be discussed in detail in Section 3. The MeHg-SeR compounds are presumably less bioavailable than MeHg-

SR due to the stronger Hg-Se bonding (*71-74*); therefore, the formation of MeHg-SeR could decrease the toxicity of MeHg but could also induce a Se deficiency.

Table 2.1. MeHg-selenocysteinate and its sulfur analog

Complex	**Bond distance**		**Bond angle**		**Coupling constant**	**Formation constant (0.3 M, 25 °C)**	
	Hg-S(e)	**Hg-C**	**C-Hg-S(e)**	**Hg-S(e)-C**	**$J_{199Hg-1H}$ (Hz)**	**log K_f**	**log K_{fc} (pH 7.4)**
MeHg-cysteinate	2.352[1]	2.084[1]	178.8[1]	100.8[1]	172.5[1]	16.7[2]	11.6[2]
MeHg-selenocysteinate	2.469[3]	2.10[3]	177.8[3]	98.5[3]	166.5[3] (in D_2O)	17.4[4]	13.4[4]

[1] (*77*)
[2] (*64*)
[3] (*73*)
[4] (*75*)

2.2 Selenium-aided Demethylation of MeHg

Methylation of inorganic Hg to MeHg is generally thought to be a microbial process mediated primarily by sulphate reducing bacteria (*78, 79*). There is no conclusive evidence that Hg methylation occurs in vivo in animals. The reverse process, MeHg demethylation, is however known to occur in vivo to a significant extent in the liver with subsequent accumulation of inorganic Hg in the kidneys in many mammals through filtration of blood (*80, 81*). Demethylation is of particular significance in the liver of marine mammals at high trophic levels. Whereas Hg in the muscle, blood, and brain is almost exclusively in the form of MeHg, high percentages of inorganic Hg are commonly found in the liver and kidneys of these animals (e.g., (*82*)). Since their Hg exposure is primarily MeHg via prey (e.g., fish), the majority of the inorganic Hg in the liver and kidneys is produced from the in vivo demethylation. Methylmercury demethylation is also possible in the brain, as inorganic Hg was found to account for more than 50% of the

total Hg in the brain of humans and monkey (*14*), including those who were not exposed to high levels of Hg^0 (*14*, *83*).

It has been hypothesized that Se may be involved in the demethylation process of MeHg (*84, 85*), though the mechanism remains unknown. Selenite has been shown to increase C-Hg cleavage in phenylmercury in the liver of rats, but not in MeHg (*86*). A more plausible pathway of Se-aided MeHg demethylation is via the formation of bis(methylmercuric)selenide, which is unstable at physiological temperature and decomposes to inorganic HgSe(s) (see Section 3).

Regardless of whether Se is directly involved in MeHg demethylation, it is clear that the produced inorganic Hg can be bound to selenides, as the presence of HgSe(s) granules has been commonly reported in the liver and kidneys of marine mammals and sea birds (*84*, *87-91*). This is likely a detoxification pathway of MeHg in high trophic level marine mammals where elimination (e.g., excretion) of MeHg cannot match the dietary intake of MeHg (*90*), potentially explaining the 1:l molar ratio of Hg and Se in these marine mammals (*84*) and the lack of toxic effect despite high concentrations of Hg commonly found in these animals (*82*).

The demethylation seems to be triggered only after a threshold concentration of MeHg is reached in the system. Palmisano et al. (*92*) suggested that Hg was first stored in the liver of dolphin as MeHg and after a threshold value (~100 µg/g wet weight) was reached, demthylation took place and the liberated inorganic Hg(II) then bound with Se to form HgSe(s). When the MeHg concentration was under the threshold value, the antagonism of Hg toxicity by Se did not occur. Similar observations on a threshold value

were reported in Arctic fox and wolverines from the Canadian Arctic (*93, 94*) and in humans (*95, 96*).

It should be noted that demethylation of MeHg does not necessarily decrease the toxicity of Hg, as the resultant inorganic Hg(II) could be more toxic due to its stronger binding affinity to –SH sites than MeHg (*97, 98*). It is most likely that the MeHg neurotoxicity may have been due, at least in part, to the inorganic Hg(II) formed from MeHg demethylation in the brain (*2, 83, 99*). However, if this inorganic Hg(II) is bound to selenides to form HgSe(s) or highly stable Hg-Se-protein complexes (see below), its neuro- or nephro-toxicity will likely be decreased.

2.3 Formation of Inorganic Hg-Se Compounds

Similar to the case of MeHg, the formation of less bioavailable inorganic Hg-SeR would also decrease the toxicity of inorganic Hg. The observation that the antagonism was most effective when Se (in the form of SeO_3^{2-}) and inorganic Hg (in the form of $HgCl_2$) were administrated simultaneously and at equimolars (*31, 40, 43, 100*) led many researchers to suggest the formation of an equimolar $(HgSe)_n$ polymer which is bound to a specific plasma protein in the blood stream of the animals (*43, 100*). This specific, $(HgSe)_n$ bonding plasma protein was later identified to be selenoprotein P (SelP) (*101*). The $(HgSe)_n$-SelP is thought to be the precursor of the crystalline HgSe(s) (*102*). Kosta et al. (*48*) showed that following exposure to inorganic Hg, Se and Hg concentrations in the brain of humans had a molar ratio of 1:1. The authors suggested that the fraction of Hg with a long biological halftime could be present as a Hg-Se compound, though the identity of the compound was not given.

While $(HgSe)_n$-SelP might explain the HgSe(s) granules in the liver and kidneys of laboratory animals to which inorganic Hg and Se are administrated simultaneously, HgSe(s) granules that are commonly observed in the liver of marine mammals are more likely a biomineralization product following the demethylation of MeHg as discussed in Section 2.2.

2.4 Redistribution of Inorganic Hg in the Presence of Se

Another possible pathway leading to the biological effects of Hg and Se is that under the influence of Se, Hg in the biological system can be redistributed among the organs (e.g., liver, kidneys). It has been observed that a single dose of Se and Hg administered simultaneously increased retention of both elements in the organism and that a redistribution of Hg in the kidneys and liver was observed compared to Hg being administered alone (*100, 103*). Komsta-Szumska and Chmielnicka (*104*) observed a major shift of inorganic Hg in rats from the kidneys to muscle after the administration of selenite. It was suggested that Se induces the release of inorganic Hg originally bound to the relatively low molecular weight (~10K Daltons) metallothionein in the red blood cell (*103*), and diverts it to high molecular weight proteins (> 60K Daltons) in rat liver and kidneys (*103, 104*). The authors assumed that Se might affect the transfer of Hg compounds from protein mercaptide to glutathione or otherwise inhibit the formation of the Hg-metallothionein complex. A similar Se-induced shift of inorganic Hg from low molecular weight to high molecular weight proteins was also demonstrated in rabbit blood, kidneys and liver (*105*). Several other studies, however, suggested that the Se

status of the animals had no effect on the distribution of inorganic Hg (*106*) and MeHg (*21*, *107*).

2.5 Selenium Inhibition of Methyl Radicals from MeHg

In contrary to the generally held view that the toxicity of MeHg is caused by the affinity of $MeHg^+$ or demethylated Hg^{2+} to the –SH containing proteins (as implied by the above four pathways), Ganther (*108*) proposed that the toxicity of MeHg might be due, at least in part, to the free methyl radicals from the dissociation of MeHg:

$$CH_3HgX \xrightarrow{\text{homolysis}} CH_3\bullet + Hg\bullet + X^- \qquad (3)$$

where X = Cl^-, OH^-, or Br^-. The Hg radicals formed could be converted to both Hg^0 and Hg^{2+}. According to this hypothesis, MeHg is taken up by membranes of the target tissues (e.g., the brain) in close proximity to lipids. The homolytic breakdown of MeHg would occur upon the initiation by radicals formed from oxygen-dependant metabolic reactions. The Se antagonism can then be explained by Se in glutathione peroxidase (GPx) decomposing peroxides which otherwise would initiate the MeHg breakdown. This hypothesis can also explain the protective effect over MeHg toxicity of other anti-oxidants such as Vitamin E (*41*, *108*, *109*) and N,N'-diphenyl-p-phenylenediamine (DPPD) (*109*). Furthermore, it could explain the lifetime of MeHg in the brain, as Hg^0 can be diffused out to the blood and exhaled from the body. However, no direct evidence has yet been reported to support this hypothesis (*110*). By their nature of being very reactive, free radicals are expected to react only with sites that are at their immediate vicinity.

2.6 Mercury-Induced Selenium Deficiency

Selenium is an essential element for animals, certain lower plants, and humans (*111*). Two primary amino acids, selenocysteine and selenomethionine, contain Se and many selenoproteins or Se-containing protein subunits have been detected in animal cells. Selenium is a micronutrient and an antioxidant, and supports normal thyroid hormone homeostasis, immunity, and fertility (*112*); its role in brain function has also recently been established (*113*). As is true for all micronutrients, adverse biological effects occur when the bioavailable Se in the biota is too low (deficiency) or too high (toxicity) (Figure 2.1).

Since the affinity of Hg^{2+} and $MeHg^{+}$ to -SeR surpasses that to -SR, it is reasonable to assume that Hg or MeHg would be bound preferentially to -SeR, which could decrease the bioavailability of Se in the biological system. Indeed, MeHg has been shown to depress the activity of GPx in rats (*21, 42, 44, 114*), without changing the total Se concentration in the organ (*21, 42, 44*). Assuming the formation constant for the MeHg-GPx complex is the same as that of the MeHg-selenocysteine complex, Arnold et al. (*75*) estimated that 1.6-47% of the selenol groups of GPx could be complexed by MeHg at total MeHg concentrations of 1-50 μM. The decrease in Se bioavailability may be negligible in humans at the normal blood MeHg level (~0.01 μM), but can be significant in MeHg contaminated populations. For example, blood MeHg concentrations up to 30 μM were reported in the 1972 epidemic of MeHg poisoning in Iraq (*75*), which could decrease the Se bioavailability by one third. Therefore, by diverting Se from selenoprotein synthesis to formation of Hg-Se complexes, Hg could cause a functional, local Se deficiency in which the function of the selenoprotein is compromised (*44, 83,*

112). It is thus possible that the observed toxicity of Hg is at least in part caused by Hg-induced Se deficiency (*21*, *112*).

This mechanism would readily explain the Hg-Se antagonism, as Hg induced Se deficiency can be simply overcome by providing the animal with more bioavailable Se. Chang and Suber (*114*) found that adding Se (in the form of Na_2SeO_3) completely alleviated the inhibitory effect of MeHg on GPx. Hoffman et al. (*38*) also reported that Se could alleviate (partially or fully) the effects of Hg on GPx, glucose-6-phosphate dehydrogenase (G-6-PDH), and oxidized glutathione (GSSG).

3. Potential Se-Hg Compounds Responsible for the Hg-Se Antagonism

While all the six proposed pathways may have contributed to the Hg-Se antagonism, at the molecular level they are all based on the same mechanism: the formation of certain Hg-Se compounds with different mobility, bioavailability, and affinity to the target sites. The identities of the Se-Hg compounds that are responsible for the Hg-Se antagonism remain unknown; however, it is likely that more than one Se-Hg compound is involved. Whereas a 1:1 molar ratio between Hg:Se is frequently reported, such as in tuna fish (*32*, *115*), in the liver of marine mammals such as belugas, ringed seals and narwhal (*46*, *47*, *102*, *116*), in the brain of river otters (*117*), and in the blood of mice (*118*) and Hg miners (*48*), Hg:Se molar ratios of < 1 and > 1 have also been reported (see (*62*)). Figure 2.2 provides a general scheme for the potential in vivo MeHg-Se reactions; the reactions between inorganic Hg(II) and Hg^0 with Se become a subset of this general scheme. Four key groups of the Hg-Se compounds are discussed below.

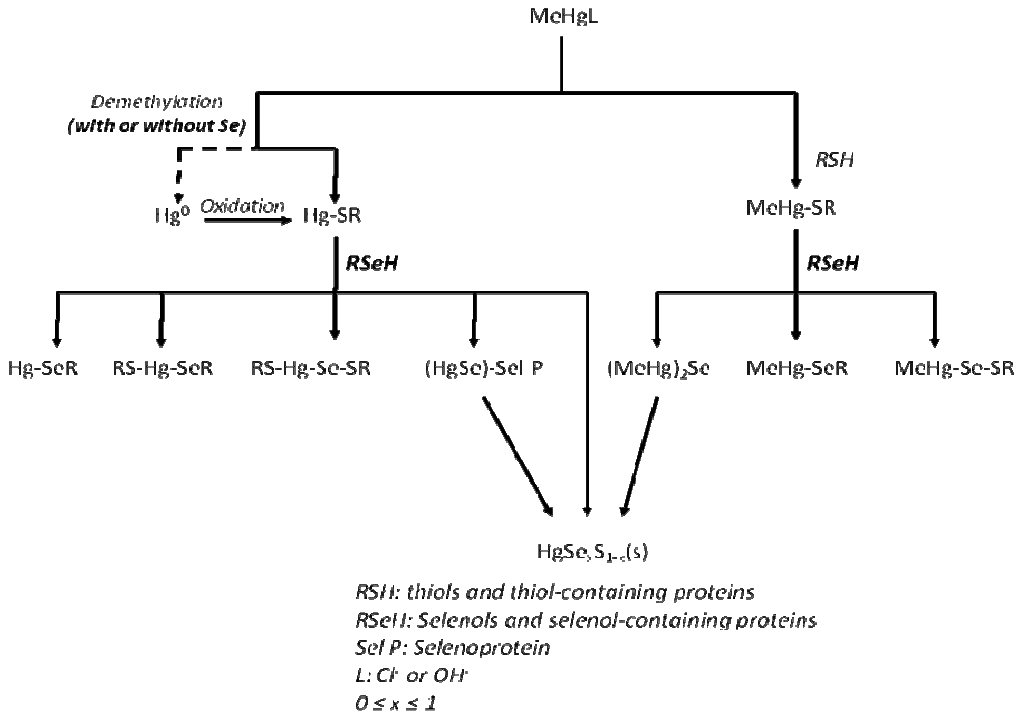

Figure 2.2 Possible Hg-Se compounds involved in the metabolism of MeHg, inorganic Hg(II) and Hg^0 in biota in the presence of Se.

3.1 Bis(methylmercuric)selenide (BMSe)

Sumino et al. (*119*) demonstrated that incubating selenite and MeHg in vitro resulted in significant release of benzene-extractable MeHg from human blood, as well as from the red blood cells, and liver, kidneys and brain homogenates of rats and mice, and muscle homogenates of raw tuna. The molar ratio of MeHg to Se in the extractant was ≥2. The benzene extractable MeHg was also detected in vivo in the blood, liver, and kidneys of mice after injection of MeHg and selenite. They concluded that selenite can liberate MeHg from sulfhydral bonds (*119*), and stated that the "liberated" MeHg loses the affinity for proteins or -SH radicals (*120*). This "liberated" benzene extractable MeHg

was later identified as bis(methylmercuric)selenide ($(MeHg)_2Se$, or BMSe) (*121, 122*), and detected in vitro in the blood of rabbits and humans (*121, 123*), and in soluble or insoluble fraction of mouse liver, kidneys, spleen, and brain (*124*). Indeed, Naganuma and Imura (*125*) reported that BMSe can be readily synthesized by mixing CH_3HgCl with glutathione at pH 7.4 followed by the addition of SeO_3^{2-}.

As BMSe is charge neutral, it could potentially enhance the transport of MeHg across the blood-brain barrier (*121*). However, it is not stable at room or physiological temperature (*121, 122*), which could explain why BMSe has not been detected in vivo (*124*). Naganuma et al. (*124*) hypothesized that the in vivo formation and decomposition of BMSe occurs repeatedly, resulting in a significant increase of MeHg in the brain of animals following the co-administration of MeHg and selenite (*119, 126*).

The formation of BMSe could also represent a chemical demethylation pathway. Although the decomposition product of BMSe has not been identified, it is possible that BMSe will produce dimethylmercury (DMHg) and HgSe(s), based on an analog with $(MeHg)_2S$ (*127*):

$$(MeHg)_2Se(s) \longrightarrow Me_2Hg + HgSe(s) \qquad (4)$$

The formed Me_2Hg could be decomposed further to MeHg:

$$Me_2Hg + H^+ \longrightarrow MeHg^+ + CH_4 \qquad (5)$$

$MeHg^+$ will react again in the presence of HSe^- (Se^{2-} is not present in any significant amount at physiological pH):

$$2MeHg^+ + HSe^- \rightleftharpoons (MeHg)_2Se(s) + H^+ \qquad (6)$$

The net reaction is thus:

$$MeHg^+ + HSe^- \longrightarrow HgSe(s) + CH_4 \qquad (7)$$

This could be one of the sources of HgSe(s) observed in animals (see below).

3.2 MeHg-Selenol Compounds (MeHg-SeR)

Sugiura et al. (*71*) were the first to study the binding affinities of $MeHg^+$ in aqueous solution with several biologically relevant Se-containing ligands including selenocysteine, selenocystine, selenomethionine, selenocysteamine, and selenocystamine. Based on the coupling constants $J_{199Hg\text{-}1H}$ from NMR, the authors found that the $MeHg^+$ affinity with selenols (RSeH) is the highest, and established the general order of binding affinity as SeH > SH ≥ Se-Se > NH_2 > S-S, $SeCH_3$.

Methylmercury complex with selenocysteine, MeHg-$_{D,L}$-selenocysteinate monohydrate, was synthesized and crystallized by Carty et al. (*73*). The crystals were found to be orthorhombic and Hg was coordinated with selenocysteine via the Se atom. Other MeHg-selenol compounds that have been characterized include MeHg-selenourea ($[CH_3HgSeC(NH_2)_2]X$ (X=Cl, Br, NO_3, ClO_4)) (*128*), MeHg-carboxybenzylselenides $CH_3HgSeCH_2Ph(COOH)$ (*129*), and Hg-selenoalkyl derivatives such as methyl(methaneselenolato)mercury(II) (MeHgSeMe), methyl(benzeneselenolato) mercury(II) (MeHgSePh) (*76*), and $MeHgSe^tBu$ (*72, 74*). None of these compounds, however, have been found in vivo analytically.

Although the Hg-Se bond length in MeHgSeR is longer than the Hg-S bond length in its sulfur counterpart, the Hg-Se bond length is marginally shorter than expected based on the relative radii (*76*), suggesting Hg-Se bonding is stronger than Hg-S bonding (*73*). This is also confirmed by NMR, which shows MeHg-SeR complexes tend to have smaller $J_{199Hg\text{-}1H}$ values than their sulfur counterparts (*76*) (Table 1). The stronger binding affinity between $MeHg^+$ and selenols implies that in the presence of RSeH, MeHg-SR

complexes will undergo ligand exchange to form MeHg-SeR (*75, 76*) (Eqn. 2). This would result in a decreased bioavailability of both MeHg (thus a decrease in potential MeHg toxicity) and Se (thus an increase in potential Se deficiency).

Of all the MeHg-selenol complexes, MeHg-selenocysteinate is of the most interest in biological systems. Selenocysteine is the form of Se that occurs in most of the known selenoproteines including GPx and SelP. While free, unbound selenocysteine may be present in vivo as a degradation product from selenoproteins and selenomethionine, the majority of it is bound in selenoproteins as selenocysteine residues. Assuming the bound selenocysteine residues have the same affinity to $MeHg^+$ as the free selenocysteine, Figure 2.3 shows the MeHg speciation in a modelled human blood system as a function of the total selenocysteine when the total cysteine concentration is 0.2 mM. As the human blood typically contains 0.5 – 2.5 μM Se (*111*) and assuming all the Se is present as selenocysteine, up to 8% MeHg in the blood would be bound as MeHg selenocysteinate. This small percentage of Se-bound Hg in human blood probably explains why there has been no conclusive evidence for the Hg-Se antagonism in humans. However, Figure 2.3 suggests that the addition of Se could be promising clinically for the treatment of patients with high MeHg exposures: if the blood Se concentration is increased by 10 times to 25 μM, nearly 50% of the MeHg would be bound to MeHg selenocysteinate. As MeHg cysteinate is thought to be the MeHg species that crosses the blood-brain barrier, this would significantly decrease the amount of MeHg that is transported to the brain and thus decrease the neurotoxicity.

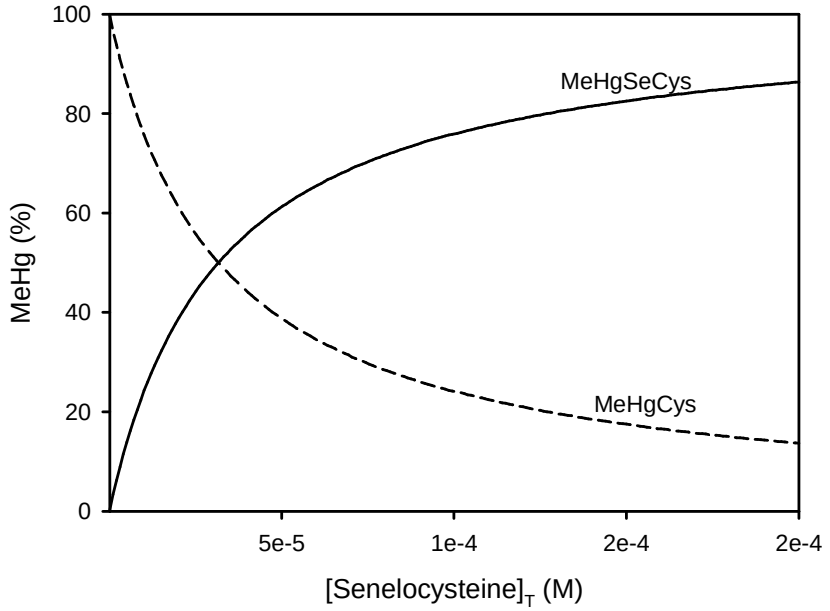

Figure 2.3. MeHg speciation in the human blood as a function of the total (free + bound) selenocysteine concentration, at a typical cysteine concentration of 2 mM (*130*). The conditional formation constants for MeHg cysteinate (MeHgCys) and MeHg selenocysteinate (MeHgSeCys) were taken from (*64*) and (*75*), respectively. The calculation was done with the computer software MINEQL+ Version 4.5 (*131*).

Selenomethionine is another Se-containing amino acid. Since the Se atom is already bound with 2 carbon atoms, its affinity to $MeHg^{+}$ is much weaker. Under physiological conditions the binding is likely via the N atom instead of the Se atom. Seppänen et al. (*132*) reported the interaction of seleno-$_{D,L}$-methionine with Hg in the liver blood of rats after being fed with fish. Seleno-$_{D,L}$-methionine was found to have a tendency to increase both MeHg and total Hg in the blood and liver, but it seemed to decrease the proportion of MeHg of total Hg. It was assumed that seleno-$_{D,L}$-methionine transfers Hg into the blood and reacts with MeHg eliminating a fraction of it. Due to the

very limited literature, the role and mechanism of selenomethionine in Hg and MeHg toxicity remains poorly understood.

3.3 Inorganic Hg-Selenol Compounds (Hg-SeR)

Inorganic Hg^{2+} has a much stronger Lewis acidity than $MeHg^{+}$ (*133*), and thus has an even higher affinity to selenols. Surprisingly, no studies have been reported on the complexation between inorganic Hg and selenolcysteine. Based on the study on Hg complexation with cysteine (*134*), Hg^{2+} is expected to form selenocysteine complexes with various stoichiometries such as HgL, HgL_2, Hg_2L_2, and Hg_3L_2 (where L represent the selenocysteine ligand), either in solution or in the solid state.

Bis(alkylselenolato)mercury(II), $Hg(SeR)_2$ (R = Me, Et and ^{t}Bu), were synthesized by Arnold et al. (*72, 74*). $Hg(SeMe)_2$ and $Hg(SeEt)_2$ have two coordinate Hg, but $Hg(Se^{t}Bu)_2$ has a distorted-tetrahedral coordination for Hg (*135*). The complex $Hg(Se^{t}Bu)_2$ is isomorphous with its sulfur analog, but $Hg(SeMe)_2$ is polymeric and has a pseudo-tetrahedral geometry like $Hg(Se^{t}Bu)_2$ as Se atoms coordinate Hg atoms by forming a bridge. $[(HgCl(py)(SeEt)_4]$ complex contains a cyclic (-Hg-SeEt-) ring system, with Hg atoms bridged by Se atoms and having pseudo-tetrahedral coordination systems. $[HgCl(py)_{0.5}(Se^{t}Bu)_4]$ is isomorphous, based on an eight-membered ring of alternating Hg and Se atoms. These HgCl(SeR) pyridinates have structures related to analogous thiolates, i.e., a distorted tetrahedral geometry for Hg. A comparison among the Hg-Se bond distances with those of Hg-S in the comparable analogs affirmed the previous findings that the Hg-Se bond is smaller in length and hence stronger than that of Hg-S (*74*). Inorganic Hg may also form compounds in the form of Hg-Se-SR, Se-Hg-SR.

3.4 $(HgSe)_n$-SelP

A particularly interesting inorganic Hg compound with Se in biological systems is the HgSe clusters bound to SelP. SelP is the major selenoprotein in the plasma (and hence the name "P" in "SelP") whose structure and many unusual properties have yet to be elucidated (*136*). It is the only selenoprotein that has multiple selenocysteine residues; human and rat SelP have ten selenocysteine, one in the N-terminal domain, and nine in the C-terminal domain. SelP is synthesized in the liver and delivers Se to certain other organs and tissues, but there is evidence that the brain synthesizes its own pool of selenoproteins (*137*).

$(HgSe)_n$-SelP was first reported by Yoneda and Suzuki (*138*) following administration of high doses of $HgCl_2$ and selenite to rats. By adding selenite and $HgCl_2$ to blood serum spiked with glutathione, they further established that selenite was first reduced to selenide, followed by reaction with Hg^{2+} to produce $(HgSe)_n$ clusters which are then bound to SelP. This binding is rather unusual because SelP seems to be the only plasma protein to bind the $(HgSe)_n$ clusters (*136*), and because the binding only occurs when $HgCl_2$ and SeO_3^{2-} were administrated simultaneously; administration of $HgCl_2$ or selenite alone did not result in its binding to SelP.

The details of the binding mechanism between $(HgSe)_n$ and SelP remain to be elucidated. Despite the abundance of thiol and selenol groups on SelP, the observation that SelP only binds $(HgSe)_n$ but not Hg^{2+} suggests that the $(HgSe)_n$-SelP bonding is not via the thiol or selenol groups (*139*). Instead, Suzuki et al. (*139*) proposed that the binding is due to an intramolecular ionic interaction. The basis for this hypothesis is that there is a large amount of amino acid residues with basic functional groups (possible

cationic centers) and acidic functional groups (possible anionic centers) in SelP. This gives rise to an intramolecular ionic interaction between the cationic and anionic centers. The formation of ionic bonds may have masked the thiol and selenol groups, which could explain why they do not directly bind with Hg^{2+}. The unit $(HgSe)_n$ complex is proposed to break and bind to the ionic bond between the cationic and anionic centers, with the cationic centers composed of imidazolyl groups of histidinyl residues being the primary binding sites for the $(HgSe)_n$ complex. Suzuki et al. (*139*) further suggested the complex is in the form of $\{(HgSe)_n\}_m$-SelP, where n is the number of Hg-Se complexes (~100) and m the number of binding sites ($\leq$ 35) in SelP. The (HgSe)-SelP is thought to be the precursor of the crystalline HgSe(s) observed in the liver and kidneys of marine mammals (*102*) (see equation 9).

By administrating $HgCl_2$ and selenite in rabbit plasma in vitro and comparing its extended x-ray absorption fine structure (EXAFS) spectrum with a laboratory synthetic analog involving $HgCl_2$, Na_2SeO_3, and GSH, Gailer et al. (*140*) provided further evidence for the presence of $(HgSe)_n$ in the plasma. However, they suggested a different structure and bonding mechanism to the SelP. Since Hg speciation in the blood plasma is dominated by Hg-thiol species which render Hg^{2+} essentially non-existing under physiological conditions, the authors proposed that selenide, once produced from selenite reduction, binds with albumin-bound Hg to form a $(HgSe)_n$ core with both Hg and Se being 4-coordinate in a probably zincblende-like structure. At the surface of the core, glutathione (or other thiol) molecules are attached via either Se or Hg atoms to make the $(HgSe)_n$ core water soluble. When this entity approaches SelP, which is rich in cysteine and selenocysteine molecules, it is plausible that two GSH molecules may be stripped off

the $(HgSe)_n$ core and two covalent bonds formed between the $(HgSe)_n$ core and SelP, a reaction which is entropically favoured. The formation of the Hg-Se-S bond was indeed confirmed by the EXAFS, but this hypothesis does not explain why SelP does not bind with Hg^{2+}.

A recent study found that the Hg in serum of Hg miners was mainly associated with protein fractions containing SelP and GPx and that the percentage of Hg bound to SelP increased with increasing serum Hg concentrations (*49*). The authors suggested that direct binding of Hg to the selenol groups of SelP is possible, particularly at higher Hg exposure concentrations.

3.5 Biominerals $HgSe_xS_{1-x}(s)$ $(0 \leq x \leq 1)$

Among all the possible Hg-Se compounds, HgSe(s) is the only one whose in vivo existence has been unambiguously confirmed by scanning or transmission electron microscopy (SEM or TEM) and X-ray microanalysis (*84*, *89*, *90*), and by XANES (*87*). Based on an operational definition as the insoluble Hg fraction after aggression extractions (*102*, *141*), HgSe(s) was reported to account for up to 50% of total Hg in the liver of ringed seals (*141*), and northern fur seals and albatrosses (*102*); a lower percentage was found in the liver of Dall's porpoises (17%) (*102*).

Several pathways can result in the formation of HgSe(s) in biological systems. The first involves the direct reaction between Hg^{2+} (or its complexes) and HSe^-:

$$Hg^{2+} + HSe^- \longrightarrow HgSe(s, \text{tiemannite}) + H^+;\ \log K_{sp,\,HgSe(s)} = 50.5 \qquad (8)$$

The second pathway is via the degradation of $(MeHg)_2Se(s)$ (see Eqn. 4 or 7). The third pathway could be via the dissociation of $(HgSe)_n$-SelP

$$(HgSe)_n\text{-SelP} \longrightarrow n\ HgSe(s) + SelP \qquad (9)$$

The relative importance of these three pathways is unknown, though HgSe(s) granules that are commonly observed in the liver of marine mammals are thought to be a biomineralization product following the demethylation of MeHg as mentioned earlier.

Pure HgSe(s), tiemannite, has the zincblende structure with all atoms tetrahedrally coordinated and a Hg-Se bond length of 2.63 Å (*142*). The biomineral HgSe(s) as observed in the liver of marine mammals, however, is unlikely to be present as pure tiemannite, due to the presence of usually much higher concentration of sulfide in biological systems which would produce HgS(s) as well. As metacinnabar and tiemannite are isostructural (*142*), they are more likely to co-exist as a mixture or a solid solution in the form of $HgSe_xS_{1-x}(s)$ (x=0-1; also known as onofrite) as commonly observed in ore deposits (*142*). In the laboratory, ternary $HgSe_xS_{1-x}$ colloids have been shown to be formed quantitatively by mixing $HgCl_2$ with sulfide and selenide at the desired molar ratios (*143*). The presence of $HgSe_xS_{1-x}(s)$ has indeed been confirmed in the liver of striped dolphin by TEM and X-ray microanalysis (*144*), and in the liver of blackfooted albatross by XANES (*87*).

Although soluble in toluene or chloroform, the solubilities of HgSe(s) and HgS(s) in aqueous solution are extremely small, with a log K_{sp} of 50.5 (see Eq. (8)) and 39.1 respectively. Therefore, $HgSe_xS_{1-x}(s)$ is essentially chemically and toxicologically inert, and represents the ultimate metabolic product of Hg and Se. The cumulative precipitation of $HgSe_xS_{1-x}$ granules over time thus provides a plausible explanation of why Hg body burden in many marine mammals increases all over the life span of the individual without reaching an equilibrium (*84*, *88*).

4. Gaps and Perspectives

Intensive studies over the past 60 years on the toxicity of Hg and Se have shed much light on the widespread Hg-Se antagonism. However, a few critical gaps remain for a full understanding of the antagonism at the molecular level.

First, what is ultimately responsible for the toxicity of Hg and MeHg? At molecular level Hg(II) and MeHg are both toxic. The differences lie in the uptake route (MeHg can readily cross the blood-brain barrier and inorganic Hg(II) does not) and in the binding affinity (Hg^{2+} has a much stronger binding affinity toward –SH sites in biological systems than $MeHg^{+}$). Therefore, should Hg(II) be present in the brain (either by MeHg demetylation or by Hg^0 oxidation), it would be much more neurotoxic than MeHg. In addition, the toxicity of MeHg could also be attributed to the CH_3 radicals produced by homolysis or to Se deficiency. The validity and relative importance of these different modes of toxic action remain to be determined.

The recent discovery of the binding between $(HgSe)_n$ clusters and SelP is exciting. With abundant –SH and –SeH groups, it remains a mystery that SelP only binds $(HgSe)_n$ clusters but not Hg^{2+} (*139*). The hypotheses of an intra-molecular ionic bonding (*139*) and of glutathione-moieties on the $(HgSe)_n$ core (*56, 140*) are extraordinary in bioinorganic chemistry, and need to be further examined by additional lines of evidence. The significance (or lack thereof) of the role of BMSe also needs to be established, as it could potentially provide a chemical pathway for Se-aided MeHg demethylation (Eqns 4-7). Although indirect evidence has suggested the in vivo presence of BMSe, direct analytical evidence is lacking due to its instability.

Another major knowledge gap in the Hg-Se antagonism is that much of the literature studies have been done with laboratory animals under laboratory exposure scenarios. The animals have been fed or directly injected with high doses of Hg (MeHg) and/or Se, often simultaneously. While acute high dosing of Hg or Se can happen accidentally in the real world (e.g., the MeHg case in Iraq), exposure to Hg or Se is usually chronic and at doses that are much lower than those used in the experimental studies. Of particular note is that simultaneous dosing of equimolar Se and Hg (or MeHg) rarely occurs outside the laboratory (*136*). Furthermore, the chemical forms commonly used in the laboratory experiments (e.g., $HgCl_2$, MeHgCl, sodium selenite) are not the forms the organisms (including humans) are exposed to. For example, Se in most human diets is present in organic forms such as selenomethionine, and MeHg in seafood that humans consume is dominated by MeHg-thiols (*65, 66*). These beg the question as to which extent the results from the laboratory-based studies can be extrapolated to the real world conditions with confidence.

These critical knowledge gaps and the often contradictory experimental results in the literature suggest that further mechanistic studies are critically needed to establish a molecular understanding of the Hg-Se antagonism. Among the most important is the gathering of direct analytical evidences to confirm or verify the possible interaction and subsequent formation of Hg-Se complexes in the biological systems (see Figure 2.2). So far the only Hg-Se compound that has been unambiguously identified in vivo is $HgSe_xS_{1-x}$. Recent development in synchrotron-based X-ray absorption spectrometric methods (e.g., EXAFS, XANES) and in hyphenated mass spectrometric techniques (e.g., HPLC/GC-ICP/ESI-MS) has opened a new horizon toward the identification and

quantification of possible Hg-Se complexes in vivo and in vitro (*65, 66, 140*). However, preservation of different chemical species during sample preparation and analysis, and the sensitivity and resolution of the detector are often the bottleneck, particularly when dealing with real-world samples (*66*).

With the aid of new analytical techniques and computational approaches, thermodynamic and kinetic constants of the key in vivo Hg-Se compounds need to be determined under physiological conditions. In vivo studies under "normal" scenarios (e.g., chronic exposure to realistic doses of Hg (or MeHg) and/or Se) should be encouraged to shed light on physiologically relevant processes, and to verify to which extent the laboratory based studies can be extended to real world situations. Such molecular level understanding of the Hg-Se antagonism is a prerequisite for the development of detoxification and remediation strategies aiming to regulate Hg and Se levels in biological systems.

Acknowledgment: Funding of this research was provided by the Natural Sciences and Engineering Council of Canada (NSERC). M.A.K.K. was supported by a NSERC Postgraduate Student – Doctoral Fellowship (PGS-D). We thank M. Hanson and three anonymous reviewers for their thorough and constructive comments on an earlier draft of this paper.

References

(1) Mergler, D., Anderson, H. A., Chan, L. H. M., Mahaffey, K. R., Murray, M., Sakamoto, M. and Stern, A. H. (2007) Methylmercury exposure and health effects in humans: a worldwide concern. *Ambio 36*, 3-11.

(2) WHO. (1990) Methylmercury, In *Environmental Health Criteria 101*, International Programme on Chemical Safety, World Health Organization, Geneva.

(3) Harada, M. (1995) Minamata disease: methylmercury poisoning in Japan caused by environmental pollution. *Crit. Rev. Toxicol. 25*, 1-24.

(4) McAlpine, D. and Araki, S. (1958) Minamata disease. An unusual neurological disorder caused by contaminated fish. *Lancet 2*, 629-631.

(5) Bakir, F., Damluji, S. F., Amin-Zaki, L., Murtadha, M., Khalidi, A., al-Rawi, N. Y., Tikriti, S., Dahahir, H. I., Clarkson, T. W., Smith, J. C. and Doherty, R. A. (1973) Methylmercury poisoning in Iraq. *Science 181*, 230-241.

(6) Gallagher, P. J. and Lee, R. L. (1980) The role of biotransformation in organic mercury neurotoxicity. *Toxicology 15*, 129-134.

(7) Zalups, R. K. and Barfuss, D. W. (1993) Intrarenal distribution of inorganic mercury and albumin after coadministration. *J. Toxicol. Environ. Health 40*, 77-103.

(8) Zalups, R. K. and Barfuss, D. W. (1996) Nephrotoxicity of inorganic mercury co-administered with L-cysteine. *Toxicol. 109*, 15-29.

(9) Gritzka, T. L. and Trump, B. F. (1968) Renal tubular lesions caused by mercuric chloride. Electron microscopic observations: degeneration of the pars recta. *Am. J. Pathol. 52*, 1225-1277.

(10) Madsen, K. M. (1980) Mercury accumulation in kidney lysosomes of proteinuric rats. *Kid. Inter. 18*, 445-453.

(11) Shenker, B. J., Mayro, J. S., Rooney, C., Vitale, L. and Shapiro, I. M. (1993) Immunotoxic effects of mercuric compounds on human lymphocytes and monocytes. IV. Alterations in cellular glutathione content. . *Immunopharmacol. Immunotoxicol. 15*, 273-290.

(12) Gstraunthaler, G., Pfaller, W. and Kotanko, P. (1983) Glutathione depletion and in vitro lipid peroxidation in mercury or maleate induced acute renal failure. *Biochem. Pharmacol. 32*, 2969-2972.

(13) Lund, B. O., Miller, D. M. and Woods, J. S. (1993) Studies on Hg(II)-induced H_2O_2 formation and oxidative stress in vivo and in vitro in rat kidney mitochondria. *Biochem. Pharmacol. 45*, 2017-2024.

(14) Friberg, L. and Mottet, N. K. (1989) Accumulation of methylmercury and inorganic mercury in the brain. *Biol. Trace Elem. Res. 21*, 201-206.

(15) Aschner, M. and Aschner, J. L. (1990) Mercury neurotoxicity: mechanisms of blood-brain barrier transport. *Neurosci. Biobehav. Rev. 14*, 169-176.

(16) Simmons-Willis, T. A., Koh, A. S., Clarkson, T. W. and Ballatori, N. (2002) Transport of a neurotoxicant by molecular mimicry: the methylmercury-L-cysteine complex is a substrate for human L-type large neutral amino acid transporter (LAT) 1 and LAT2. *Biochem. J. 367*, 239-246.

(17) Mokrzan, E. M., Kerper, L. E., Ballatori, N. and Clarkson, T. W. (1995) Methylmercury-thiol uptake into cultured brain capillary endothelial cells on amino acid system L. *J. Pharmacol. Exp. Ther. 272*, 1277-1284.

(18) Kerper, L. E., Ballatori, N. and Clarkson, T. W. (1992) Methylmercury transport across the blood-brain barrier by an amino acid carrier. *Am. J. Physiol. 262*, R761-R765.

(19) Atchison, W. D. and Hare, M. F. (1994) Mechanisms of methylmercury-induced neurotoxicity. *FASEB J. 8*, 622–629.

(20) Kim, Y.-J., Chai, Y.-G. and Ryu, J.-C. (2005) Selenoprotein W as molecular target of methylmercury in human neuronal cells is down-regulated by GSH depletion. *Biochem. Biophys. Res. Commun. 330*, 1095-1102.

(21) Watanabe, C., Yin, K., Y., K. and Satoh, H. (1999) In utero exposure to methylmercury and Se deficiency converge on the neurobehavioral outcome in mice. *Neurotoxicol. Teratol. 21*, 83-88.

(22) Myers, G. J. and Davidson, P. W. (1998) Prenatal methylmercury exposure and children: neurologic, developmental, and behavioral research. *Environ. Health Perspect. 106*, 841-847.

(23) Iyengar, G. V. and Rapp, A. S. O. (2001) Human placenta as a “duel” biomarker for monitoring fatal and maternal environment with special reference to potentially toxic trace elements. Part 3: toxic trace elements in placenta and placenta as a biomarker for these elements. *Sci. Total Environ. 280*, 221-238.

(24) Grandjean, P., Weihe, P., White, R. F., Debes, F., Araki, S., Yokoyama, K., Murata, K., Sorensen, N., Dahl, R. and Jorgensen, P. J. (1997) Cognitive deficit in

7-year-old children with prenatal exposure to methylmercury. *Neurotoxicol. Teratol. 19*, 417-428.

(25) Harada, M. (1978) Congenital Minamata disease: intrauterine methylmercury poisoning. *Teratol. 18*, 285-288.

(26) Gilbert, S. G. and Grant-Webster, K. S. (1995) Neurobehavioral effects of developmental methylmercury exposure. *Environ. Health Perspect. 103*, 135-142.

(27) Choi, A. L. and Grandjean, P. (2008) Methylmercury exposure and health effects in humans. *Environ. Chem. 5*, 112-120.

(28) Salonen, J. T., Seppanen, K., Nyyssonen, K., Korpela, H., Kauhanen, J., Kantola, M., Tuomilehto, J., Esterbauer, H., Tatzber, F. and et al. (1995) Intake of mercury from fish, lipid peroxidation, and the risk of myocardial infarction and coronary, cardiovascular, and any death in eastern Finnish men. *Circulation 91*, 645-655.

(29) Sakamoto, M., Nakano, A. and Akagi, H. (2001) Declining Minamata male birth ratio associated with increased male fetal death due to heavy methylmercury pollution. *Environ. Res. 87*, 92-98.

(30) Itai, Y., Fujino, T., Ueno, K. and Motomatsu, Y. (2004) An epidemiological study of the incidence of abnormal pregnancy in areas heavily contaminated with methylmercury. *Environ. Sci. 11*, 83-97.

(31) Pařízek, J. and Ošádalová, I. (1967) The protective effect of small amounts of selenite in sublimate intoxication. *Experientia 23*, 142-143.

(32) Ganther, H. E., Goudie, C., Sunde, M. L., Kopecky, M. J. and Wagner, P. (1972) Selenium: relation to decreased toxicity of methylmercury added to diets containing tuna. *Science 175*, 1122-1124.

(33) Belzile, N., Wu, G.-J., Chen, Y.-W. and Appanna, V. D. (2006) Detoxification of selenite and mercury by reduction and mutual protection in the assimilation of both elements by *Pseudomonas fluorescens*. *Sci. Total Environ. 367*, 704-714.

(34) Belzile, N., Chen, Y.-W., Gunn, J. M., Tong, J., Alarie, Y., Delonchamp, T. and Lang, C. Y. (2006) The effect of selenium on mercury assimilation by freshwater organisms. *Can. J. Fish. Aquat. Sci. 63*, 1-10.

(35) Chen, Y.-W., Belzile, N. and Gunn, J. M. (2001) Antagonistic effect of selenium on mercury assimilation by fish populations near Sudbury metal smelters? *Limnol. Oceanogr. 46*, 1814-1818.

(36) Sell, J. L. and Horani, F. G. (1976) Influence of selenium on toxicity and metabolism of methylmercury in chicks and quail. *Nutr. Rep. Int. 14*, 439-447.

(37) Hill, C. H. (1974) Reversal of selenium toxicity in chicks by mercury, copper, and cadmium. *J. Nutr. 104*, 593-598.

(38) Hoffman, D. J. and Heinz, G. H. (1998) Effects of mercury and selenium on glutathione metabolism and oxidative stress in mallard ducks. *Environ. Toxicol. Chem. 17*, 161-166.

(39) Newland, M. C., Reed, M. N., LeBlanc, A. and Donlin, W. D. (2006) Brain and blood mercury and selenium after chronic and developmental exposure to methylmercury. *Neurotoxicol. 27*, 710-720.

(40) Chmielnicka, J., Komsta-Szumska, E. and Jedrychowski, R. (1979) Organ and subcellular distribution of mercury in rats as dependent on the time of exposure to sodium selenite. *Environ. Res. 20*, 80-86.

(41) Beyrouty, P. and Chan, H. M. (2006) Co-consumption of selenium and vitamin E altered the reproductive and developmental toxicity of methylmercury in rats. *Neurotoxicol. Teratol. 28*, 49-58.

(42) Fredriksson, A., Gardlund, A. T., Bergman, K., Oskarsson, A., Ohlin, B., Danielsson, B. and Archer, T. (1993) Effects of maternal dietary supplementation with selenite on the postnatal development of rat offspring exposed to methyl mercury in utero. *Pharmacol. Toxicol. 72*, 377-382.

(43) Naganuma, A., Ishii, Y. and Imura, N. (1984) Effect of administration sequence of mercuric chloride and sodium selenite on their fates and toxicities in mice. *Ecotoxicol. Environ. Safety 8*, 572-580.

(44) Nishikido, N., Furuyashiki, K., Naganuma, A., Suzuki, T. and Imuram, H. (1987) Maternal selenium deficiency enhances the fetolethal toxicity of methyl mercury. *Toxicol. Appl. Pharmacol. 88*, 322-328.

(45) Hansen, J. C., Kristensen, P. and Al-Masri, S. N. (1981) Mercury/selenium interaction. A comparative study on pigs. *Nord. Vet. Med. 33*, 57-64.

(46) Koeman, J. H., Peeters, W., Koudstaal-Hol, C., Tijoe, P. S. and de Goeij, J. J. M. (1973) Mercury-selenium correlations in marine mammals. *Nature 245*, 385-386.

(47) Koeman, J. H., van de Ven, W. S. M., de Goeij, J. J. M., Tijoe, P. S. and van Haaften, J. L. (1975) Mercury and selenium in marine mammals and birds. *Sci. Total Environ. 3*, 279-287.

(48) Kosta, L., Byrne, A. R. and Zelenko, V. (1975) Correlation between selenium and mercury in man following exposure to inorganic mercury. *Nature 254*, 238-239.

(49) Chen, C., Yu, H., Zhao, J., Li, B., Qu, L., Liu, S., Zhang, P. and Chai, Z. (2006) The roles of serum selenium and selenoproteins on mercury toxicity in environmental and occupational exposure. *Environ. Health Perspect. 114*, 297-301.

(50) Huckabee, J. W. and Griffith, N. A. (1974) Toxicit of mercury and selenium to the eggs of carp (*Cyprinus carpio*). *Trans. Am. Fish. Soc. 103*, 822-825.

(51) Birge, W. J., Roberts, O. W. and Black, J. A. (1976) Toxicity of metal mistures to chick embryos. *Bull. Environ. Contam. Toxicol. 16*, 314-318.

(52) Sukra, Y., Sastrohadinoto, S., Haeruman, H. H. J. and Bird, H. R. (1976) Effect of selenium and mercury on survival of chick embryos. *Poult. Sci. 55*, 1423-1428.

(53) Glickstein, N. (1978) Acute Toxicity of Mercury and Selenium to *Crassostrea gigas* Embryos and *Cancer magister* Larvae. *Mar. Biol. 49*, 113-117.

(54) Palmisano, F., Cardellicchio, N. and Zambonin, P. G. (1995) Speciation of mercury in dolphin liver: a two-stage mechanism for the demethylation accumulation process and role of selenium. *Mar. Environ. Res. 40*, 109-121.

(55) Yang, D.-Y., Chen, Y.-W., Gunn, J. M. and Belzile, N. (2008) Selenium and mercury in organisms: interactions and mechanisms. *Environ. Rev. 16*, 71-92.

(56) Gailer, J. (2007) Arsenic-selenium and mercury-selenium bonds in biology. *Coord. Chem. Rev. 251*, 234-254.

(57) Rais, D. and Vilar, R. (2006) Mercury: organometallic chemistry, In *Encyclopedia of Inorganic Chemistry*, John Wiley and Sons.

(58) Bock, A. (2006) Selenium proteins containing selenocysteine, In *Encyclopedia of Inorganic Chemistry*, John Wiley and Sons.

(59) Back, T. G. (2006) Selenium: organoselenium chemistry, In *Encyclopedia of Inorganic Chemistry*, John Wiley and Sons.

(60) Fitzgerald, W. F., Lamborg, C. H. and Hammerschmidt, C. R. (2007) Marine biogeochemical cycling of mercury. *Chem. Rev. 107*, 641-662.

(61) Pelletier, E. (1985) Mercury-selenium interactions in aquatic organisms: a review. *Mar. Environ. Res. 18*, 111-132.

(62) Cuvin-Aralar, M. L. A. and Furness, R. W. (1991) Mercury and selenium interaction: a review. *Ecotoxicol. Environ. Saf. 21*, 348-364.

(63) Skerfving, S. (1978) Interaction between selenium and methylmercury. *Environ. Health Perspect. 25*, 57-65.

(64) Reid, R. S. and Rabenstein, D. L. (1981) Nuclear magnetic resonance studies of the solution chemistry of metal complexes. XVII. Formation constants for the complexation of methylmercury by sulfhydryl-containing amino acids and related molecules. *Can. J. Chem. 59*, 1505-1514.

(65) Harris, H. H., Pickering, I. J. and George, G. N. (2003) The chemical form of mercury in fish. *Science 301*, 1203.

(66) Lemes, M. and Wang, F. (2009) Methylmercury speciation in fish muscle by HPLC-ICP-MS following enzymatic hydrolysis. *J. Anal. At. Spectrom. 24*, 663-668.

(67) Rabenstein, D. L. (1978) The chemistry of methylmercury toxicology. *J. Chem. Edu. 55*, 292-296.

(68) Rabenstein, D. L. and Evans, C. A. (1978) The mobility of methylmercury in biological systems. *Bioinorg. Chem. 8*, 107-114.

(69) Rabenstein, D. L., Isab, A. A. and Reid, R. S. (1982) A proton nuclear magnetic resonance study of the binding of methylmercury in human erythrocytes. *Biochim. Biophys. Acta 720*, 53-64.

(70) Rabenstein, D. L. and Reid, R. S. (1984) Nuclear magnetic resonance studies of the solution chemistry of metal complexes. 20. ligand-exchange kinetics of methylmercury(II)-thiol complexes. *Inorg. Chem. 23*, 1246-1250.

(71) Sugiura, Y., Tamai, Y. and Tanaka, H. (1978) Selenium protection against mercury toxicity: High binding affinity of methylmercury by selenium-containing ligands in comparision with sulphur-contaning ligands. *Bioinorg. Chem. 9*, 167-180.

(72) Arnold, A. P. and Canty, A. J. (1981) Synthesis, structure and spectroscopic studies of mercury(II) selenolates and MeHgSeBu^{t}. *Inorg. Chim. Acta 55*, 171-176.

(73) Carty, A. J., Malone, S. F., Taylor, N. J. and Canty, A. J. (1983) Synthesis, spectroscopic, and x-ray structural characterization of methylmercury-D,L-selenocysteinate monohydrate, a key model for the methylmercury(II)-selenoprotein interaction. *J. Inorg. Biochem. 18*, 291-300.

(74) Arnold, A. P., Canty, A. J., Skelton, B. W. and White, A. H. (1982) Mercury(II) selenolates. Crystal structures of polymeric $Hg(SeMe)_2$ and the tetrameric pyridinates $[\{HgCl(py)(SeEt)\}_4]$ and $[\{HgCl(py)_{0.5}[Se(CMe_3)]\}_4]$ *J. Chem. Soc. Dalton Trans. 3*, 607-613.

(75) Arnold, A. P., Tan, K. S. and Rabenstein, D. L. (1986) Nuclear magnetic resonance studies of the solution chemistry of metal complexes. 23. Complexation

of methylmercury by selenohydryl-containing amino acids and related molecules. *Inorg. Chem. 25*, 2433-2437.

(76) Canty, A. J., Carty, A. J. and Malone, S. F. (1983) Methylmercury(II) selenolates. Synthesis and characterization of MeHgSeMe and MeHgSePh and ^{1}H and ^{199}Hg NMR studies of ligand exchange in methylmercury(II) thiolates and selenolates, including amino acid complexes. *J. Inorg. Biochem. 19*, 133-142.

(77) Taylor, N. J., Wong, Y. S., Chieh, P. C. and Carty, A. J. (1975) Syntheses, x-ray crystal structure, and vibrational spectra of L-cysteinatomethylmercury(II) monohydrate. *J. Chem. Soc. Dalton Trans. Inorg. Chem.*, 438-442.

(78) Compeau, G. C. and Bartha, R. (1985) Sulfate-reducing bacteria: principal methylators of mercury in anoxic estuarine sediment. *Appl. Environ. Microbiol. 50*, 498-502.

(79) Ekstrom, E. B., Morel, F. M. M. and Benoit, J. M. (2003) Mercury methylation independent of the acetyl-coenzyme: A pathway in sulfate-reducing bacteria *Appl. Environ. Microbiol. 69*, 5414-5422.

(80) Berlin, M., Carlson, J. and Norseth, T. (1975) Dose-dependence of methylmercury metabolism. *Arch. Environ. Health 30*, 307-313.

(81) Magos, L., Bakir, F., Clarkson, T. W., Al-Jawad, A. M. and Al-Softi, M. H. (1976) Tissue levels of mercury in autopsy specimens of liver and kidney. *Bull. WHO 53*, 93-96.

(82) Lockhart, W. L., Stern, G. A., Wagemann, R., Hunt, R. V., Metner, D. A., DeLaronde, J., Dunn, B., Stewart, R. E. A., Hyatt, C. K., Harwood, L. and Mount, K. (2005) Concentrations of mercury in tissues of beluga whales (*Delphinapterus*

leucas) from several communities in the Canadian Arctic from 1981 to 2002. *Sci. Total Environ. 351/352*, 391-412.

(83) Vahter, M. E., Mottet, N. K., Friberg, L. T., Lind, S. B., Charleston, J. S. and Burbacher, T. M. (1995) Demethylation of methyl mercury in different brain sites of *Macaca fascicularis* monkeys during long-term subclinical methyl mercury exposure. *Toxicol. Appl. Pharmacol. 134*, 273-284.

(84) Martoja, R. and Berry, J. P. (1980) Identification of tiemannite as a probable product of demethylation of mercury by selenium in cetaceans. a complement to the scheme of the biological cycle of mercury. *Vie Milieu 30*, 7-10.

(85) Storelli, M. M., Ceci, E. and Marcotrigiano, G. O. (1998) Comparison of total mercury, methylmercury, and selenium in muscle tissues and in the liver of *Stenella coeruleoalba* (Meyen) and *Caretta caretta* (Linnaeus). *Bull. Environ. Contam. Toxicol. 61*, 541-547.

(86) Fang, S. C. (1974) Induction of carbon-mercury cleavage enzymes in rat liver by dietary selenite. *Res. Comm. Chem. Pathol. Pharmacol. 9*, 579-582.

(87) Arai, T., Ikemoto, T., Hokura, A., Terada, Y., Kunito, T., Tanabe, S. and Nakai, I. (2004) Chemical forms of mercury and cadmium accumulated in marine mammals and seabirds as determined by XAFS analysis *Environ. Sci. Technol. 38*, 6468-6474.

(88) Martoja, R. and Viale, D. (1977) Accumulation de granules de seleniure mercurique dans le foie d'odontocetes (Mammiferes, Cetaces): un mecanisme possible de detoxication du methylmercure par le selenium. *C. R. Hebd. Seanc. Acad. Sci. Paris D 285*, 109-112.

(89) Nigro, M. (1994) Mercury and selenium localization in macrophages of the striped dolphin, *Stenella coeruleoalba*. *J. Mar. Biol. Ass. UK 74*, 975-978.

(90) Nigro, M. and Leonzio, C. (1996) Intracellular storage of mercury and selenium in different marine vertebrates. *Mar. Ecol. Prog. Ser. 135*, 137-143.

(91) Rawson, A. J., Bradley, J. P., Teetsov, A., Rice, S. B., Haller, E. M. and Patton, G. W. (1995) A role for airborne particulates in high mercury levels of some cetaceans. *Ecotoxicol. Environ. Saf. 30*, 309-314.

(92) Palmisano, F., Cardellicchio, N. and Zambonin, P. G. (1995) Speciation of mercury in dolphin liver: a two-stage mechanism for the demethylation accumulation process and role of selenium. *Mar. Environ. Res. 40*, 1-12.

(93) Hoekstra, P. F., Braune, B. M., Elkin, B., Armstrong, F. A. J. and Muir, D. C. G. (2003) Concentrations of selected essential and non-essential elements in arctic fox (Alopex lagopus) and wolverines (Gulo gulo) from the Canadian Arctic. *Sci. Total Environ. 309*, 81-92.

(94) Vaal, M., van der Wal, J. T., Hoekstra, J. and Hermens, J. (1997) Variation in the sensitivity of aquatic species in relation to the classification of environmental pollutants. *Chemosphere 35*, 1311-1327.

(95) Hansen, J. C. and Pedersen, H. S. (1986) Environmental exposure to heavy metals in North Greenland. *Arc. Med. Res. 41*, 21-34.

(96) Hansen, J. C. (1988) Blood mercury concentrations in birthgiving Greenlandic women. *Arc. Med. Res. 47*, 175-178.

(97) Zhang, J., Wang, F., House, J. D. and Page, B. (2004) Thiols in wetland interstitial waters and their role in mercury and methylmercury speciation. *Limnol. Oceanogr. 49*, 2276-2286.

(98) Magos, L. and Webb, M. (1980) The interactions of selenium with cadmium and mercury. *Crit. Rev. Toxicol. 8*, 1-42.

(99) Clarkson, T. W. (1969) Isotope exchange methods in study of the biotransformation of organomercurial compounds in experimental animals, In *Chemical Fallout* (Miller, M. W. and Berg, G. G., Eds.) p 274, Charles C. Thomas, Springfield, Illinois.

(100) Burk, R. F., Foster, K. A., Greenfield, P. M. K. and Kiker, K. W. (1974) Binding of simultaneously administered inorganic selenium and mercury to rat plasmaprotein. *Proc. Soc. Exp. Biol. Med. 145*, 782-785.

(101) Yoneda, S. and Suzuki, K. T. (1997) Equimolar Hg-Se complex binds to selenoprotein P. *Biochem. Biophys. Res. Commun. 231*, 7-11.

(102) Ikemoto, T., Kunito, T., Tanaka, H., Baba, N., Miyazaki, N. and Tanabe, S. (2004) Detoxification mechanism of heavy metals in marine mammals and seabirds: Interaction of selenium with mercury, silver, copper, zinc, and cadmium in liver. *Arch. Environ. Contam. Toxicol. 47*, 402-413.

(103) Chen, R. W., Whanger, P. D. and Fang, S. C. (1974) Diversion of mercury binding in rat tissues by selenium: a possible mechanism of protection. *Pharmacol. Res. Commun. 6*, 571-579.

(104) Komsta-Szumska, E. and Chmielnicka, J. (1977) Binding of mercury and selenium in subcellular fractions of rat liver and kidneys following separate and joint administration. *Arch. Toxicol. 38*, 217-228.

(105) Naganuma, A. and Imura, N. (1980) Changes in distribution of mercury and selenium in soluble fractions of rabbit tissues after simultaneous administration. *Pharmacol. Biochem. Behav. 13*, 537-544.

(106) Burk, R. F., Jordan, H. E. J. and Kiker, K. W. (1977) Some effects of selenium status on inorganic mercury metabolism in the rat. *Toxicol. Appl. Pharmacol. 40*, 71-82.

(107) Balthrop, J., Wade, J. and Braddon-Galloway, S. (1986) Mercury distribution studies involving complexes of low-molecular weight thiols and methylmercury. *Bull. Environ. Contamin. Toxicol. 37*, 890-898.

(108) Ganther, H. E. (1978) Modification of methyl mercury toxicity and metabolism by selenium and vitamin E: Possible mechanisms. *Environ. Health Perspect. 25*, 71-76.

(109) Welsh, S. (1979) The protective effect of vitamin E and N,N'-diphenyl-p-phenylenediamine (DPPD) against methyl mercury toxicity in the rat. *J. Nutr. 109*, 1673- 1681.

(110) Sheline, J. and Schmidt-Nielsen, B. (1977) Methyl mercury-selenium: interaction in killifish, *Fundulus heteroclitus*, in *physiological responses of marine biota to pollutants* (Vemberg, F., Ed.) pp 119-130, Symposium, Milford, CN.

(111) Reilly, C. (2006) *Selenium in food and health*, Springer, New York.

(112) Raymond, L. J. and Ralston, N. V. C. (2004) Mercury: selenium interactions and health implications. *Seychelles Med. Den. J. 7*, 72-77.

(113) Schweizer, U. and Schomburg, L. (2006) Chapter 21. Selenium, selenoproteins and brain function, In *Selenium. Its Molecular Biology and Role in Human Health, Second Edition* (Hatfield, D. L., Berry, M. J. and Gladyshev, V. N., Eds.) pp 233-248, Springer, New York.

(114) Chang, L. W. and Suber, R. (1982) Protective effect of selenium on methyl mercury toxicity: a possible mechanism. *Bull. Environ. Contam. Toxicol. 29*, 285-289.

(115) Ganther, H. E. and Sunde, M. S. (1974) Effect of tune fish and selenium on the toxicity of methylmercury. A progress report. *J. Food Sci. 39*, 1-5.

(116) Wagemann, R. and Armstrong, F. A. J. (1988) Trace metal determination in animal tissues: an interlaboratory comparison. *Talanta 35*, 545-551.

(117) Haines, K. J. R., Evans, R. D. and O'Brien, M. (2004) Relationship between mercury and selenium in the brain of river otter (*Lutra canadensis*) and wild mink (*Mustela vison*) from Nova Scotia, Canada. *Mat. Geoenviron. 51*, 1028-1030.

(118) Naganuma, A., Satoh, H., Yamamoto, R., Suzuki, T. and Imura, N. (1979) Effect of selenium on determination of mercury in animal tissues. *Anal. Biochem. 98*, 287-292.

(119) Sumino, K., Yamamoto, R. and Kitamura, S. (1977) A role of selenium against methyl mercury toxicity. *Nature 268*, 73-74.

(120) Sumino, K., Yamamoto, R. and Kitamura, S. (1979) Mechanism of methylmercury release from bound type in bloodstream or tissues. *Biochem. Biophys. Res. Commun. 86*, 735-741.

(121) Naganuma, A. and Imura, N. (1980) Bis(methylmercuric) selenide as a reaction product from methylmercury and selenite in rabbit blood. *Res. Comm. Chem. Pathol. Pharmacol. 27*, 163-173.

(122) Magos, L., Webb, M. and Hudson, A. R. (1979) Complex formation between selenium and methylmercury. *Chem. -Biol. Interactions 28*, 359-362.

(123) Masukowa, T., Kito, H., Hayashi, M. and Iwata, H. (1982) Formation and possible role of bis(methylmercury) selenide in rats treated with methylmercury and selenite. *Biochem. Pharmacol. 31*, 75-78.

(124) Naganuma, A., Kojima, Y. and Imura, N. (1980) Interaction of methylmercury and selenium in mouse: formation and decomposition of bis(methylmercuric)selenide *Res. Comm. Chem. Pathol. Pharmacol. 30*, 301-316.

(125) Naganuma, A. and Imura, N. (1981) New method for Bis(methylmercury) selenide synthesis from methylmercuric chloride, sodium selenite and reduced glutathione. *Chemosphere 10*, 441-443.

(126) Prohaska, J. R. and Ganther, H. E. (1977) Interactions between selenium and methylmercury in rat brain. *Chem. Biol. Interact. 16*, 155-167.

(127) Craig, P. J. and Bartlett, P. D. (1978) The role of hydrogen sulphide in environmental transport of mercury. *Nature 275*, 635 - 637.

(128) Carty, A. J., Malone, S. F. and Taylor, N. J. (1979) The selenium-mercury interaction: synthesis, spectroscopic and x-ray structural studies of methylmercury-selenourea complexes. *J. Organometal. Chem. 172*, 201-211.

(129) Pelletier, E., Sauriol, F. and Wharf, I. (1987) Preparation and characterization of new organomercury(II)selenolates. *Inorg. Chim. Acta 138*, 99-101.

(130) Mills, B. J. and Lang, C. A. (1996) Differential distribution of free and bound glutathione and cyst(e)ine in human blood. *Biochem. Pharmacol. 52*, 401-406.

(131) Schecher, W. D. and McAvoy, D. C. (2003) MINEQL+: a chemical equilibrium program for personal computers - User's manual, Environmental Research Software, Hallowell, ME.

(132) Seppänen, K., Laatikainen, R., Salonen, J. T., Kantola, M., Lötjönen, S., Harri, M., Nurminen, L., Kaikkonen, J. and Nyyssönen, K. (1998) Mercury-binding capacity of organic and inorganic selenium in rat blood and liver. *Biol. Trace Elem. Res. 65*, 197-210.

(133) Martell, A. E. and Hancock, R. D. (1995) *Metal complexes in aqueous solutions*, Springer.

(134) Taylor, N. J. and Carty, A. J. (1977) Nature of Hg^{2+}-L-cysteine complexes implicated in mercury biochemistry. *J. Am. Chem. Soc 99*, 6143-6145.

(135) Kunchur, N. R. (1964) Polymer structure of mercury tert-butyl mercaptide. *Nature 204*, 468.

(136) Burk, R. F. and Hill, K. E. (2005) Selenoprotein P: An extracellular protein with unique physical characteristics and a role in selenium homeostasis *Ann. Rev. Nutr. 25*, 215-235.

(137) Gladyshev, V. N. (2006) Chapter 9. Selenoproteins and selenoproteomes, in *selenium. its molecular biology and role in human health, second edition* (Hatfield, D. L., Berry, M. J. and Gladyshev, V. N., Eds.) pp 99-110, Springer, New York.

(138) Yoneda, S. and Suzuki, K. T. (1997) Detoxification of mercury by selenium by binding of equimolar Hg-Se complex to a specific plasma protein. *Toxicol. Appl. Pharmacol. 143*, 274-280.

(139) Suzuki, K. T., Sasakura, C. and Yoneda, S. (1998) Binding sites for the (Hg-Se) complex on selenoprotein P. *Biochim. Biophys. Acta 1429*, 102-112.

(140) Gailer, J., George, G. N., Pickering, I. J., Madden, S., Prince, R. C., Yu, E. Y., Denton, M. B., Younis, H. S. and Aposhian, H. V. (2000) Structure basis of the antagonism between inorganic mercury and selenium in mammals. *Chem. Res. Toxicol. 13*, 1135-1142.

(141) Wagemann, R., Trebacz, E., Boila, G. and Lockhart, W. L. (2000) Mercury species in the liver of ringed seals. *Sci. Total Environ. 261*, 21-32.

(142) Earley, J. W. (1950) Description and synthesis of the selenide minerals. *Am. Minerol. 35*, 337-364.

(143) Kuno, M., Higginson, K. A., Qadri, S. B., Yousuf, M., Lee, S. H., Davis, B. L. and Mattoussi, H. (2003) Molecular clusters of binary and ternary mercury chalcogenides: Colloidal synthesis, characterization, and optical spectra *J. Phys. Chem. B. 107*, 5758-5767.

(144) Ng, P. S., Li, H., Matsumoto, K., Yamazaki, S., Kogure, T., Tagai, T. and Nagasawa, H. (2001) Striped dolphin detoxificates mercury as insoluble Hg(S, Se) in the liver. *Proc. Japan. Acad. Ser. B 77*, 178-183.

Preface to Chapter 3

This chapter is based on the following manuscript published in the journal "*Dalton Transactions*". Full citation of the paper is as follows:

> Khan, M. A. K.; Asaduzzaman, A. M.; Schreckenbach, G.; Wang, F. Synthesis, Characterization and Structures of Methylmercury Complexes with Selenoamino Acids. *Dalton Transac.* **2009**, 5766-5772.

This manuscript focuses on the synthesis and characterization of four methylmercury selenoamino acid (MeHgSeAA) complexes to study their molecular structures and similarity – dissimilarity with their sulphur counter parts. X-ray crystallography and quantum chemical calculations are used to show that all the complexes are chemically and structurally similar to their counterparts with slightly stronger binding affinity of Hg to Se than to S which may account for the antagonism and toxicity respectively in biological systems. This chapter expands our knowledge about MeHgSeAA complexes from the point where only one MeHgSeAA complex was known.

Chapter 3: Synthesis, Characterization and Structures of Methylmercury Complexes with Selenoamino Acids

Summary

Four new methylmercury-selenoamino acid complexes were synthesized, including methylmercury-$_{L}$-selenoglutathionate, methylmercury-$_{D,L}$-selenopenicillaminate, and two methylmercury-$_{L}$-selenomethioninate complexes (one via a Hg-Se bonding and the other Hg-N bonding). All the complexes were characterized by NMR (^{1}H, ^{13}C, ^{77}Se and ^{199}Hg), FT-IR and mass spectra. Their molecular structures were established by single crystal X-ray crystallography (for the Hg-N bonding methylmercury-$_{L}$-selenomethioninate) and by quantum mechanical calculations using Gaussian-03 with the hybrid functional B3LYP/SDD. All four complexes were found to chemically and structurally resemble their sulfur analogues, with a slightly stronger binding affinity of Hg to Se than to S, suggesting chemical and structural mimicry might play a role in methylmercury-selenium antagonism in biological systems.

Introduction

Mercury (Hg) is a global contaminant and has received much scientific attention since the outbreak of the Minamata disease in the 1950s (*1, 2*). Of most concern is monomethylmercury (MeHg) which is a developmental neurotoxin (*1, 2*); it (presumably in the form of a $_{L}$-cysteine complex (*3*)) can cross the blood-brain barrier and the placental barrier, irreversibly binds to high-molecular weight, –SH containing biomolecules in astrocytes, and results in neuronal impairment, injury and death (*4*). The toxicity of MeHg in animals including humans is known to be alleviated by selenium (Se) (*5, 6*). Though the mechanism for this MeHg-Se antagonism is not yet fully understood, one of the most plausible pathways is via the formation of MeHg complexes with Se-containing compounds, particularly selenoamino acids (*7*). Due to the chemical similarity, Se can be incorporated in place of sulfur in amino acids, and can interact with MeHg. The MeHg-Se antagonism could then be explained if the MeHg-selenoamino acid complexes are less toxic and/or act as intermediates for further detoxification. The former seems to be the case with MeHg-selenocysteinate in which the Hg-Se bonding was found to be marginally stronger than its sulfur analogue (*8*). However, MeHg-selenocystainate is the only MeHg-selenoamino acid compound that has been synthesized and characterized so far, and it remains unknown whether other MeHg-selenoamino acid compounds behave in a similar fashion.

Here we report the synthesis, characterization and structures of four new MeHg-selenoamino acid complexes, including MeHg-$_{L}$-selenoglutathionate, MeHg-$_{D,L}$-selenopenicilaminate, and two MeHg-$_{L}$-selenomethioninate complexes (one via a Hg-Se bonding and the other Hg-N bonding) (Figure 3.1). Selenomethione is a common form of dietary selenium, and is randomly incorporated into proteins due to

its chemical and structural mimicry to methionine (*9*). Selenoglutathione can be a physiological source of selenocysteine and may interact with MeHg as a carrier in between the cells and across the blood-brain barrier (*10*). Selenopenicillamine is known to bind $MeHg^+$ strongly (*11*), and its sulfur analogue, penicillamine, has been clinically used for detoxification of mercury (*12, 13*).

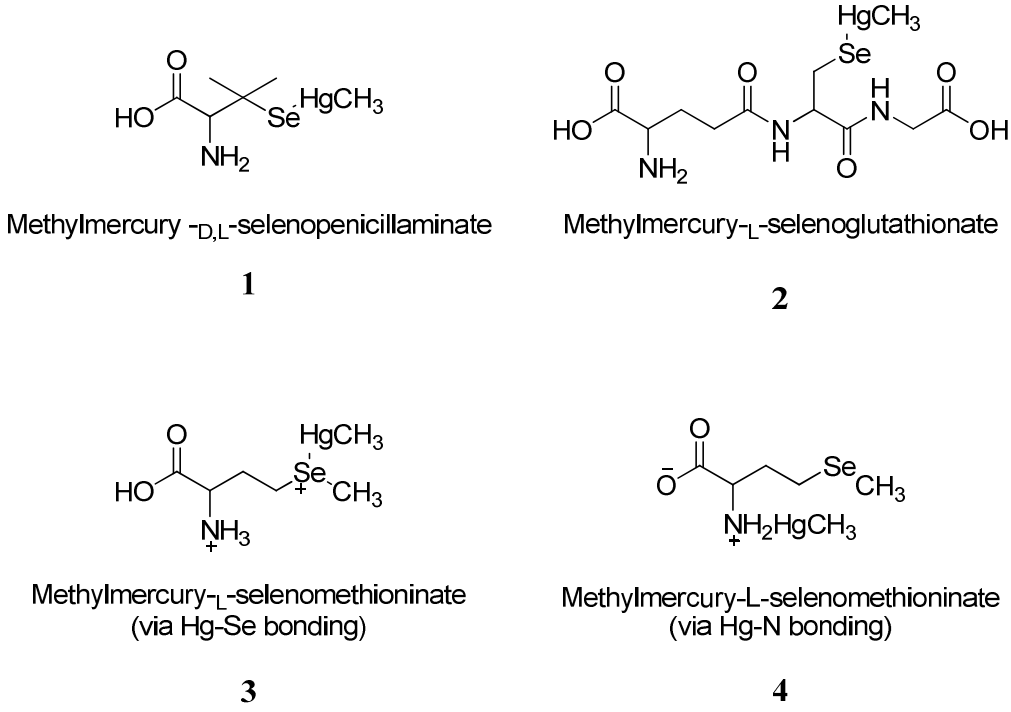

Figure 3.1. Four new methylmercury-selenoamino acid complexes studied in this work

Experimental

Reagents and apparatus

Methylmercury hydroxide, $_{D,L}$-penicillamine, and Na_2SeO_3 were purchased from Alfa Aesar, $_L$-glutathione (reduced form) from Sigma-Aldrich, and $_L$-selenomethionine from CalBioChem. All of the chemicals were of ACS grade or greater, and were used as received. Ultrapure deionized water (Milli-Q Element;

Millipore) was used as the laboratory water in all the experiments. All reactions were carried out under an inert atmosphere of Ar.

^{1}H and ^{13}C NMR spectra were recorded in D_2O on a Bruker AMX 500 MHz NMR spectrometer equipped with a 5-mm broadband probe. Chemical shifts δ were reported in ppm relative to TMS and coupling constants J in Hz. The ^{1}H NMR spectra were referenced to residue of D_2O at δ = 4.75 ppm. $^{77}Se\{^{1}H\}$ and $^{199}Hg\{^{1}H\}$ NMR spectra were recorded in D_2O on a Bruker AMX 600 MHz NMR spectrometer equipped with a 5 mm broadband probe, with referencing 114.3676223 Hz as 0 ppm frequency for ^{77}Se and 107.4043151 Hz as 0 ppm frequency for ^{199}Hg. Mass spectra were recorded in a methanol and water (10:90 v:v) solution on an Agilent G6410A triple quadrupole mass spectrometer with electrospray ionization. Solid-state IR spectra were recorded on KBr on a Thermo-Nicolet model 1605 FT-IR. UV-Vis spectra were recorded in water on a Cary 500 spectrophotometer (Varian).

Synthesis of $_{L}$-selenoglutathione and $_{D,L}$-selenopenicillamine

Synthesis of $_{L}$-selenoglutathione was carried out following (*14*). Briefly, to 50-mL deoxygenated Milli-Q water, 0.3241 g (0.98 mmol) of Na_2SeO_3 was added. The pH was adjusted to 8.75 by adding 4M NaOH. 0.2500 g (0.81 mmol) of $_{L}$-glutathione was added to the mixture and stirred for 3.5 h. After evaporation of the solvent in vacuum, the product was kept under Ar at 4°C. Yield: 0.4219 g, 75%. ^{1}H NMR (500 MHz, D_2O, 25 °C): δ = 3.59-3.68 (q, $^{2}J_{H,H}$ = 44 Hz, $CysH^{\alpha}$, 1H), 3.27-3.29 (t, $^{2}J_{H,H}$ = 13 Hz, $GluH^{\alpha}$, 1H), 3.16-3.19 (dd, $^{2}J_{H,H}$ = 19 Hz, $GlyH^{\alpha}$, 2H), 2.80-2.85 (q, $^{2}J_{H,H}$ = 24 Hz, $CysH^{\beta}$, 2H), 2.24-2.35 (multiplet, $GluH^{\gamma}$, 2H), 1.76-1.90 (multiplet, $GluH^{\beta}$, 2H).

$_{D,L}$-selenopenicillamine was synthesized following a similar procedure. Briefly, to 50-mL deoxygenated Milli-Q water, 0.3252 g (0.98 mmol) of Na_2SeO_3 was added. The pH was adjusted to 10.5 by adding 4M NaOH. 0.1203 g (0.81 mmol) of $_{D,L}$-penicillamine was added to the mixture and stirred for 3.5 h. After evaporation of the solvent in vacuum, the product was kept under Ar at 4°C. Yield: 0.1265 g, 80 %. ^{1}H NMR (500 MHz, D_2O, 25 °C): δ = 3.39-3.41 (d, $^2J_{H,H}$ = 10 Hz, NH_2, 2H), 3.24-3.25 (d, $^2J_{H,H}$ = 8 Hz, CH-COOH, 1H), 1.44-1.46 (d, $^2J_{H,H}$ = 7 Hz, Se-H, 1H), 1.26-1.36 (q, $^2J_{H,H}$ = 50 Hz, CH_3, 6H).

Synthesis of MeHg-selenoamino acid complexes

The MeHg-selenoamino acid complexes were synthesized following a procedure modified from that for the synthesis of MeHg-selenocysteinate (*11*). An example of reactions involved is given in Scheme 3.1. In general, to 50-mL deoxygenated Milli-Q water, a selenoamino acid ($_{D,L}$-selenopenicillamine, $_L$-selenoglutathione, or $_L$-selenomethionine) was added. The pH was adjusted by adding 4M NaOH at their respective pKa values for the –SeH group (10.5 for $_{D,L}$-selenopenicillamine, 8.75 for $_L$-selenoglutathione and 9.21 for $_L$-selenomethionine); a further set of synthesis was conducted with $_L$-selenomethionine at pH ~0.5 by adding conc. HNO_3. Equimolar CH_3HgOH was added and the mixture was stirred for 3.5 h. Any elemental Se produced was filtered by passing the solution through a 0.45-µm hydrophilic polypropylene membrane filter (PALL Life Sciences). The filtrate was collected and the solvent was evaporated in vacuum, and the product was kept under Ar at 4°C.

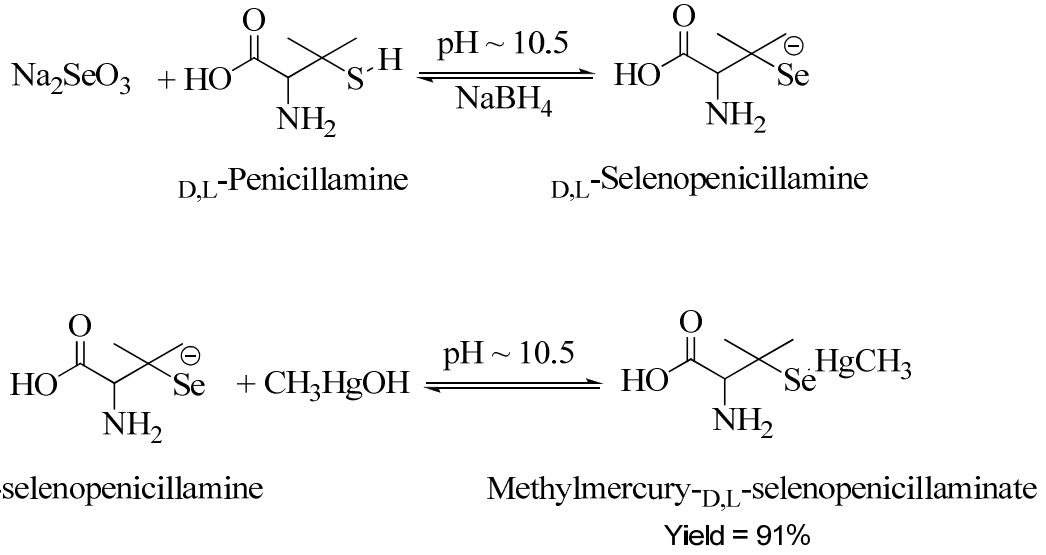

Scheme 3.1. A general reaction scheme using $_{D,L}$-penicillamine as an example

Methylmercury-$_{D,L}$-selenopenicillaminate (Complex 1). Complex **1** was synthesized following the general procedure described above with 0.1578 g (0.80 mmol) of $_{D,L}$-selenopenicillamine. Yield: 0.3000 g, 91%. ESI-MS (*m*/*z*): Calc. for $C_6H_{13}HgNO_2Se$ $[M+1]^+$: 412.982. Found: 412.956. FT-IR (KBr, cm^{-1}): 3454 (b, N–H), 2966, 2912 (s, C-H), 1641 (s, C=O). ^1H NMR (500 MHz, D_2O, 25 °C): δ = 3.90 (s, CH-COOH, 1H), 3.49 (s, NH_2, 2H), 1.44-1.54 (d, CH_3, 3H), 0.92-1.02 (d, CH_3, 3H), 0.78 (s, Hg-CH_3, 3H). ^{13}C NMR (600 MHz, D_2O, 25 °C): δ = 178.3 (C=O), 67.57 (CH), 34.13 (C-CH_3), 32.78 (C-CH_3), 16.45 (C(CH_3), 5.01 (CH_3-Hg). ^{77}Se NMR (600 MHz, D_2O, 25 °C): δ = 1278.92. ^{199}Hg NMR (600 MHz, D_2O, 25 °C): δ = -557.81.

Methylmercury-$_{L}$-selenoglutathionate (Complex 2). Complex **2** was synthesized following the general procedure described above with 0.3520 g (0.99 mmole) of $_{L}$-selenoglutathione. Yield: 0.3447 g, 61%. ESI-MS (*m*/*z*): Calc. for $C_{11}H_{19}HgN_3O_6Se$ $[M+1]^+$: 571.014. Found: 526.100 (M-COOH). FT-IR (KBr, cm^{-1}): 3347 (s, N–H), 2975, 2925 (s, C-H), 1733 (s, C=O). ^1H NMR (500 MHz, D_2O,

25 °C): δ = 8.55-8.61 (d, $^{2}J_{H,H}$ = 35 Hz, CysNH, 1H), 8.28-8.30 (t, $^{2}J_{H,H}$ = 12 Hz, free GlyNH, 1H), 8.22-8.24 (t, $^{2}J_{H,H}$ = 12 Hz, bound GlyNH, 1H), 4.65-4.68 (dist. t, $^{2}J_{H,H}$ = 18 Hz, CysH$^{\alpha}$, 1H), 3.81-3.85 (quintet, $^{2}J_{H,H}$ = 23 Hz, GluH$^{\alpha}$, 1H), 3.74-3.79 (quintet, $^{2}J_{H,H}$ = 33 Hz, GlyH$^{\alpha}$, 1H), 2.96-3.00 (q, $^{2}J_{H,H}$ = 24 Hz, CysH$^{\beta}$, 2H), 2.47-2.58 (m, $^{2}J_{H,H}$ = 63 Hz, GluH$^{\gamma}$, 2H), 2.12-2.19 (quintet, $^{2}J_{H,H}$ = 37 Hz, GluH$^{\beta}$, 2H), 0.89 (s, CH_3-Hg, 3H). ^{13}C NMR (600 MHz, D_2O, 25 °C): δ = 176.47-176.68 (t, $^{2}J_{C,C}$ = 31 Hz, GlyCOO), 175.24 (s, GluCON), 174.82 (s, GluCOO), 172.56-172.63 (d, $^{2}J_{C,C}$ = 11 Hz, Cys$_{b(bound)}$CON), 172.02-172.14 (q, $^{2}J_{C,C}$ = 18 Hz, Cys$_{f(free)}$CON), 61.88 (s, Cys$_b$C$^{\alpha}$), 56.76 (s, Cys$_f$C$^{\alpha}$), 52.89 (s, GluC$^{\alpha}$), 39.08 (s, Cys$_b$C$^{\beta}$), 31.66-31.96 (q, $^{2}J_{C,C}$ = 45 Hz, GluC$^{\gamma}$), 29.25 (s, GluC$^{\beta}$), 26.76-26.91 (dist. t, $^{2}J_{C,C}$ = 22 Hz, Cys$_f$C$^{\beta}$), 5.51 (s, C-Hg). ^{77}Se NMR (600 MHz, D_2O, 25 °C): δ = 1317.66. ^{199}Hg NMR (600 MHz, D_2O, 25 °C): δ = -761.93.

The Hg-Se bonding MeHg-$_L$-selenomethioninate (Complex 3). Complex **3** was synthesized following the general procedure described above with 0.2107 g (1.07 mmol) of $_L$-selenomethionine at pH = 1.5. Yield: 0.2186 g, 49%. ESI-MS (*m*/*z*): Calc. for $C_6H_{15}HgNO_2Se^{2+}$ $[M+1]^+$: 414.996. Found: 414.996. FT-IR (KBr, cm^{-1}): 3454 (b, N–H), 2966, 2912 (s, C-H), 1640 (s, C=O). ^{1}H NMR (500 MHz, D_2O, 25 °C): δ = 3.99-4.02 (t, $^{2}J_{H,H}$ = 13 Hz, CH, 1H), 2.99-3.10 (multiplet, $^{2}J_{H,H}$ = 53 Hz, C-CH_2, 2H), 2.43 (s, CH_3-Se, 3H), 2.15-2.31 (multiplet, $^{2}J_{H,H}$ = 80 Hz, Se-CH_2, 2H), 0.96 (s, CH_3-Hg, 3H). ^{13}C NMR (600 MHz, D_2O, 25 °C): δ = 173.8 (C=O), 81.1 (CH), 50.0(Se–CH_3), 46.9 (–CH_2), 31.7 (–CH_2), 1.2 (Hg-CH_3). ^{77}Se NMR (600 MHz, D_2O, 25 °C): δ = 857.38. ^{199}Hg NMR (600 MHz, D_2O, 25 °C): δ = -950.29.

The Hg-N bonding MeHg-$_L$-selenomethioninate (Complex 4). Complex **4** was synthesized following the general procedure described above with 0.2113 g (1.08 mmol) of $_L$-selenomethionine at pH = 9.0 Yield: 0.2305 g, 52%. ESI-MS (*m*/*z*): Calc.

for $C_6H_{13}HgNO_2Se$ $[M+1]^+$: 410.723; Found: 410.721. FT-IR (KBr, cm^{-1}): 3151 (b, N–H), 2995, 2924 (s, C-H), 1640 (s, C=O). ^1H NMR (500 MHz, D_2O, 25 °C): δ = 3.98-4.00 (t, $^2J_{H,H}$ = 12 Hz, CH, 1H), 2.57-2.69 (multiplet, $^2J_{H,H}$ = 58 Hz, C-CH_2, 2H), 2.06-2.21 (multiplet, $^2J_{H,H}$ = 71 Hz, Se-CH_2, 2H), 2.00 (s, CH_3-Se, 3H), 0.86 (s, CH_3-Hg, 3H). ^{13}C NMR (600 MHz, D_2O, 25 °C): δ = 179.2 (C=O), 56.7 (CH), 33.6 (–CH_2), 20.4 (–CH_2), 3.7 (Se–CH_3), -1.7 (Hg-CH_3). ^{77}Se NMR (600 MHz, D_2O, 25 °C): δ = 67.93. ^{199}Hg NMR (600 MHz, D_2O, 25 °C): δ = -860.99.

Single crystal X-ray crystallography

Suitable crystals of Complex **4** were obtained from an aqueous solution by slow evaporation of the solvent in vacuum. The crystal (colorless plate; 7×80×200 µm) was mounted on a Bruker 4-circle single-crystal diffractometer equipped with an APEX CCD area detector using graphite-monochromated Mo K_α (λ = 0.71073 Å) radiation. The crystal-glass-fiber end was dipped in epoxy and the crystal coated prior to data collection. In excess of a hemisphere of intensity data was collected (293 K) to 60° 2θ using a frame width of 0.3° and a frame time of 30 s, at a crystal-to-detector distance of 5 cm. Integration of the intensity data was carried out using the SAINT program (*15*), along with standard corrections (for Lorentz, polarization and background effects). A total of 12371 reflections were integrated, corrected for absorption effects using the SADABS program (*15*), and identical reflections (at different Ψ angles) combined using the XPREP program (*15*), to give a total of 5389 reflections in the Ewald sphere. The rapid data collection (<48 h) and the epoxy coating on the crystal prevented any measurable deterioration, and a time-decay correction was not employed. Systematically absent reflections are consistent with space group $P2_1$, with 3080 unique data with a Laue (2/m) merging of 2.3% (Friedel pairs were not merged). Scattering curves for neutral atoms, together with anomalous

dispersion corrections, were taken from International Tables for X-ray Crystallography (*16*). The Bruker SHELXTL program was used for the refinement of the crystal structure with initial coordinates of all non-hydrogen atoms. Least-squares refinement (based on Fo^2 and all 3080 data) for a model involving anisotropic displacement of all non-hydrogen atoms converged to an R1 index of 5.3% (2732 observed unique reflections $|F_0| > 4\sigma F_0$) and wR2 index of 11.3% for all data. The absolute structural configuration was clearly established [Flack parameter = 0.02(2)]. Residual peaks in the difference-Fourier map conforming to sensible H positions were inserted into the model and allowed to refine with the following constraints for chemically equivalent H atoms: (1) the donor-atom - H distances were restrained to equal the observed electron density maxima (as opposed to the internuclear distance) as suggested by the software, and (2) the isotropic displacement parameters were restrained to be equal. There were some indications for minor disorder in the terminal SeMe group, but a satisfactory model could not be developed (see Appendix A); bond lengths for this part of the molecule should be treated with caution. The program MERCURY2.2 was used for molecular geometry and drawing (*17*). Crystallographic details for Complex **4** are given in Table A1 in Appendix A.

Quantum mechanical calculations

Standard molecular orientations were used in building the molecules of Complexes **1**–**4** using the graphical user interface of Gaussian, GaussView 3.09 (*18*). All structures were fully optimized using Gaussian-03 (*19*) without imposing any symmetry constraints. The hybrid functional, B3LYP (*20, 21*), was used for all calculations. However, to probe how the exchange and correlation functionals affect the structure and electronic properties calculations, at least one structure was optimized with the PBE functional (*22*) which yielded similar structural properties

with the B3LYP calculations. The Stuttgart-Dresden basis set (SDD) (*23*) for the Hg atom was used with the respective effective core potential to treat the (scalar) relativistic effects for the heavier atom and 6-31+G(p) basis for all other atoms. Structures of a few systems were optimized in the solution using the Conductor Polarizable Continuum Model (CPCM) (*24*) implemented in the Gaussian-03 package.

When establishing structural data by quantum mechanical calculations, it is important to verify that the methodology used is suitable and the results are reliable. One way of ensuring this is to "calibrate" the method for similar types of compounds that have well-established experimental data. MeHg cysteine (*25*) and MeHg selenocysteine (*11*), the crystal structures of which were experimentally characterized, were used for this purpose. For example, the experimental bond distances of C-Hg, Hg-S and S-C determined by X-ray crystallography for MeHg-cysteinate are 2.10, 2.35 and 1.81 Å, respectively and the C-Hg-S bond angle is 177.6º (*25*). The corresponding values from the quantum mechanical calculations are 2.11, 2.39, 1.85 Å and 177.05º, respectively, which are within 1% differences from the experimental values. For MeHg-selenocysteine, the experimental bond distances of C-Se and Se-Hg are 1.99 Å and 2.47 Å, respectively, and the C-Hg-Se angle is 177.8º (*11*), and the corresponding values from the calculations were 1.99 Å, 2.51 Å, and 177.7º, respectively. All calculated structural parameters of both compounds were found to be within 1% differences from the experimental values.

Results and discussion

Although the formation constant for Complex **1** (MeHg-$_{D,L}$-selenopenicillaminate) was previously reported (*11*), this is the first time this complex

is isolated and characterized. Complexes 2-**4** are reported for the first time. All of the compounds are relatively unstable after prolonged exposure at room temperature and tend to decompose to a black precipitate which is identified to be HgSe. Therefore all of these compounds were stored at 4 °C under an Ar atmosphere.

IR characterization

All of the compounds yield a colorless solution in D_2O and do not absorb significantly in the visible range. The IR spectra of these compounds show a typical C=O band close to 1640 cm^{-1}. Except for Complex **3** where N is bonded to Hg, all the N–H stretching bands are above 3340 cm^{-1}, suggesting the N–H bond in these compounds is hydrogen bonded (Table 3.1). Other bands in the 2800-3450 cm^{-1} region (not shown in Table 3.2) are an indication for a strongly hydrogen bonded zwitterionic amino acid part of the molecule (*11*). ν(Hg-C) was assigned to bands at 545 cm^{-1} (Complex **1**), 594 cm^{-1} (Complex **2**), 540 cm^{-1} (Complex **3**), and 541 cm^{-1} (Complex **4**), respectively, and are similar to those reported for MeHg-selenocysteinate (536 cm^{-1}) (*11*), $MeHgSeBu^t$ (534 cm^{-1}) (*26*), and $MeHgSeCH_2Ph(COOH)$ (536 cm^{-1}) (*27*), as well as their S-analogues (MeHg-methionine: 542 cm^{-1} (*28*); MeHg-cysteinate: 538 cm^{-1} (*25*)). The ν(Hg-N) band generally appears between 400 to 700 cm^{-1} (*28*), and thus may overlap with the ν(Hg-C) band in Complex **4**.

NMR characterization

^1H NMR spectra of Complexes **1**-**4** are shown in Figure B1 in Appendix B. All the ^1H and $^{13}C\{^1H\}$ spectra of Complexes **1**–**4** exhibited chemical shifts that are closely related to those observed for related sulfur analogues, such as Cu(I)-glutathionate (*29*), MeHg-methioninate (at low and high pH) (*30*), mercury-dimethioninate (*31*), MeHg-selenocysteaminate, MeHg-selenocystinate, MeHg-

selenocystaminate, MeHg $_L$-selenoprophylaminate (*32*). In all the complexes, the methyl protons of MeHg are within a δ range of 0.86-0.96 ppm, similar to those reported for MeHg-selenolate complexes (*32*) and for MeHg-selenourea complexes (*33*).

Table 3.1. Selected IR, NMR and MS characterizations of Complexes **1**– **4**

Complex	**1**	**2**	**3**	**4**
IR (KBr,cm^{-1})	545 (Hg-C), 3454 (N–H), 1641 (C=O)	594 (Hg-C), 3347 (N–H), 1733 (C=O)	540 (Hg-C), 3151 (N–H), 1640 (C=O)	541 (Hg-C), 3454 (N–H), 1640 (C=O)
^{1}H NMR (δ/ppm)	3.90 (s, CH-COOH, 1H), 0.78 (s, Hg-CH_3, 3H)	4.65-4.68 (dist. t, $^2J_{H,H}$ = 18 Hz, $CysH^{\alpha}$, 1H), 0.89 (s, CH_3-Hg, 3H)	3.99-4.02 (t, $^2J_{H,H}$ = 13 Hz, CH, 1H), 0.96 (s, CH_3-Hg, 3H)	3.98-4.00(t, $^2J_{H,H}$ = 12 Hz, CH, 1H), 0.86 (s, CH_3-Hg, 3H)
^{13}C NMR (δ/ppm)	178.3 (C=O), 5.01 (Hg-CH_3)	176.47-176.68 (t, $^2J_{C,C}$ = 31 Hz, GlyCOO), 5.51 (Hg-CH_3)	173.8 (C=O), 1.2 (Hg-CH_3)	179.2 (C=O), -1.7 (Hg-CH_3)
^{77}Se (δ/ppm)	1278.92	1317.66	857.38	67.93
^{199}Hg (δ/ppm)	-557.81	-761.93	-950.29	-860.99
$J_{199Hg\text{-}1H}$	191	201	232	213
m/z – theoretical $[M^+]$	412.9818	571.0145	414.9963	410.7229
m/z – experimental $[M^+]$	412.9563	526.1000 ($[M\text{-}COOH]^+$)	414.9960	410.7206

Depending on the pH, the binding of MeHg and selenomethionine can be dominated either via the Hg-Se bonding (Complex **3**) or the Hg-N bonding (Complex **4**). The ^{1}H NMR spectra of Complexes **3** and **4** exhibited the expected chemical shift pattern for the C**H**$_2$ protons as of their S-analogues (see Figure B1 in Appendix B) (*30*). At pH < 2 the methyl protons are de-shielded and the downfield move indicates MeHg binding with Se (Complex **3**). At higher pH (Complex **4),** the methyl protons approach each other and the chemical shift of the –CH_2 protons is affected which indicates the binding of MeHg to the –NH_2 group.

^{77}Se NMR signals of Complexes **1**-**3** are significantly different from that of Complex **4**. In Complexes **1**-**3** Se is directly bonded with $MeHg^+$ and thus experiences a deshielding effect from Hg. In Complex **4**, such a deshielding effect is absent as Se is bonded with -NH_2 instead and the peak thus appears at a very high field at δ 67.93 ppm.

A similar but reverse trend was observed in the ^{199}Hg NMR where Complex **1** showed a high-field peak compared to other compounds. In Complex **1**, the soft Lewis acid $MeHg^+$ forms a strong covalent bond with the soft Lewis base -SeH and experiences less deshielding as the electron donating property of the adjacent methylene protons may compensate, whereas $MeHg^+$ in compound **3** is the most deshielded because of its binding with the positive Se. In Complex **4** this effect is somewhat less than that in Complex **3**, most probably due to the close proximity of the carboxylate group and therefore the availability of lone-pair electron on the oxygen atom. Deshielding is medium in Complex **2** due to the electronic effect from the backbone structure of the tri-peptide.

Methylene satellite peaks appear on both sides of the MeHg peak with a *J* value ranging from 191 Hz to 232 Hz. This coupling is due to a Fermi contact interaction and the *J* value increases with increasing contribution of the mercury 6s orbital to the C-Hg bond, as seen in Complexes **1**-**3** (Table 3.1). In Complex **4**, MeHg binds with the N-atom of the amino group and showing the usual *J* value ($J_{199Hg-1H}$ = 213 Hz). Similar *J* values were reported for MeHg complexes with methionine (223 Hz) (*30*), selenocysteine (164.3 Hz) and selenocysteamine (162.0 Hz) (*32*), and selenourea (190-196 Hz) (*33*). Comparing the *J* values with the S-analogues showed that these values are slightly lower for Se complexes than those for S complexes. For example, Complex **4** has a $J_{199Hg-1H}$ value of 213 Hz, whereas its S-analogue has a *J*

value of 217.4 Hz (*32*). A similar trend was also reported for other complexes such as MeHgXMe (158.2 Hz when X=S and 155.3 Hz when X=Se) and MeHgXPh (168.4 Hz when X=S and 164.5 Hz when X=Se) (*34*), indicating that $MeHg^+$ has more affinity for Se than for S. The binding affinity of MeHg in aqueous solution has been generally observed to follow the order of SeH > SH ≥ Se-Se > NH_2 > S-S, $SeCH_3$ (*32*). The *J* values also indicate that the Hg-C bond has more 's' character and confirm the high covalency of MeHg-Se bond and involvement of d-d back bonding (*32, 33*).

Arnold et al. (*11*) reported a lower *J* value for Complex **1** (168.0 Hz) based on a ligand exchange reaction carried out in D_2O. The authors pointed out that the exchange between their various protonated forms is fast on the NMR time scale and the chemical shifts of the carbon-bonded ligand protons are the weighted averages of the chemical shifts of the various protonated species. In the present study, Complex **1** was purified and isolated and the ligand exchange reactions were absent, and thus the higher *J* value (191.0 Hz) is expected to be more reliable.

Structural properties

X-ray crystallography was done successfully only with Complex **4**. Structural data for Complexes **1-4** were obtained based on quantum mechanical calculations and are listed in Appendix C. As mentioned earlier, the quantum mechanical calculation approach was verified by the excellent agreement between the calculated structure and the experimentally determined structure of MeHg-selenocysteinate. Furthermore, Table 3.2 shows that the quantum mechanical calculations also reproduced well the experimental structure of Complex **4**, with one exception on the Hg-O bonding as detailed below.

Some key structural parameters of all the four compounds are listed in Table 3.3. The Hg-Se bond length decreases from Complex **3** to **1**. This increased bond strength is due to an increase in *sp* hybridization of Hg by a decrease in the *s* character in the C-Hg bond, which is in agreement with the order of the $J(^{199}Hg\text{-}^{1}H)$ coupling constant (Table 3.1). Complex **4** is an exception as MeHg is not bounded with Se but rather with N; this hybridization does not affect the bond length between C-Hg and Se-C bonds.

Table 3.2. Comparison between the quantum mechanical calculations and x-ray crystallography on the structure of Complex **4**

	X-ray crystallography	Quantum mechanical calculations
Bond distance (Å)		
C(1)-Se	1.936 (15)	1.971
Se-C(2)	1.912 (22)	1.985
C(5)-O(1)	1.256 (12)	1.338
C(5)-O(2)	1.243 (10)	1.214
C(4)-C(5)	1.524 (19)	1.549
Hg-N(1)	2.114 (10)	2.086
Hg-C(6)	2.082 (13)	2.098
Hg-O(2)	2.640 (7)	4.146
Bond angle (°)		
C(6)-Hg-N(1)	172.0 (0.8)	177.2
C(6)-Hg-O(2)	118.3 (0.8)	147.0

The structure of MeHg-selenopenicillaminate (Complex **1**) is very close to the structure of MeHg-selenocysteinate where the two hydrogen atoms of the CH_2 group bonded to Se are replaced by the methyl group. However, the bond distance between C-Se is slightly longer (0.03 Å) in the selenopenicillamine complex than that in the

selenocysteine complex. This observation is expected as the two attached electron releasing groups (CH_3) increase the electron density around the carbon atom which eventually weakens the bonding between C and Se. In the MeHg-selenoglutathionate (Complex **2**) the carbon atom bonded to the selenium atom has similar neighbours as in MeHg-selenocysteinate and therefore the C-Se bond distance is similar to those of the selenocysteine complexes. The large groups attached in the tail induce a slight (0.02 Å) bond lengthening between Se-Hg.

Table 3.3. Bond distances and bond angles for Complexes **1**-**4** and their S-analogues (values in parentheses) based on quantum mechanical calculations.

Complex	Bond distance (Å)				Bond angle (º)		
	C-Hg	Hg-Se(S)	Se(S)-C	Hg-N	C-Hg-Se(S)	C-Se(S)-Hg	C-Hg-N
1	2.12	2.51 (2.41)	1.99 (1.88)	-	175.33 (175.94)	106.78 (108.65)	
2	2.12	2.52 (2.43)	2.03 (1.88)	-	173.00 (172.93)	104.26 (106.67)	
3	2.12	2.69 (2.60)	2.00 (1.86)	-	177.49 (177.90)	105.55 (108.16)	
4	2.10	-	-	2.08	177.10 (177.21)	-	177.18 (177.21)
4*	2.17	-	-	2.34	149.18	-	

* Optimized in solution

Structural calculations further confirmed that the binding atom of selenomethionine with $MeHg^+$ is different at two different pH values. At lower pH (pH 0.5), $MeHg^+$ binds to Se (Complex **3**) and most of the structural parameters (Table 3.3) are consistent with those of the cysteine, penicillamine and glutathionine

analogues. The coordination number of the Se atom in selenomethionine is, however, one more than the corresponding value in the other complexes and hence the Se-Hg bond distance is longer. At higher pH (8), $MeHg^+$ binds to the amine group of selenomethionine (Complex **4**). The binding of $MeHg^+$ to the amine group develops a positive charge on the nitrogen atom and a negative charge on the carboxylic group. Such a strongly charge-separated single molecule is not stable in the gas phase. Instead, a stable structure in solution is calculated (Table 3.3) which is, however, still not consistent with the experimental results. The Hg-N bond distance is calculated to be 2.34 Å, which is 0.26 Å longer than the experimental value (*29, 34*). The largest discrepancy observed is in the N(1)-Hg-C(6) bond angle, which is around 28º lower than the experimentally reported value. By compensating some of the intermolecular interactions by adding one more proton to the carboxylic group, the recalculated Hg-N bond distance and N-Hg-C bond angle are in very good agreement with the corresponding experimental values (Table 3.2), further confirming the deprotonation of the carboxylic acid group. The disagreement in Hg-O(2) distance and C(6)-Hg-O(2) angle between experimentally and theoretically determined values are due to the absence of the 3D solid-state structure in the calculations. A comprehensive study on the 3D solid-state structure would be needed to determine the extent of intermolecular interactions but this is beyond the scope of current study.

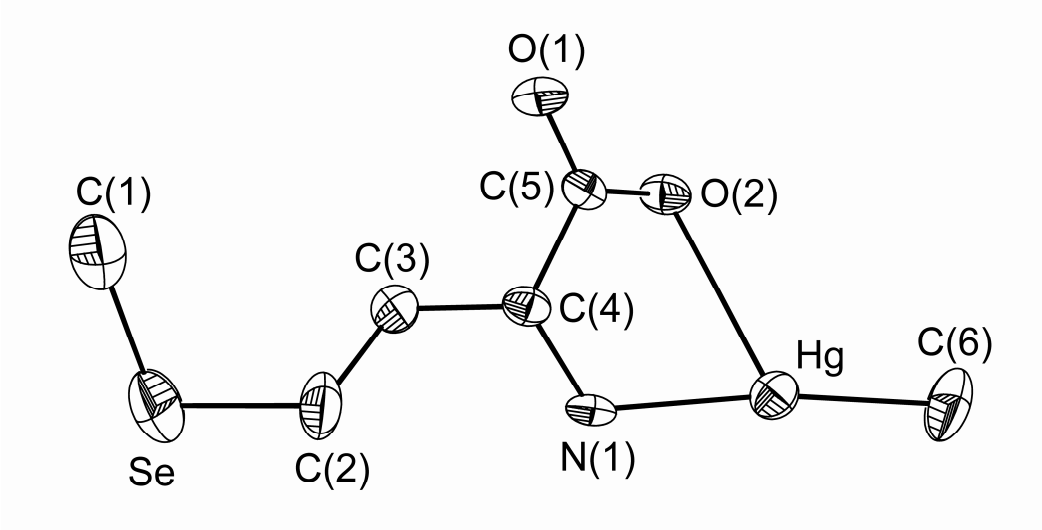

Figure 3.2. Crystal structure of Complex **4** (hydrogens are omitted for clarity)

The ORTEP plot of Complex **4** based on X-ray crystallography is shown in Figure 3.2. The Hg-N bond distance (2.114(10)) is similar to other compounds reported such as 2.10 Å in H_2NHgCl, 2.13 (3) Å in $[MeHg)_2(pen)]$ (pen = $_{D,L}$-penicillamine) and 2.08 Å in Hg(II) succinimide. The bond distance between Hg-O (2.640(7)) is shorter than the sums of their van der Waals radii (*ca*. 3.0 Å) which indicate a weak bond. The presence of two additional weak Hg-O (carboxylate) bonds are shown by the intramolecular Hg-O(1) distance of 2.70(3) Å and an intermolecular Hg-O(2) contact of 2.640(7) Å. These contacts presumably reflect ionic interactions resulting from the zwitterionic nature $[CH_3HgNH_2^+CH(COO^-)CH_2CH_2SeCH_3]$ of the complex, resulting in a significantly smaller bond angle (C1-Hg-N1=172.0(0.8)).

Toxicological significance

A comparison between Complexes **1**-**4** and their S-analogues reported in the literature shows that replacing the sulphur atom by the selenium atom does not change the structure significantly (see also Figure 3.3). Due to the larger radius of selenium, the structural parameters that are directly related to the selenium atom are however

slightly changed (Table 3.3). Although the Hg-Se bond length in MeHgSeR is longer than the Hg-S bond length in its sulfur counterpart MeHgSR, the Hg-Se bond length is marginally shorter than expected based on the relative radii, as observed earlier for MeHg-selenocysteinate (*8*). This is in agreement with the higher nucleophilicity of selenols than that of thiols (*33*).

The stronger binding affinity between $MeHg^{+}$ and selenols implies that in the presence of RSeH, MeHg-SR complexes tend to undergo ligand exchange to form MeHg-SeR (*11, 35*):

$$MeHgSR + RSeH \rightleftharpoons MeHgSeR + RSH$$

This could potentially result in a decreased bioavailability of both MeHg (thus a decrease in potential MeHg toxicity) and Se (thus an increase in potential Se deficiency) (*7*).

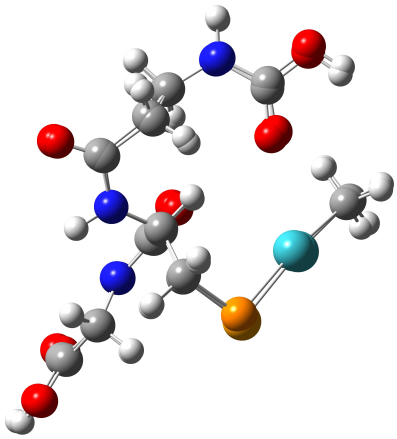

Figure 3.3. Superimposed structures of Complex **2** with its S-analogue. White, grey, cyan, orange, red and blue balls represent hydrogen, carbon, mercury, sulfur (selenium), oxygen and nitrogen atoms, respectively.

In addition, it should be noted that the selenol group in selenoamino acids has a much lower pKa value than the thiol group in their sulfur analogues. For instance, the selenol group in selenocysteine and selenoglutathione has a pKa value of 5.2 and 5.3, respectively, whereas the pKa value for the thiol group in cysteine and glutathione is 8.3 and 8.7, respectively (*36*). Therefore, at physiological pH selenolates (-Se^-) are the primary form of selenols while their S-analogues are primarily in the un-dissociated –SH form. Due to this reason and also for the rapid ligand exchange mechanism with the MeHg-thiolate complexes, a significant portion of the MeHg in the biological systems is expected to be bounded as MeHg-selenol complexes which could protect the cells from oxidative damage (*37*). The ratio of selenol- to thiol-bound MeHg is dependent on the selenium status of the organism which could be regulated dietary (e.g., by supplementing Se dietary which usually contains selenocysteine and selenomethionine) or clinically (e.g., by administrating selenopenicillamine). Furthermore, the observation that the MeHg-selenoamino acid complexes can decompose to black precipitates (HgSe) provides a new possible pathway for demethylation and detoxification of MeHg. In vivo formation of black HgSe(s) in liver and kidneys of rats and marine mammals has been frequently reported (*38-43*). Although the metabolic pathway for the formation of HgSe(s) is not well understood, it is generally thought to be via the interaction between inorganic Hg and selenoproteins (*44, 45*). Further studies are being conducted in our laboratory to probe the significance of MeHg-selenoamino acids as intermediates in the formation of biomineral HgSe(s).

Conclusion

Four new methylmercury-selenoamino acid complexes with potential importance in biological and clinical mercury-selenium antagonism were synthesized and characterized. All four complexes were found to chemically and structurally resemble their sulfur analogues, with a slightly stronger binding affinity of mercury to selenium than to sulfur. Further studies on their thermodynamic properties, in vivo occurrence, and toxicological importance are warranted.

Acknowledgement

This research was funded by the Natural Science and Engineering Council (NSERC) of Canada (FW, GS). MAKK was supported by an NSERC PGS-D fellowship. GS and AMdA acknowledge additional funding from the EJLB Foundation (http://www.ejlb.qc.ca/) and the University of Manitoba. Quantum mechanical calculations were enabled by the use of WestGrid computing resources, which are funded in part by the Canada Foundation for Innovation (CFI), Alberta Innovation and Science, BC Advanced Education, and the participating research institutions. WestGrid equipment is provided by IBM, Hewlett Packard and SGI. We thank Kirk Murat for taking all the NMR spectra, Mark Cooper, Peter H.M. Budzelaar, and Frank C. Hawthorne for X-ray crystallography, Marcos Lemes for assistance in the synthesis and MS characterization, and Akef Afaneh for useful discussion on theoretical calculations. The crystallography equipment was supported by a Canada Research Chair in Crystallography and Mineralogy and NSERC and CFI grants (to Frank C. Hawthorne).

References

(1) WHO. (1990) Methylmercury, International programme on chemical safety, World Health Organization, Geneva.

(2) Harada, M. (1995) Minamata disease: Methylmercury poisoning in Japan caused by environmental pollution. *Crit. Rev. Toxicol. 25*, 1-24.

(3) Aschner, M. and Clarkson, T. W. (1989) Methylmercury uptake across bovine brain capillary endothelial cells in vitro: the role of amino acids. *Pharmacol. Toxicol. 64*, 293-297.

(4) Aschner, M., Aschner, J. L. and Kimelberg, H. K. (1992) Methylmercury neurotoxicity and its uptake across blood-brain barrier. *Vulner. Brain Environ. Risks 2*, 3-17.

(5) Ganther, H. E., Goudie, C., Sunde, M. L., Kopecky, M. J. and P., W. (1972) Selenium: relation to decreased toxicity of methylmercury added to diets containing tuna. *Science 175*, 1122-1124.

(6) Cuvin-Aralar, M. L. A. and Furness, R. W. (1991) Mercury and selenium interaction: a review. *Ecotoxicol. Environ. Saf. 21*, 348-364.

(7) Khan, M. A. K. and Wang, F. (2009) Mercury-selenium compounds and their toxicological significance: toward a molecular understanding of the mercury-selenium antagonism. *Environ. Toxicol. Chem. 28*, 1567-1577.

(8) Carty, A. J., Malone, S. F., Taylor, N. J. and Canty, A. J. (1983) Synthesis, spectroscopic and X-ray structural characterization of methylmercury-D,L-selenocysteinate monohydrate, a key model for the methylmercury(II)-selenoprotein interaction. *J. Inorg. Biochem. 18*, 291-300.

(9) Reilly, C. (2006) *Selenium in Food and Health.*, 2nd ed., Springer, New York.

(10) Kerper, L. E., Ballatori, N. and Clarkson, T. W. (1992) Methylmercury transport across the blood-brain barrier by an amino acid carrier. *Am. J. Physiol. 262*, R761-R765.

(11) Arnold, A. P., Tan, K.-S. and Rabenstein, D. L. (1986) Nuclear magnetic resonance studies of the solution chemistry of metal complexes. 23. Complexation by selenohydryl-containing amino acids and related molecules. *Inorg. Chem. 25*, 2433-2437.

(12) Clarkson, T. W. (1972) The pharmacology of mercury compounds. . *Annu. Rev. Pharmacol. 12*, 375-406.

(13) Margel, S. (1981) A novel approach for heavy metal poisoning treatment, a model. Mercury poisoning by means of chelating microspheres: hemoperfusion and oral administration. *J. Med. Chem. 24*, 1263-1266.

(14) Ogasawara, Y., Lacourciere, G. and Stadtman, T. C. (2001) Formation of a selenium-substituted rhodanese by reaction with selenite and glutathione: possible role of a protein perselenide in a selenium delivery system. *Proc. Natl. Acad. Sci. U S A 98*, 9494-9498.

(15) Bruker. (2004) *APEX 2*, *SAINT*, *XPREP* and *SADABS*, WI, USA.

(16) Wilson, A. J. C. E. (1992) *International Tables for X-ray Crystallography*, Vol. C, Kluwer, Dordrecht, The Netherlands.

(17) Macrae, C. F., Edgington, P. R., McCabe, P., Pidcock, E., Shields, G. P., Taylor, R., Towler, M. and van de Streek, J. (2006) Mercury: visualization and analysis of crystal structures. *J. Appl. Cryst. 39*, 453-457.

(18) Dennington II, R., Keith, T., Millam, J., Eppinnett, K., Hovell, W. L. and Gilliland, R. (2003) GaussView, Version 3.09, Semichem, Inc., Shawnee Mission, KS.

(19) Frisch, M. J., Trucks, G. W., Schlegel, H. B., Scuseria, G. E., Robb, M. A., Cheeseman, J. R., Montgomery, J. A., Vreven, T., Kudin, K. N., Burant, J. C., Millam, J. M., Iyengar, S. S., Tomasi, J., Barone, V., Mennucci, B., Cossi, M., Scalmani, G., Rega, N., Petersson, G. A., Nakatsuji, H., Hada, M., Ehara, M., Toyota, K., Fukuda, R., Hasegawa, J., Ishida, M., Nakajima, T., Honda, Y., Kitao, O., Nakai, H., Klene, M., Li, X., Knox, J. E., Hratchian, H. P., Cross, J. B., Bakken, V., Adamo, C., Jaramillo, J., Gomperts, R., Stratmann, R. E., Yazyev, O., Austin, A. J., Cammi, R., C. Pomelli, C., Ochterski, J. W., Ayala, P. Y., Morokuma, K., Voth, G. A., Salvador, P., Dannenberg, J. J., Zakrzewski, V. G., Dapprich, S., Daniels, A. D., Strain, M. C., Farkas, O., Malick, D. K., Rabuck, A. D., Raghavachari, K., Foresman, J. B., Ortiz, J. V., Cui, Q., Baboul, A. G., Clifford, S., Cioslowski, J., Stefanov, B. B., Liu, G., Liashenko, A., Piskorz, P., Komaromi, I., Martin, R. L., Fox, D. J., Keith, T., Al-Laham, M. A., Peng, C. Y., Nanayakkara, A., Challacombe, M., Gill, P. M. W., Johnson, B., Chen, W., Wong, M. W., Gonzalez, C., Pople, J. A. and GAUSSIAN-03, R. C. (2004) GAUSSIAN-03, Gaussian, Inc., Wallingford, CT.

(20) Becke, A. D. (1993) Density-functional thermochemistry. III. The role of exact exchange. *J. Chem. Phys. 98*, 5648-5652.

(21) Lee, C., Yong, W. and Parr, R. G. (1988) Development of the Colle-Salvetti correlation-energy formula into a functional of the electron density. *Phys. Rev. B 37*, 785-789.

(22) Perdew, J. P., Burke, K. and Ernzerhof, M. (1996) Generalized gradient approximation made simple. *Phys. Rev. Lett. 77*, 3865-3868.

(23) Figgen, D., Rauhut, G., Dolg, M. and Stoll, H. (2005) Energy-consistent pseudopotentials for group 11 and 12 atoms: adjustment to multi-configuration Dirac-Hartree-Fock data. *Chem. Phys. 311*, 227-244.

(24) Cossi, M., Rega, N., Scalmani, G. and Barone, V. (2003) Energies, structures, and electronic properties of molecules in solution with the C-PCM solvation method. *J. Comp. Chem. 24*, 669-681.

(25) Taylor, N. J., Wong, Y. S., Chieh, P. C. and Carty, A. J. (1975) Syntheses, X-ray crystal structure and vibrational spectra of L-Cysteinato(methyl)mercury(II)monohydrate. *J. C. S. Dalton 5*, 438-442.

(26) Arnold, A. P. and Canty, A. J. (1981) Synthesis, structure and spectroscopic studies of mercury(II) selenolates and $MeHgSeBu^t$. *Inorg. Chim. Acta 55*, 171-176.

(27) Pelletier, E., Sauriol, F. and Wharf, I. (1987) Preparation and characterization of new organomercury(II)selenolates. *Inorg. Chim. Acta 138*, 99-101.

(28) Wong, Y. S., Carty, A. J. and Chieh, P. C. (1977) Crystal structure of (DL-methioninato)methylmercury(II). *J. C. S. Dalton Transac. 12*, 1157-1160.

(29) Corazza, A., Harvey, I. and Sadler, P. J. (1996) ^{1}H, ^{13}C-NMR and X-ray absorption studies of copper(I) glutathione complexes. *Eur. J. Biochem. 236*, 697-705.

(30) Fairhurst, M. T. and Rabenstein, D. L. (1975) Nuclear magnetic resonance studies of the solution chemistry of metal complexes. XII. binding of methylmercury by methionine. *Inorg. Chem. 14*, 1413-1415.

(31) Birgersson, B., Drakenberg, T. and Neville, G. A. (1973) Mercury(II) complexes of methionine. *Acta Chem. Scand. 27*, 3953-3960.

(32) Sugiura, Y., Tamai, Y. and Tanaka, H. (1978) Selenium protection against mercury toxicity: high binding affinity of methylmercury by selenium-containing ligands in comparision with sulphur-contaning ligands. *Bioinorg. Chem. 9*, 167-180.

(33) Carty, A. J., Malone, S. F. and Taylor, N. J. (1979) The selenium-mercury interaction: synthesis, spectroscopic and x-ray structural studies of methylmercury-selenourea complexes. . *J. Organomet. Chem. 172*, 201-211.

(34) Wong, Y. S., Taylor, N. J., Chieh, P. C. and Carty, A. J. (1974) Models for the methylmercury-protein interaction. Comparison of the molecular structures of methyl-L-cysteinatomercury(II) and methyl-DL-methioninemercury(II). *J. Chem. Soc. Chem. Comm.*, 625-626.

(35) Canty, A. J., Carty, A. J. and Malone, S. F. (1983) Methylmercury(II) selenolates. Synthesis and characterization og MeHgSeMe and MeHgSePh, and ^{1}H and ^{199}Hg nmr studies of ligand exchange in MeHg(II) thiolates and selenolates, including amino acid complexes. *J. Inorg. Biochem. 19*, 133-142.

(36) Huber, R. E. and Criddle, R. S. (1967) Comparison of the chemical properties of selenocysteine and selenocystine with their sulfur analogs. *Arch. Biochem. Biophys. 122*, 164-173.

(37) Splittgerber, A. G. and Tappel, A. L. (1979) Inhibition of glutathione peroxidase by cadmium and other metal ions. *Arch. Biochem. Biophys. 197*, 534-542.

(38) Cikrt, M. and Benko, V. (1989) Mercury-selenium interaction: Distribution and excretion of $^{203}Hg^{2+}$ in rats after simultaneous administration of selenite or selenate. *Toxicol. Lett. 48*, 159-164.

(39) Magos, L., Clarkson, T. W. and Hudson, A. R. (1983) Differences in the effects of selenite and biological selenium on the chemical form and distribution of mercury after the simultaneous administration of $HgCl_2$ and selenium to rats. *J. Pharmacol. Expt. Ther. 228*, 478-483.

(40) Martoja, R. and Viale, D. (1977) Accumulation of mercuric selenide granules in the liver of Odontocetes (Mammifers, Cetacea): a possible method of detoxification of methylmercury by selenium. *C. R. Hebd. Seanc. Acad. Sci. Paris D 285*, 109-112.

(41) Nigro, M. and Leonzio, C. (1996) Intracellular storage of mercury and selenium in different marine vertebrates. *Mar. Ecol. Prog. Ser. 135*, 137-143.

(42) Rawson, A. J., Bradley, J. P., Teetsov, A., Rice, S. B., Haller, E. M. and Patton, G. W. (1995) A role for airborne particulates in high mercury levels of some cetaceans. *Ecotoxicol. Environ. Saf. 30*, 309-314.

(43) Arai, T., T., I., A., H., Terada, Y., Kunito, T., Tanabe, S. and Nakai, I. (2004) Chemical forms of mercury and cadmium accumulated in marine mammals and seabirds as determined by XAFS analysis. *Environ. Sci. Technol. 38*, 6468-6474.

(44) Gailer, J., George, G. N., Pickering, I. J., Madden, S., Prince, R. C., Yu, E. Y., Denton, M. B., Younis, H. S. and Aposhian, H. V. (2000) Structural basis of the antagonism between inorganic mercury and selenium in mammals. . *Chem. Res. Toxicol. 13*, 1135-1142.

(45) Suzuki, K. T., Sasakura, C. and Yoneda, S. (1998) Binding sites for the (Hg-Se) complex on selenoprotein P. *Biochim. Biophys. Acta 1429*, 102-112.

Preface to Chapter 4

This chapter is based on the following manuscript submitted in the journal "*Chemical Research in Toxicology*". Full citation of the paper is as follows:

> **Khan, M. A. K.**; Wang, F. Chemical Demethylation of Methylmercury by Selenoamino Acids. *Chem. Res. Toxicol.* **2010**, 23, 1202–1206.

The fate of methylmercury selenoamino acid (MeHgSeAA) complexes (reported in chapter 3) at physiological conditions is discussed in this chapter by using spectroscopic methods like ^{1}H and ^{199}Hg nmr and X-ray powder diffraction (XRD). This chapter explains the mechanism leading to the antagonism of methylmercury and selenium in biological systems and the formation of the end product of the antagonism, $HgSe_{(s)}$. Quantum chemical calculations also provide evidences for each step of the mechanism.

Chapter 4: Chemical Demethylation of Methylmercury by Selenoamino Acids

Abstract

A new chemical demethylation pathway for methylmercury under physiologically and environmentally relevant conditions is reported. The pathway involves the reaction between methylmercury and a selenoamino acid ($_{L}$-selenocysteine, $_{L}$-selenoglutathione, $_{D,L}$-selenopenicillamine, or $_{L}$-selenomethionine) via the formation of bis(methylmercuric)selenide and dimethylmercury as intermediates. The final degradation product is HgSe(s).

Introduction

Methylmercury (CH_3Hg^+ and its complexes; MeHg hereafter) is a known developmental neurotoxin (*1*), capable of crossing the placental (*2*) and blood-brain (*3*) barriers causing neurological damage and death in humans in extreme cases (*4, 5*). Produced mainly in the aquatic environment by microbial-mediated methylation of inorganic Hg (*6*), MeHg biomagnifies along food chains, resulting in elevated concentrations in high trophic level animals such as predatory fish and marine mammals and in humans via dietary consumption of these animals (*1, 5*). Much less is, however, known about the demethylation process once MeHg is formed (*7*). Due to the kinetic stability of the C-Hg bond (*8*), MeHg demethylation in the aquatic environment is thought to occur primarily via photolysis or microbial processes (*7*). The only established mechanism for chemical demethylation of MeHg in nature is the reaction between MeHg and H_2S via a bis(methylmercuric)sulfide ($(CH_3Hg)_2S$) intermediate, ultimately forming HgS(s) (*9, 10*).

MeHg demethylation, however, is known to occur in vivo in animals, particularly in the liver of marine mammals, and Se has long been postulated to be involved in this demethylation process (*11*). Indirect evidence has suggested that the Se-aided demethylation may have involved the formation of bis(methylmercuric)selenide ($(CH_3Hg)_2Se$) (*12, 13*), similar to $(CH_3Hg)_2S$ in the H_2S case, but the presence of $(CH_3Hg)_2Se$ has never been analytically proven due to its in vivo instability (*13*), and the pathway leading to the formation of $(CH_3Hg)_2Se$ remains unknown.

When synthesizing MeHg complexes with several selenoamino acids (*14*),

we noticed the formation of a black precipitate from their aqueous solutions after various storage times. NMR, X-ray diffraction (XRD), and mass spectrometry studies were subsequently carried out to characterize the reactions, which revealed a new chemical demethylation pathway of MeHg in the presence of selenoamino acids. Four selenoamino acids were studied, including $_{L}$-selenocysteine (CSeH), $_{L}$-selenoglutathione (GSeH), $_{D,L}$-selenopenicillamine (SePen), and $_{L}$-selenomethionine (SeMet). All the four selenoamino acids were shown to be capable of demethylating MeHg under physiologically and environmentally relevant conditions.

Materials and Methods

Reagents and Apparatus. Methylmercury hydroxide, $_{D,L}$-penicillamine, and Na_2SeO_3 were purchased from Alfa Aesar, methylmercury chloride, $_{L}$-selenocystine, $_{L}$-glutathione (reduced form), ethanol (anhydrous, 99.8%), and ethyl alcohol from Sigma-Aldrich, $_{L}$-selenomethionine from CalBioChem, and benzene from Fluka. All of the chemicals were of ACS grade or greater, and were used as received. $_{L}$-selenocysteine was prepared from $_{L}$-selenocystine following the procedure of Carty et al. (*15*). $_{L}$-selenoglutathione and $_{D,L}$-selenopenicillamine were prepared from $_{L}$-glutathione and $_{D,L}$-penicillamine, respectively, following the procedure of Khan et al. (*14*). Ultrapure deionized water (Milli-Q Element; Millipore) was used as the laboratory water in all the experiments. All reactions were carried out under an inert atmosphere of Ar.

Real-time NMR Spectra. Real-time ^{1}H and ^{199}Hg NMR spectra were

collected at 37ºC. For the MeHg-SeMet study, a 0.1 M $_{L}$-selenomethionine solution was added to 0.1 M CH_3HgOH solution at pH 9.0 in a standard NMR tube. ^{1}H NMR spectra were then recorded in D_2O on a Bruker AMX 500 MHz NMR spectrometer equipped with a 5-mm broadband probe at various time intervals after the mixing. Chemical shifts δ were reported in ppm relative to TMS and coupling constants J in Hz. ^{1}H NMR spectra were referenced to residue of D_2O at δ = 4.75 ppm. ^{199}Hg NMR spectra were recorded in D_2O on a Bruker AMX 600 MHz NMR spectrometer equipped with a 5 mm broadband probe, with referencing 107.4043151 Hz as 0 ppm frequency for ^{199}Hg. Real-time ^{1}H and ^{199}Hg NMR spectra of CH_3HgOH in the presence of CSeH, GSeH, or SePen were studied following a similar procedure except that $_{L}$-selenomethionine was replaced with $_{L}$-selenocysteine, $_{L}$-selenoglutathione and $_{D,L}$-selenopenicillamine, respectively, and that pH was adjusted to 10.5 when working with $_{D,L}$-selenopenicillamine.

X-ray Powder Diffraction. Black precipitate from the above tubes was collected by filtration through a 0.45µm hydrophilic polypropylene membrane filter (PALL Life Sciences), washed with copious amount of milli-Q water and dried at room temperature for 3 days. Powder XRD patterns of the solid were obtained using Philips PW3830/40 X-ray generator with PW1710 with a Rigaku diffractometer with Cu/ $K_{\alpha 1}$ radiation source (k = 1.54059 Å). MDI Datascan/Jade (v. 7.5) data collection and processing software were used. PDF 4.0 database was cross checked to compare and identify the XRD pattern and compound respectively.

Synthesis of bis(methylmercury)selenide. $(CH_3Hg)_2Se$ was synthesized

following the method reported by Naganuma and Imura (*16*). Briefly, 8 mM of $_L$-glutathione (GSH) was dissolved in 100 mL ultrapure water and the pH of the solution was adjusted to 7.4 with 4 M NaOH. 1 mM of CH_3HgCl was dissolved in the solution followed by the addition of 0.4 mM Na_2SeO_3 under vigorous shaking. After a few minutes, the solution was extracted with 100 mL benzene. The benzene layer was collected from the separatory funnel, washed with 100 mL 0.5% GSH (pH 7.4) and then two times with 100 mL ultrapure water. The volume of the solvent was reduced to 10 mL by rotary evaporation (Büchi Rotavapor) at 50ºC. 15 mL of ethyl alcohol was added to this volume and evaporated again until the appearance of silvery flake-like crystals. The solution was cooled and the crsytals were recrystallized from ethanol at 60 ºC. ^{199}Hg NMR was taken from a 1 mM $(CH_3Hg)_2Se$ in 3 mL toluene-d at 37 ºC following the same procedure as described above.

GC/MS Analysis. Mass spectra of the gas phase of a MeHg-selenoamino acid solution were obtained from a gas chromatograph (GC 3800, Varian) interfaced with a triple quadrupole mass spectrometer (MS 320, Varian). 3 mL of 1 mM CH_3HgOH-SeMet solution was heated in a 4 mL amber vial with silicon septa (from Wheaton) at 37ºC. The gas phase of the head space was injected directly to a 30 m VF-5MS capillary column (i.d. 0.25 mm) through a split/splitless inlet. The injector temperature was set at 265 °C and the ion source at 230 °C, and the helium carrier-gas flow was 1 mL/min. Mass spectra were collected by electron ionization at 70 eV with a resolution (Δm) of 1 amu, a scan range from 40 to 600 amu, and a scan speed of 30.46 scans/min.

Results

Real-time ^{1}H and ^{199}Hg NMR spectra collected at 37ºC are shown in Figure 4.1 for a 0.1 M CH_3HgOH solution with the addition of a 0.1 M SeMet at pH 9.0. The pH of 9.0 was chosen according to the pKa value of the amine group of SeMet which has been shown to be the optimal pH for the synthesis of $CH_3HgSeMet$ (via the Hg-N bonding) (*14*). Addition of SeMet into CH_3HgOH resulted in a $\delta(^{1}H)$ shift of the $–CH_3Hg$ peak from 0.94 (Figure 4.1a) to 0.88 ppm (Figure 4.1b) and a $\delta(^{199}Hg)$ shift of the $–CH_3Hg$ peak from -1014.07 ppm (Figure 4.1e) to -861.00 ppm (Figure 4.1f), due to the formation of MeHgSeMet as previously reported (*14*). Ten min after the addition, however, the $–CH_3Hg$ peak was split into a triplet, with a new peak evident at δ 0.23 ppm (Figure 4.1c) suggesting the formation of a new species in the solution. This was verified by the ^{199}Hg NMR spectra, as the initial $–CH_3Hg$ peak at δ -861.00 (Figure 4.1f) diminished rapidly within 10 min with a new peak showing up at δ 27.0 ppm (Figure 4.1g and 4.2b). Both the new ^{1}H peak and the new ^{199}Hg NMR peak, however, disappeared at t = 150 min (Figure 4.1d and 4.1h). Traces of a black precipitate were evident during this time frame. Similar time-dependent changes in the ^{1}H and ^{199}NMR spectra were observed in the CH_3HgOH solution in the presence of CSeH, GSeH, or SePen (Table 4.1 and Figure 4.2b-4.2e).

We attributed this change in the NMR spectra to the formation of $(CH_3Hg)_2Se$ as an intermediate in the MeHg-selenoamino acid solution. This was confirmed by a comparison of the new ^{199}NMR peak formed in situ in the solution (δ = 26.6 – 27.6; Figure 4.2b-e) with that of a purified and crystalized $(CH_3Hg)_2Se$ dissolved in

toluene-d (δ = 25.2 ppm; Figure 4.2a). The slight difference in the δ values is due to the different solvents used: toluene-d was used to dissolve the purified $(CH_3Hg)_2Se$ due to its low solubility in water. The ^1H NMR spectrum of $(CH_3Hg)_2Se$ (Figure 4.1c and Table 4.1) is also very similar to that of its sulfur analog $(CH_3Hg)_2S$ where peaks at δ 0.77 and 0.27 ppm were reported (*17*). Furthermore, the 10 min time frame for the formation of $(CH_3Hg)_2Se$ as observed from Figure 4.1 and Table 4.1 was in good agreement with an earlier in vivo study (*18*) where Hg and Se concentrations in mouse brain were increased after being simultaneously administered with CH_3HgCl and Na_2SeO_3. To our knowledge, Figure 4.1 and Figure 4.2 are the first direct analytical evidence for the presence of $(CH_3Hg)_2Se$ in the MeHg-selenoamino acid system.

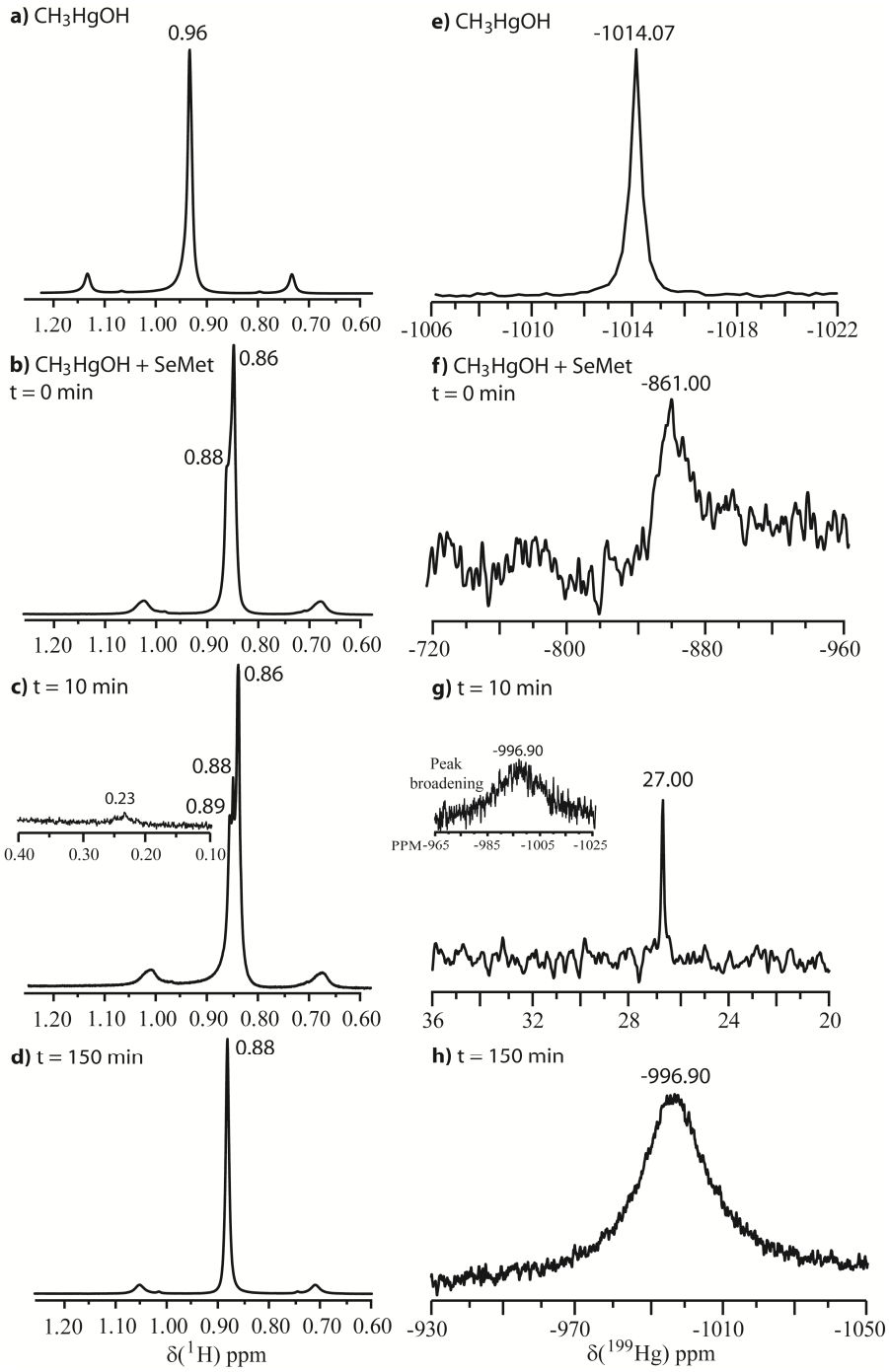

Figure 4.1. Real-time ^{1}H (a-d) and ^{199}Hg (e-h) NMR spectra of a 0.1 M CH_3HgOH solution at various time intervals after the addition of 0.1 M $_L$-selenomethionine at pH = 9.0 and t = 37 ºC.

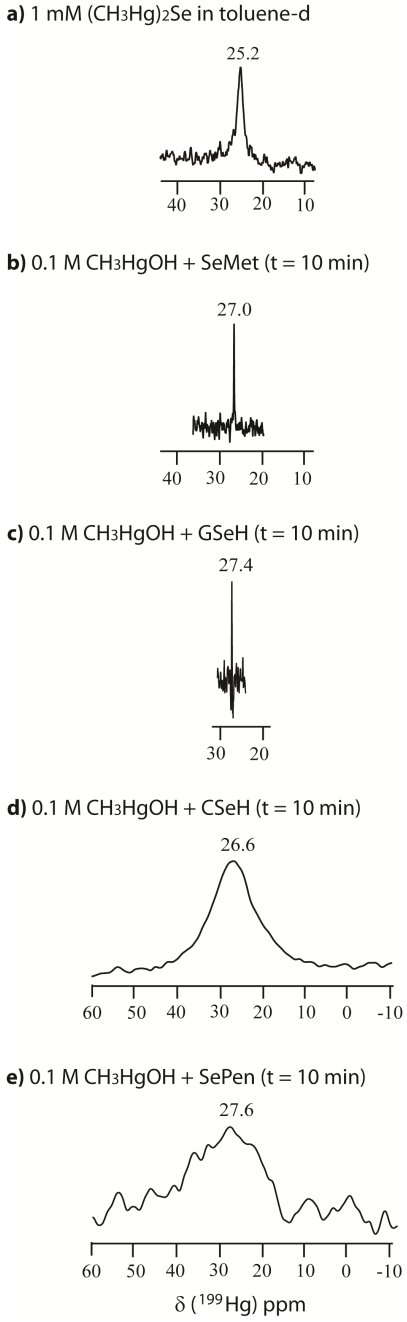

Figure 4.2. ^{199}Hg NMR spectra of 1 mM synthesized $(CH_3Hg)_2Se$ in toluene-d (a) and 0.1 M CH3HgOH solution 10 min after the addition of various selenoamino acids (b-e). All the spectra were obtained at pH = 9.0 and t = 37 ºC. Note that the y-axes were not to the same scale.

We did not observe any ^{1}H peak corresponding to $(CH_3)_2Hg$ which was predicted to be a decomposition product of $(CH_3Hg)_2Se$ (see also Equation 3 in Scheme 4.1 below) (*11*). This is probably due to the subsequent decomposition of $(CH_3)_2Hg$ to CH_3Hg^+ which is indicated by the reappearance of the peaks similar to those of CH_3HgOH at t = 150 min (Figure 4.1d and 4.1h). The presence of a $(CH_3)_2Hg$ intermediate was confirmed by the mass spectrum of the headspace of a solution containing CH_3HgOH and SeMet (Figure 4.3), which showed characterisitic isotopic and fragmentation patterns of $(CH_3)_2Hg$ (*19*).

Table 4.1. Changes in ^{1}H and ^{199}Hg NMR chemical shifts in a CH_3HgOH solution with the addition of various selenoamino acids.

Step	Changes in chemical shifts of C**H**$_3$**Hg**OH with the addition of							
	CSeH		GSeH		SePen		SeMet	
	^{1}H	^{199}Hg	^{1}H	^{199}Hg	^{1}H	^{199}Hg	^{1}H	^{199}Hg
t = 0: Formation of MeHg complex	0.81	-645.00	0.89	-761.93	0.78	-557.81	0.86	-860.99
t = 15 min: Formation of $(CH_3Hg)_2Se$	0.85; 0.20	26.65	0.93; 0.21	27.41	0.81; 0.18	27.57	0.89; 0.23	27.00
t = 150 min: Decomposition of $(CH_3Hg)_2Se$	0.84	-1005.00	0.90	-990.38	0.79	-1006.93	0.88	-996.90

We further invstigated the dependence of the formation of the black precipitate on the molar ratio of CH_3HgOH and the selenoamino acid. A series of 50 μM CH_3HgOH solutions was prepared at a pH corresponding to the pKa value of the –SeH group (for CSeH, GSeH, and SePen) or the pKa value of the -NH_2

group (for SeMet) under Ar at room temperature with constant stirring. Various amounts of the corresponding selenoamino acid were added to create a [MeHg]/[Se] molar ratio gradient from 1:0.1 to 1:3. Bulk amount of a black precipitate was observed after 12 hr when the [MeHg]/[[Se] ratio was 1:3, after 24 hr when the ratio was 1:2, and after 1 week when the ratio was 1:1; no precipitate was observed even after 1 month when [MeHg]/[Se] > 1.0.

The black precipitate was collected by filtration through a 0.45µm hydrophilic polypropylene membrane filter (PALL Life Sciences), followed by being washed with copious amount of milli-Q water and dried at room temperature for 3 days. The XRD pattern of the dried black solid (Figure 4.4) contains peaks characteristic of cubic HgSe (*20*), with scattering angles (2θ) of 25.3°, 29.3°, 42.0°, 49.6°, 67.0° and 76.7° due to Bragg's scattering of 1 1 1, 2 0 0, 2 2 0, 3 1 1, 3 3 1 and 4 2 2, respectively. The particle size was calculated using Scherrer's and Bragg's equations (*20*), i.e. $d = n\lambda/(2 \sin \theta)$ where n=1 respectively (Table 4.2). The particles size is found to be less than 30 nm for the precipitate from the reaction of MeHg with all the four selenoamino acids studied.

Table 4.2. Calculation of particle diameter and lattice spacing from the powder XRD pattern (for intense peaks only).

h k l planes	2θ	θ	FWHM	Lattice Spacing (nm)	Particle size (nm)
1 1 1	25.26	12.63	0.48	0.3523	29.63
2 2 0	42.00	21.00	0.52	0.2150	28.58
3 1 1	49.65	24.83	0.54	0.1835	28.31

Discussion

Mechanism of MeHg Demythylation by Selenoamino Acids. Based on the above results, Scheme 4.1 is proposed for the chemical demethylation of MeHg by selenoamino acids. Reaction 1a shows the formation of a 1:1 MeHg complex with a specific selenoamino acid (CSeH, GSeH, or SePen) via a Hg-Se bonding, as demonstrated in our earlier report (*14*), as well as by Figure 4.1a and 4.1e. Reaction 2a shows that the MeHg-selenoamino acid complex is not stable and undergoes oxidation to form a diselenide and $(CH_3Hg)_2Se$ (Figure 4.1c and 4.1g). The formation of diselenides from selenoamino acids has been reported in the literature (*21, 22*).

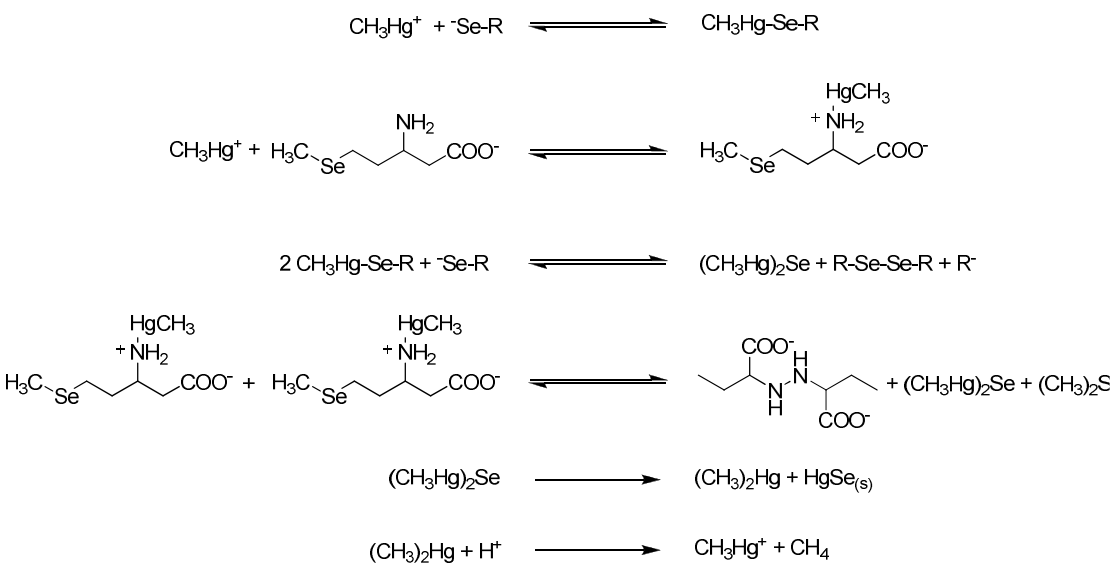

Scheme 4.1. Chemical demethylation of methylmercury by selenoamino acids. $^{-}$Se-R in Reactions (1a) and (2a) represents CSeH, GSeH, or SePen.

A distinction, however, needs to be made in the case of the reaction between MeHg and SeMet, as the complex is formed via a Hg-N bonding (Reaction 1b) under environmentally or physiologically relevant pHs (*14*). We propose that the subsequent formation of $(CH_3Hg)_2Se$ from this complex is due to the deselenization reaction (Reaction 2b), which is known to occur for SeMet producing also dimethylselenide (*23-25*).

The formation of $(CH_3Hg)_2Se$ (Reactions 2a and 2b) is an equilibrium process as demonstrated by the peak broadening effect in Figure 4.1g. Similar to $(CH_3Hg)_2S$ (*9, 10*), $(CH_3Hg)_2Se$ readily degrades to $(CH_3)_2Hg$ and HgSe(s) (Reaction 3) as proposed earlier (*11*) and demonstrated by Figure 4.3 and Figure 4.4, respecyively. The formed $(CH_3)_2Hg$ is decomposed further to CH_3Hg^+ (Reaction 4) (*9, 10*). Based on Figure 4.1 and Figure 4.2, we estimate that the half-life of $(CH_3Hg)_2Se$ is in the order of 1 hr.

The net reaction is thus the formation of black HgSe nanoparticles (Figure 4.4). The small sizes of the HgSe(s) particles formed from the demethylation process are likely due to the size quantization effect of selenoamino acids. We have recently shown that nanoparticles of HgSe of similar sizes could be formed from the reaction of inorganic Hg and sodium selenite in the presence of glutathione (*20*).

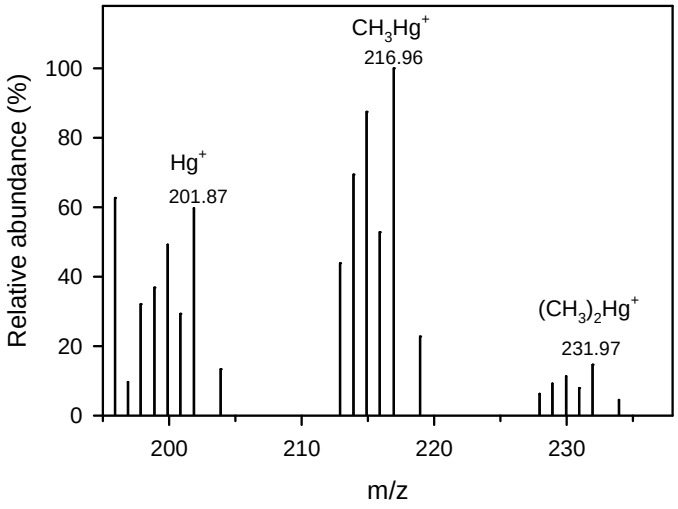

Figure 4.3. Mass spectrum of the headspace of a 1 mM CH_3HgOH-SeMet solution heated to 37 ºC, showing the characteristic isotopic and fragmentation patterns of $(CH_3)_2Hg$.

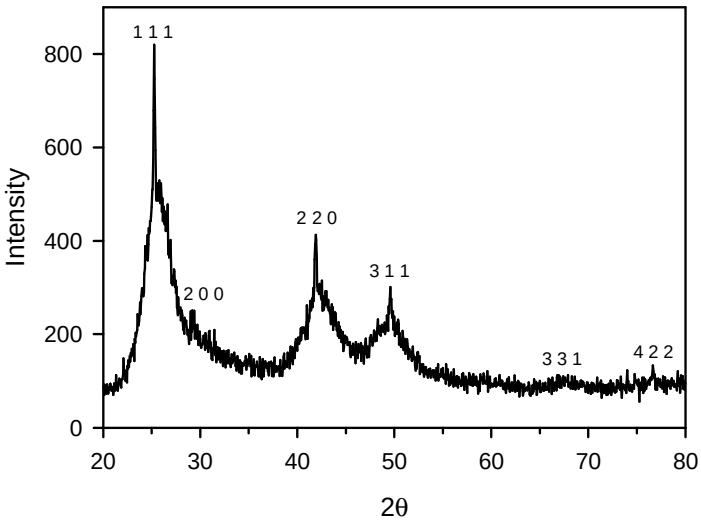

Figure 4.4. XRD pattern of the black solid formed from the degradation of MeHgSeMet after being dried at room temperature. Similar patterns were shown from other MeHg-selenoamino acid complexes.

Biological and Environmental Implications. While the Hg-Se antagonism is the most well-documented toxicological antagonism and Se has long been thought to have played a role in in vivo MeHg demethylation (*11*), this is the first time that a mechanistic pathway has been proposed for Se-aided MeHg demethylation. Different from earlier in vivo or in vitro studies where MeHg and sodium selenite were simultaneously administered to animals (e.g., (*26, 27*)), Scheme 4.1 suggests that the Se does not need to be in the sodium selenite form. Instead, any selenoamino acid could initiate the reaction, followed by oxidation or deselenization to produce $(CH_3Hg)_2Se$ which subsequently decomposes to HgSe(s). Therefore, Scheme 1 may explain the observed HgSe(s) granules in the liver of marine mammals where exposure to Hg is almost exclusively via dietary uptake of MeHg (*28*, *29*).

Scheme 1 also provides an alternative pathway for MeHg crossing the blood-brain barrier. While the generally held view attributes the blood-brain transport of MeHg to the structural mimicry of MeHg-$_L$-cysteinate with methionine (*3*), a recent study suggested that only the L_α regions of the two compounds are similar which questions the mode of transport (*30*). Instead, Scheme 1 suggests that the $(CH_3Hg)_2Se$ could potentially be involved in the blood-brain transfer due to its high lipophilicity. This would explain the earlier observation that after the injection of $(CH_3Hg)_2Se$, concentrations of Hg and Se in the brain became higher in mouse than when it is administered with MeHg and/or Na_2SeO_3 (*13*).

Furthermore, it is possible that selenoamino acid-aided MeHg demethylation to HgSe(s) may occur in the aquatic environment where MeHg is primarily formed. Though there has been no report on the concentrations of selenoamino acids in natural waters, nanomolar to micromolar levels of their sulfur counterparts have been reported in surface and sediment pore waters (e.g., (*31*, *32*)).

Acknowledgements

This research was funded by the Natural Science and Engineering Council (NSERC) of Canada (F.W.). M.A.K.K. was supported by an NSERC PGS-D fellowship. We thank K. Murat for taking all the NMR spectra, W. Buchannon for GC-MS analysis, N. Ball for X-ray power diffraction analysis, and M. Lemes for laboratory assistance.

References

(1) WHO. (1990) Methylmercury, In *Environmental Health Criteria 101*, International programme on chemical safety, World Health Organization, Geneva.

(2) Myers, G. J. and Davidson, P. W. (1998) Prenatal methylmercury exposure and children: neurologic, developmental, and behavioral research. *Environ. Health Perspect. 106*, 841-847.

(3) Aschner, M. and Aschner, J. L. (1990) Mercury neurotoxicity: mechanisms of blood-brain barrier transport. *Neurosci. Biobehav. Rev. 14*, 169-176.

(4) Harada, M. (1995) Minamata disease: methylmercury poisoning in Japan caused by environmental pollution. *Crit. Rev. Toxicol. 25*, 1-24.

(5) Mergler, D., Anderson, H. A., Chan, L. H. M., Mahaffey, K. R., Murray, M., Sakamoto, M. and Stern, A. H. (2007) Methylmercury exposure and health effects in humans: a worldwide concern. *Ambio 36*, 3-11.

(6) Compeau, G. C. and Bartha, R. (1985) Sulfate-reducing bacteria: principal methylators of mercury in anoxic estuarine sediment. *Appl. Environ. Microbiol. 50*, 498-502.

(7) Fitzgerald, W. F., Lamborg, C. H. and Hammerschmidt, C. R. (2007) Marine biogeochemical cycling of mercury. *Chem. Rev. 107*, 641-662.

(8) Stumm, W. and Morgan, J. J. (1996) *Aquatic Chemistry*, 3rd ed., Wiley, New York.

(9) Craig, P. J. and Bartlett, P. D. (1978) The role of hydrogen sulphide in environmental transport of mercury. *Nature 275*, 635 - 637.

(10) Rowland, I. R., Davies, M. J. and Grasso, P. (1977) Volatilisation of methylmercuric chloride by hydrogen sulphide. *Nature 265*, 718 - 719.

(11) Khan, M. A. K. and Wang, F. (2009) Mercury-selenium compounds and their toxicological significance: toward a molecular understanding of the mercury-selenium antagonism. *Environ. Toxicol. Chem. 28*, 1567-1577.

(12) Masukawa, T., Kito, H., Hayashi, M. and Iwata, H. (1982) Formation and possible role of bis(methylmercury) selenide in rats treated with methylmercury and selenite. *Biochem. Pharmacol. 31*, 75-78.

(13) Naganuma, A., Kojima, Y. and Imura, N. (1980) Interaction of methylmercury and selenium in mouse: formation and decomposition of bis(methylmercuric)selenide. *Res. Comm. Chem. Pathol. Pharmacol. 30*, 301-316.

(14) Khan, M. A. K., Asaduzzaman, A. M., Schreckenbach, G. and Wang, F. (2009) Synthesis, characterization and structures of methylmercury complexes with selenoamino acids. *Dalton Transac.*, 5766-5772.

(15) Carty, A. J., Malone, S. F., Taylor, N. J. and Canty, A. J. (1983) Synthesis, spectroscopic, and x-ray structural characterization of methylmercury-$_{D,L}$-selenocysteinate monohydrate, a key model for the methylmercury(II)-selenoprotein interaction. *J. Inorg. Biochem. 18*, 291-300.

(16) Naganuma, A. and Imura, N. (1981) New method for bis(methylmercury) selenide synthesis from methylmercuric chloride, sodium selenite and reduced glutathione. *Chemosphere 10*, 441-443.

(17) Higa, K. T. and Fallis, K. A. (2002) The Synthesis of II-VI binary alloys and organometallic compounds via Me_3SiOR elimination reactions. *J. Cluster Sci. 13*, 533-541.

(18) Naganuma, A. and Imura, N. (1980) Bis(methylmercuric) selenide as a reaction product from methylmercury and selenite in rabbit blood. *Res. Comm. Chem. Pathol. Pharmacol. 27*, 163-173.

(19) NIST. (2010) NIST Standard Reference Database 69: NIST Chemistry WebBook, National Institute of Standards and Technology.

(20) Khan, M. A. K. and Wang, F. (2009) Reversible dissolution of glutathione-mediated $HgSe_xS_{1-x}$ nanoparticles and possible significance in Hg-Se antagonism. *Chem. Res. Toxicol. 22*, 1827-1832.

(21) Tsai, J. H., Hiserodt, R. D., Ho, C.-T., Hartman, T. G. and Rosen, R. T. (1998) Determination of volatile organic selenium compounds from the Maillard reaction in a selenomethionine-glucose model system. *J. Agric. Food Chem. 46*, 2541-2545.

(22) Mounicou, S., Shah, M., Meija, J., Caruso, J. A., Vonderheideb, A. P. and Shannb, J. (2006) Localization and speciation of selenium and mercury in *Brassica juncea*—implications for Se–Hg antagonism. *J. Anal. At. Spectrom. 21*, 404-412.

(23) Stauffer, C. S. and Datta, A. (2002) Efficient synthesis of (S,S)-ethambutol from L-methionine. *Tetrahedron 58*, 9765-9767.

(24) Młochowski, J., Kloc, K., Lisiak, R., Potaczek, P. and Wójtowicz, H. (2007) Developments in the chemistry of selenaheterocyclic compounds of practical importance in synthesis and medicinal biology. *ARKIVOC VI*, 14-46.

(25) Młochowski, J. and Giurg, M. (2008) New Trends in Chemistry and Application of Aromatic and Related Selenaheterocycles. *Top. Heterocycl. Chem. 7*, 287-340.

(26) Fang, S. C. (1974) Induction of carbon-mercury cleavage enzymes in rat liver by dietary selenite. *Res. Comm. Chem. Pathol. Pharmacol. 9*, 579-582.

(27) Norseth, T. and Clarkson, T. W. (1970) Studies on the biotransformation of ^{203}Hg-labelled methyl mercury chloride in rats. *Arch. Environ. Health 21,* 717-727.

(28) Arai, T., Ikemoto, T., Hokura, A., Terada, Y., Kunito, T., Tanabe, S. and Nakai, I. (2004) Chemical forms of mercury and cadmium accumulated in marine mammals and seabirds as determined by XAFS analysis *Environ. Sci. Technol. 38,* 6468-6474.

(29) Palmisano, F., Cardellicchio, N. and Zambonin, P. G. (1995) Speciation of mercury in dolphin liver: a two-stage mechanism for the demethylation accumulation process and role of selenium. *Mar. Environ. Res. 40,* 109-121.

(30) Hoffmeyer, R. E., Singh, S. P., Doonan, C. J., Ross, A. R. S., Hughes, R. J., Pickering, I. J. and George, G. N. (2006) Molecular mimicry in mercury toxicology. *Chem. Res. Toxicol. 19,* 753-759.

(31) Zhang, J., Wang, F., House, J. D. and Page, B. (2004) Thiols in wetland interstitial waters and their role in mercury and methylmercury speciation. *Limnol. Oceanogr. 49,* 2276-2286.

(32) Al-Farawati, R. and van den Berg, C. M. G. (2001) Thiols in coastal waters of the Western North Sea and English Channel. *Environ. Sci. Technol. 35,* 1902-1911.

Preface to Chapter 5

This chapter is based on the following manuscript submitted in the journal "*Chemical Research in Toxicology*". Full citation of the paper is as follows:

> **Khan, M. A. K.**; Wang, F. Reversible Dissolution of Glutathione-Mediated $HgSe_xS_{1-x}$ Nanoparticles and Possible Significance in Hg-Se antagonism. *Chem. Res. Toxicol.* **2009**, *22* (11), 1827–1832.

This chapter focuses on the fate of inorganic mercury at physiological conditions. Formation of the biomineral, $HgSe_xS_{1-x}(s)$ ($0<x\leq1$), as the end product of the Hg-Se antagonism is established by UV-visible spectroscopy, infrared spectroscopy, microbeam scanning electron microscopy, transmission electron microscopy, x-ray diffraction, and x-ray photoelectron spectroscopy. This chapter is related to the previous chapters on the theme of the antagonism of mercury as both organic and inorganic form of mercury may enter and biotransform into each other in biological systems.

Chapter 5: Reversible Dissolution of Glutathione-Mediated $HgSe_xS_{1-x}$ Nanoparticles and Possible Significance in Hg-Se antagonism

Abstract

A new pathway is proposed for the in vivo biomineralization of $HgSe_xS_{1-x}(s)$ ($0<x\leq1$) which is thought to be the ultimate metabolic product responsible for the Hg-Se antagonism in biological systems. The pathway involves the reaction of Hg(II) with selenite in the presence of glutathione (GSH). The resulting GSH-mediated $HgSe_xS_{1-x}$ nanoclusters are reversibly soluble depending on the pH which could account for the distribution pattern of $HgSe_xS_{1-x}(s)$ in different tissues. The HgSe species involved and the nature of bonding were studied by UV-visible spectroscopy, infrared spectroscopy, microprobe scanning electron microscopy, transmission electron microscopy, x-ray diffraction, and x-ray photoelectron spectroscopy.

Introduction

The toxicological antagonism between mercury (Hg) and selenium (Se) has been known for many decades. Although the mechanism is yet to be fully understood, the key step most likely involves the formation of in vivo Hg-Se complexes that are less reactive, less bioavailable and/or less toxic (*1, 2*). Among the possible in vivo Hg-Se complexes, the inorganic HgSe(s) is the least soluble and most likely the final metabolic product. The presence of HgSe(s) granules has been analytically confirmed in the liver and kidneys of many marine mammals and sea birds (*3-8*). Two major questions however remain a subject of debate: how is HgSe(s) formed in vivo? And why is HgSe(s) only present in the liver and kidneys but not in other tissues?

Suzuki and colleagues were the first to propose the role of selenoprotein P (SelP) in solubilizing HgSe in the blood plasma (*9-11*). By adding selenite (SeO_3^{2-}) and $HgCl_2$ to glutathione (GSH)-spiked rat and rabbit blood serum, they proposed the formation of a $(HgSe)_n$ polymer which is kept "soluble" in the plasma by binding to SelP. The observation that SelP only binds with the $(HgSe)_n$ polymer but not the free Hg^{2+} ions led them to suggest an unusual binding where the polymer is held by the intramolecular ionic bond between the cationic and anionic centers of SelP, instead of direct bonding to the thiol or selenol groups of SelP (*9*). However, binding to SelP is not the only mechanism to keep HgSe soluble. It has been known for almost 30 years that a water soluble black complex can be formed by the reaction of Hg(II), selenite, and GSH in a buffered solution (pH 7.4) (*12*). Gailer et al. (*13*) identified this complex as a $(HgSe)_n$ core with GSH bound at the surface.

When making the water soluble HgSe solution following the procedure of Gailer et al. (*13*), we noticed that upon acidification a black precipitate was formed and that the precipitation-dissolution was reversible simply by adjusting the pH of the solution. Here we report the characterization of this pH reversible precipitation-dissolution which involves a soluble $HgSe_xS_{1-x}$ complex ($0<x\leq1$) with GSH, GSH-mediated $HgSe_xS_{1-x}$ nanoclusters, and ultimately $HgSe_xS_{1-x}$ nanoparticles. The reactions not only provide a new and simple means to synthesizing small sizes (~ 9 nm) $HgSe_xS_{1-x}$ nanoparticles, but also shed new light into the biomineralization and tissue distribution of HgSe in biological systems.

Materials and Methods

All reagents (ACS grade or higher) were obtained from Sigma-Aldrich and used without further purification.

Preparation of the GSH-Mediated HgSe Species (A and B)

The dissolved HgSe species (A) was prepared following the procedure described by (*13*). In brief, 0.75 mmol of GSH was dissolved in 1.2 mL of phosphate buffered saline (PBS) buffer and the pH was adjusted to 7.4 by adding 4.0 M NaOH. The solution was incubated for 15 min at 37ºC before 160 µL of a solution containing 0.47 mmol each of Na_2SeO_3 and $HgCl_2$ in the PBS buffer were added. This immediately produced a black solution which was stable (i.e., without any visible precipitate) at pH 7.4 or higher for at least one month at room temperature.

Upon acidification by 3.0 M HNO_3 to a final pH of ~3.5, a black precipitate (Species B) was formed which could be solublized in the same solution upon addition of

4 M NaOH to pH > 7.0. Species B was found to be stable (i.e., capable of being re-solubilized) for at least 6 hr at room temperature.

Preparation of the Insoluble $HgSe_xS_{1-x}$ nanoparticles (C and D)

The above black precipitate (Species B) was collected by filtration through a 0.45µm hydrophilic polypropylene membrane filter (PALL Life Sciences), washed with copious amount of Milli-Q (Millipore Milli-Q Element) water to remove any un-reacted GSH, and dried at room temperature for 3 days. The isolated precipitate (Species C) was insoluble in water in the pH range studied (2 – 10) with or without GSH.

After a prolonged storage (more than 2 weeks) of Species A at room temperature, its subsequent acidification yielded another black precipitate (Species D) which was collected by following the same procedure as Species C. Species D was found to be of different crystalline nature and composition from Species C.

Characterization of the Hg-Se species

The UV-visible absorption spectrum of the black solution containing Species A was collected on a Varian Cary 500 spectrophotometer. The solution was further characterized by transmission electron microscopy (TEM) and x-ray photoelectron spectroscopy (XPS). In both cases, a droplet of the solution was placed on a carbon grid and mica respectively and dried under high vacuum for 3 days before being analyzed. The TEM analysis was done on a JEOL 2000 FX analytical transmission electron microscope at various acceleration potentials. The XPS was carried out on a Kratos AXIS ULTRA X-ray photoelectron spectrophotometer (XPS) with the Mg K lines being used for excitation. The position of the core levels was calibrated relative to the C 1s line (284.6 eV).

The solid species C and D were analyzed by X-ray powder diffraction (XRD) and microprobe scanning electron microscopy (MSEM). The XRD was done on a Rigaku diffractometer with a Cu/ $K_{\alpha 1}$ radiation source (k = 1.54059 Å) with the software MDI Datascan/Jade (v. 7.5) for data collection and processing. PDF 4.0 database was cross checked for compound identification. The MSEM was carried out on a CAMECA SX100 electron microprobe with PGT EDS and 5 WDS spectrometers. Pyrite, Bi_2Se_3 and HgTe were used as reference materials for the quantification of S, Se and Hg respectively. Infrared (IR) spectra were also obtained for unwashed Species C in KBr on a Thermo-Nicolet Nexus 870 FT-IR at a resolution of 4 cm^{-1}.

Results and Discussion

Reversible Dissolution-Precipitation of the Glutathione-Mediated Hg-Se Species

Change in pH has a dramatic effect on the solubility of the GSH-mediated HgSe species. At pH ≥7.0, the species is soluble (Species A), forming a black solution. However, when the solution is acidified to pH 3.5, a black precipitate (Species B) is formed. This precipitation-dissolution process is reversible simply by changing the pH of the solution.

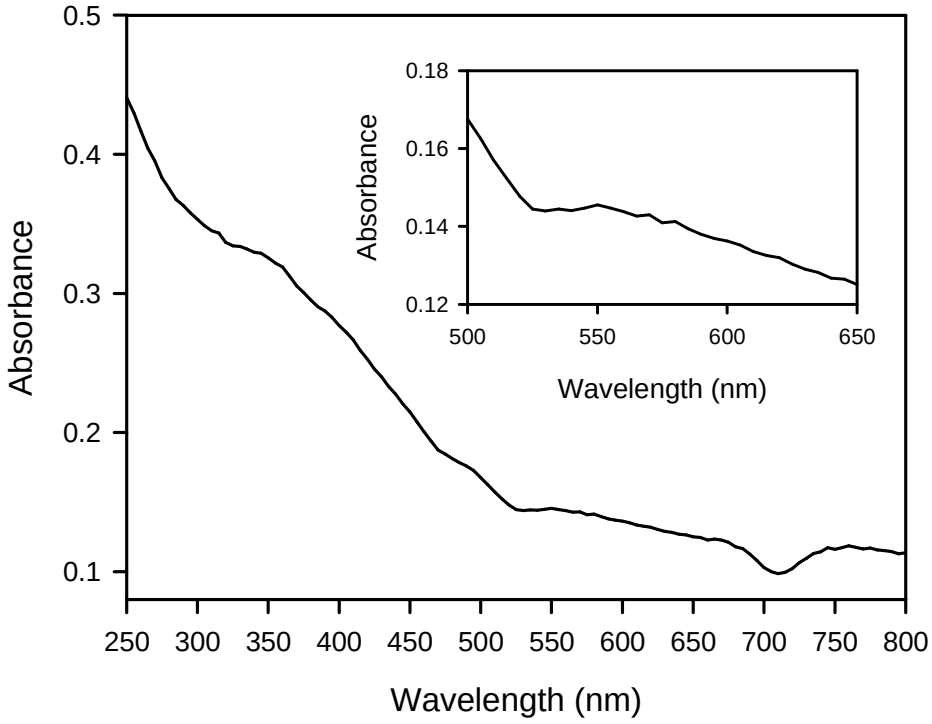

Figure 5.1. UV-vis spectra of the dissolved GS-HgSe species (species A at pH 7.4)

UV-visible absorption spectra (Figure 5.1) showed a distinct absorption maximum at ~550 nm for the dissolved species A, similar to what has been reported for $HgSe_{1-x}S_x$ nanoparticles in mineral oil (*14*) or acetone (*15*). TEM showed that the dissolved species, upon vacuum drying, is present as spherical aggregates with a diameter of <5 nm (Figure 5.2).

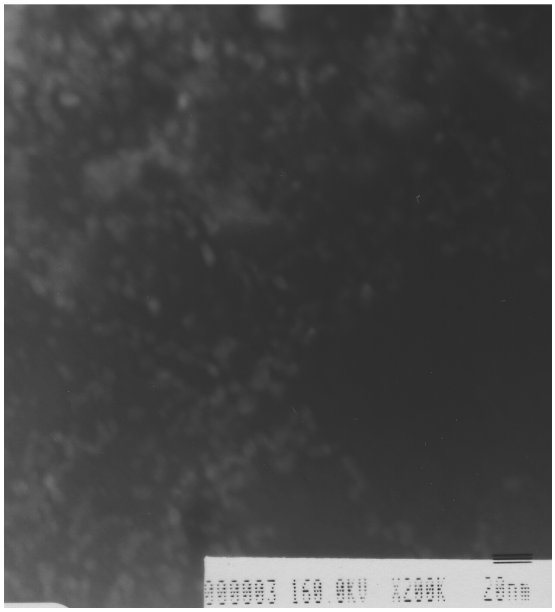

Figure 5.2. TEM micrograph of the dissolved GS-HgSe species (species A at pH 7.4; after being vacuum dried) at 200K magnification

No peaks of elements other than C, O, N, Na, S, Hg, and Se were observed on the wide-scan XPS spectra of Species A after being vacuum dried. The Hg 4f peak at 99.3 eV (Figure 5.3a) could be indicative of a Hg-Se bond (100.05 eV; (*16*)) or Hg(0) (b.e. = 99.2-99.8 eV; (*17*)) resulted from the reduction of Hg(II) by GSH; the resolution of the instrument (±1.0 eV) did not allow for the distinction between these two possibilities. However, the Se 3d peak at 53.2 eV (Figure 5.3b) supports the presence of a Hg-Se bond (*16, 18*). The Hg 4f peak at 103.4 eV at pH 7.4 (Figure 5.3a) is indicative of a Hg-S bond (*19-21*), as the high-energy component is known to increase with increasing pH (*22*). This is also supported by the S 2p peak. As shown in Figure 5.3c, deconvolution of the S 2p gives rise to a doublet at 162.7 eV (S $2p_{3/2}$) and 163.8 eV (S $2p_{1/2}$) with a ~3:1 area ratio. The binding energy of the S $2p_{3/2}$ photoelectrons at 162.7 eV is an exact match for the Hg-S bond reported elsewhere (*22, 23*). The XPS spectra thus suggest that species A

contains –S-Hg-Se-. The S $2p_{1/2}$ peak at 163.8 eV is likely due to the un-bound S which can interact with the HgSe core electronically through space as discussed below. C (1s), O (1s), and N (1s) give their characteristic peaks at the expected binding energies and are not shown in Figure 5.3.

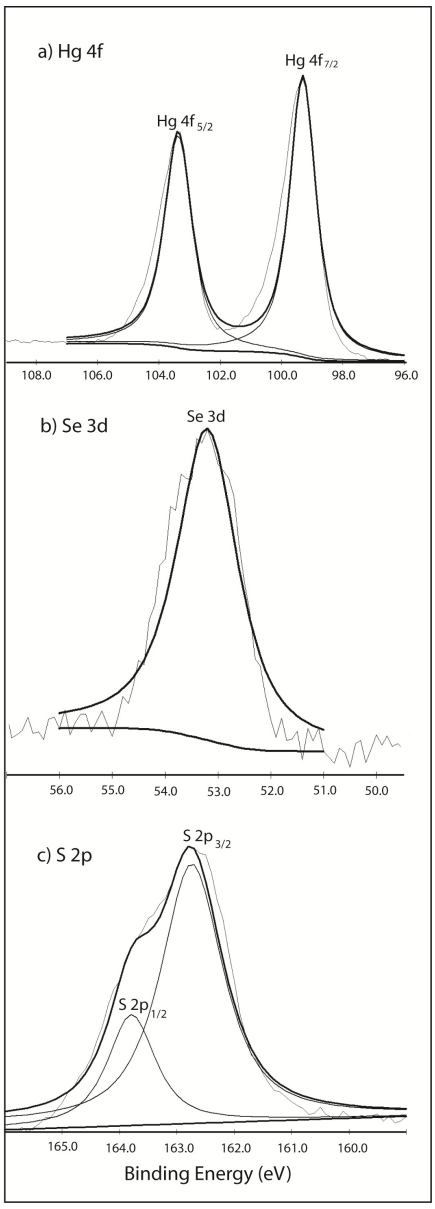

Figure 5.3. XPS spectra of the dissolved GS-HgSe species (Species A at pH 7.4) after being vacuum dried.

Insoluble $HgSe_xS_{1-x}$ nanoparticles

The powder XRD pattern of Species C (Figure 5.4a) shows features characteristic of cubic HgSe(s), with peaks at scattering angles (2θ) of 25.3°, 29.2°, 41.9°, 49.6°, 66.9° and 76.7° corresponding to Bragg's scattering of 1 1 1, 2 0 0, 2 2 0, 3 1 1, 3 3 1 and 4 2 2 crystal planes of cubic HgSe, respectively. The particle size (D) and lattice spacings (d) were estimated by using Scherrer's equation and the Bragg's equation, respectively. At a selected 2θ:

$$D = 0.9\lambda/\beta \cos\theta$$

$$d = n\lambda/(2 \sin\theta)$$

where λ is the frequency of the X-ray, β is the full width at half maximum (FWHM) of the peak, and n =1. As shown in Table 5.1, the particle size is calculated to be ~ 9 nm. HgSe nanoparticles of this size range have been previously produced by reacting Hg(II) with freshly prepared selenide or polyselenides (*16*), or with organic selenide at high temperature (*21*). In the present study, the size quantization is possible due to the presence of excess GSH molecules which form a covalent bond with the nanoparticle core and thus stabilize the nanoparticles. The role of GSH is further supported by the IR spectrum of the unwashed nanoparticles (Figure 5.5) where a reminiscence of the organic moiety is evident.

Table 5.1. Particle Size and Lattice Spacing of HgSe(s) nanoparticles (Species C) calculated from the powder XRD (Figure 5.4a)

h k l planes	2θ	FWHM (average ± s.d.)	lattice spacing (Å)	particle size (nm)
1 1 1	25.26	1.63 ± 0.02	3.524	8.7
2 2 0	41.90	1.57 ± 0.03	2.154	9.5
3 1 1	49.60	1.59 ± 0.02	1.836	9.6

Powder XRD of the solid formed after more than 2 weeks of storage of the black solution at room temperature (Species D), however, yielded a different pattern (Figure 5.4b) which, with database search, matched with onofrite or $HgSe_xS_{1-x}$ ($0<x<1$). Four major, rather broad peaks were observed, three of which were present in between the angles of diffraction (2θ) for HgSe and HgS. The d values (lattice spacing) of the three peaks (2θ = 30.38, 43.20 and 51.36°, corresponding to Bragg's scattering of 2 0 0, 2 2 0, and 3 1 1, respectively) were calculated to be 2.950, 2.090 and 1.780 Å, from which a lattice constant a_0 of 5.9253 Å was calculated for the solid. Based on Vegard's law that a linear correlation exists between the lattice constant and the chemical composition (molar fraction) of a solid, the ratio of HgSe and HgS in this solid was estimated to be 0.7:0.3. This ratio is in excellent agreement with the MSEM analysis of solid D, which revealed that the product consisted of Hg, Se and S with a composition of approximately $HgSe_{0.7}S_{0.3}$. Particle size calculation using Scherrer's equation for this solid yielded a similar size as for Species C.

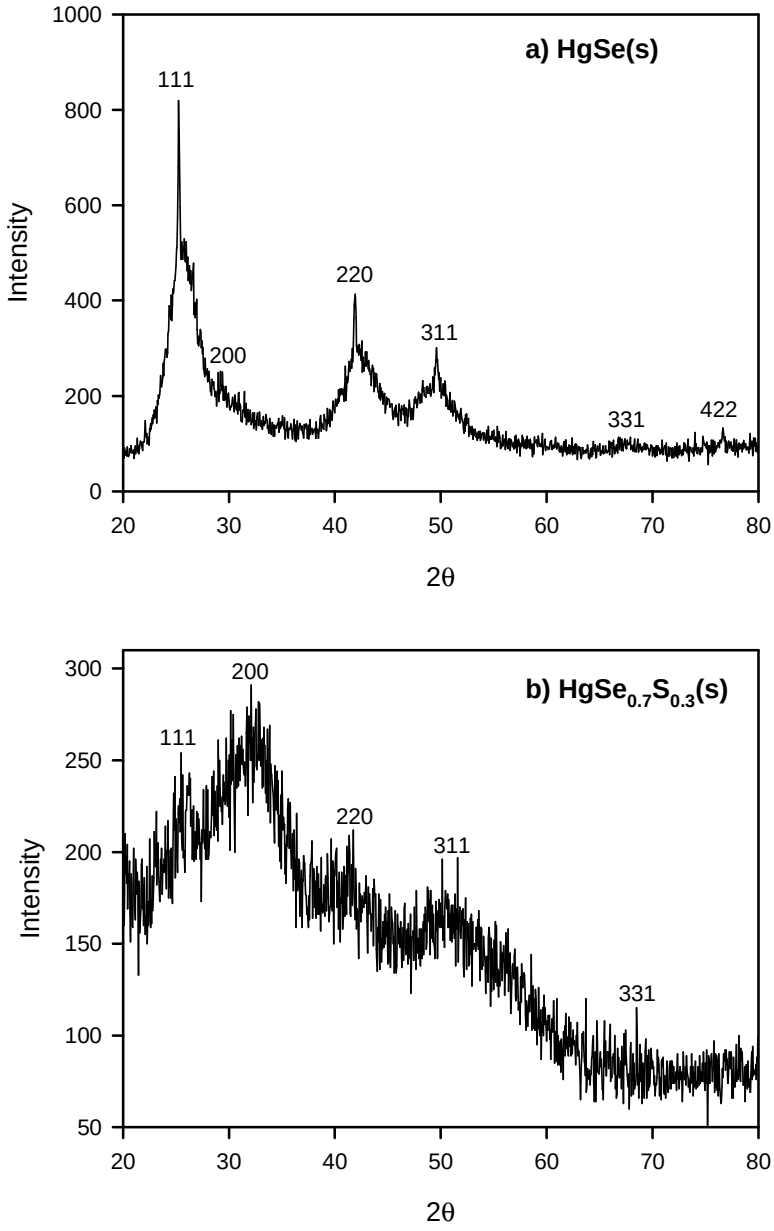

Figure 5.4. XRD pattern of a) HgSe(s) nanoparticles formed by acidification of a freshly prepared GS-HgSe solution and b) $HgSe_{0.7}S_{0.3}$(s) nanoparticles formed by acidification of a GS-HgSe solution that had been kept for two weeks under the room temperature. In both cases, the precipitate was filtered through a 0.45 um membrane, and air dried at room temperature before being analyzed.

Mechanistic Aspects

Several mechanisms have been proposed to explain the interaction between GSH and Au-nanoparticles (*24-26*). To account for the pH dependent assembly-disassembly of GSH-mediated Au-nanoparticles, Lim et al. (2008) proposed that the hydrogen bonding of the carboxylic acid groups of GSH molecules is primarily responsible for the interparticle interaction between GSH-mediated Au nanoparticles. Our observation that dissolution-precipitation of GSH-mediated HgSe nanoparticles is reversible upon change of pH agrees well with this hydrogen bonding mechanism.

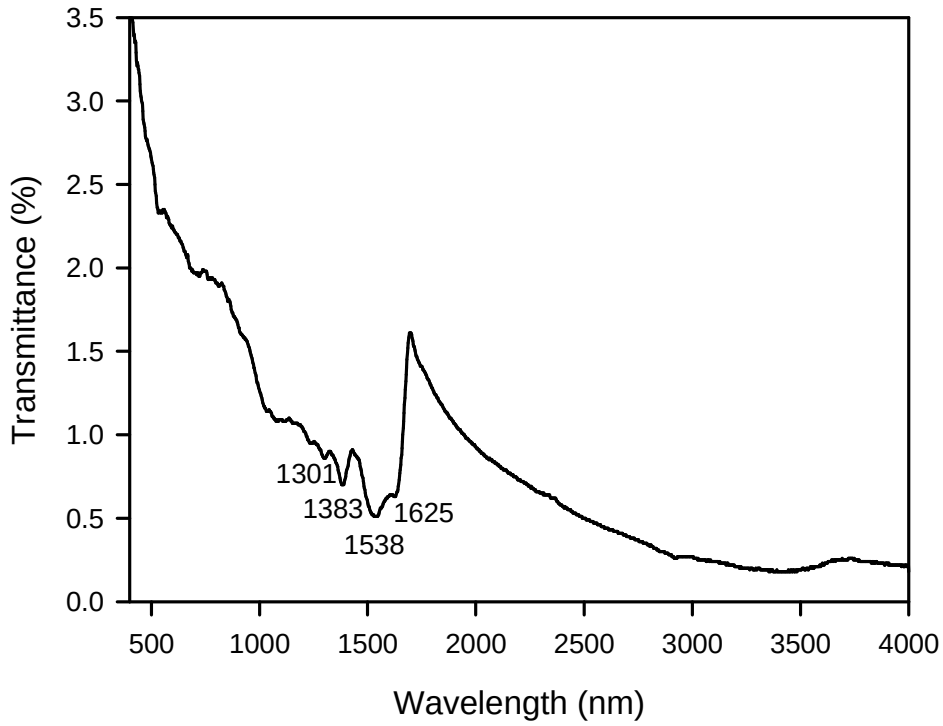

Figure 5.5. IR spectrum of the unwashed HgSe nanoparticles in KBr.

Based on the well known chemistry between GSH and Na_2SeO_3 (*27-30*) and the interparticle interaction model (*26*), the following chemical reactions (Scheme 5.1) and

interparticle interactions (Scheme 5.2) are proposed for the formation of $HgSe_xS_{1-x}$ nanoparticles in the GSH-SeO_3^{2-}-Hg(II) system.

$$GSH + SeO_3^{2-} \longrightarrow GSSG + GSSeSG + HSe^- \quad (1a)$$

$$GSSeSG \longrightarrow GSSG + HSe^- \quad (1b)$$

$$GSH \xrightarrow{Desulfurization} \gamma\text{–}_L\text{-glutamyl-}_L\text{-anayl-}_L\text{-glycine} + HS^- \quad (1c)$$

$$xHSe^- + (1-x)\,HS^- + HgL + GSH \longrightarrow GS\text{-}HgSe_xS_{1-x}\ (\text{Species A}) \quad (2a)$$

$$n\,(GS\text{-}HgSe_xS_{1-x}) + H^+ \rightleftharpoons (GS\text{-}HgSe_xS_{1-x})_n\ (\text{Species B}) \quad (2b)$$

$$(GS\text{-}HgSe_xS_{1-x})_n \longrightarrow n\,GSH + (HgSe_xS_{1-x})_n(s)\ (\text{Species C \& D}) \quad (2c)$$

$$GSSeSG \longrightarrow GSSe^- + GSH \quad (3a)$$

$$GSSe^- + HgL \longrightarrow GS\text{-}Se\text{-}Hg \quad (3b)$$

Scheme 5.1. General chemical reactions involved in the formation of $HgSe_{1-x}S_x$ nanoparticles. The value of x ($0<x\leq1$) is dependent on the extent of GSH desulfurization: x=1 when there is no desulfurization. L is a complexing ligand for Hg^{2+}.

Reactions 1a and 1b are known to occur at physiological pH (*27, 29*). The formation of GSSeSG from the reaction of GSH with SeO_3^{2-} ion (Reaction 1a) was reported by Ganther (*31*). GSSeSG is not stable and breaks down to GSSG and HSe^- (Reaction 1b) (*29, 30*). A desulfurization process can also occur to GSH forming a tripeptide γ-glutamyl-alayl-glycine and inorganic sulfide HS^- (Reaction 1c; (*32-36*).

In the absence of GSH, selenide and sulfide react rapidly with Hg(II) to form insoluble $HgSe_xS_{1-x}(s)$ (the value of x is dependent on the relative concentration of selenide and sulfide). However, in the presence of excess amount of GSH as is the case in

this study, we propose that the $HgSe_xS_{1-x}$ species formed is immediately bonded to GSH to form the soluble GS-$HgSe_xS_{1-x}$ species (Species A; Reaction 2a). Upon acidification, the carboxylic acid groups are prontonated and can form hydrogen bonding with other GS-$HgSe_xS_{1-x}$ resulting in $(GS\text{-}HgSe_xS_{1-x})_n$ nanoclusters (Species B; Reaction 2b) which gives rise to the black precipitate. The presence of GSH once again prevents Species B from aggregating into $HgSe_xS_{1-x}(s)$ and keeps the reaction 2b reversible.

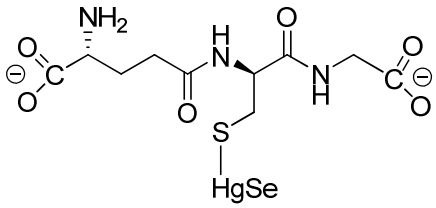

A. GSH-mediated soluble HgSe complex: GS-HgSe

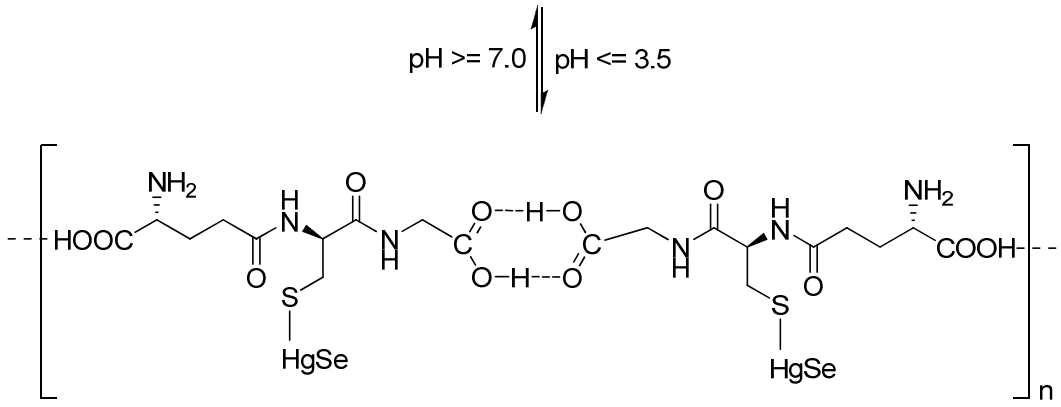

B. GSH-mediated insoluble HgSe nanoclusters: $(GS\text{-}HgSe)_n$

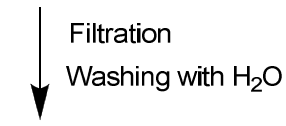

$HgSe_{(S)}$

C. Insoluble nanoparticles: HgSe(s)

Scheme 5.2. Interparticle interactions involved in the formation of HgSe nanoparticles.

The dynamics among Species A, B and C is further depicted in Scheme 5.2. The structure of GSH in Scheme 5.2 was first reported on Au-nanoparticles (*26*) based on DFT computational data (*37*), and supported in the present case by the XPS spectra which indicate the presence of two types of S (Figure 5.3c). The carboxylic acid groups of both the glutamate moiety (pKa = 2.05) and the glycine moiety (pKa = 3.5) of GSH can form hydrogen bonding; however, the observation that the black precipitate forms when pH <= 3.5 suggests that the latter is primarily responsible. At pH > 3.5, the clustering is either hindered or not favoured as a result of the deprotonation of the acid groups.

The difference between Species C and D is likely related to the extent of the desulfurization process of GSH which controls the concentration of inorganic sulfide HS^- in the system. In the case of solid D, the black solution containing A had been stored for more than 2 weeks at room temperature during which time the GSH desulfurization occurred and thus resulted in a mixed solid $HgSe_{0.7}S_{0.3}$. The experimental condition in this study (pH 7.4 and ambient temperature) is indeed favorable for the desulfurization process as was reported in refs (*32-36, 38*). In contrary, Solid C was formed by acidifying a freshly prepared black solution containing A in which case the desulfurization was minimal and thus the final solid was pure HgSe. Schemes 5.1 and 5.2 provide a new and simple way of synthesizing $HgSe_xS_{1-x}$ nanoparticles in aqueous media.

Of key interest in Schemes 5.1 and 5.2 is the nature of the bonding among S, Hg and Se. There are several possibilities: i) S-Hg-Se covalent bonding; iii) surface bonding between S and a (HgSe) nanoparticle, i.e., S-(HgSe), and iii) S-Se-Hg covalent bonding. The XPS spectra (Figure 5.3) demonstrated the presence of both Hg-S and Hg-Se in

Species A, supporting S-Hg-Se covalent bonding (type i). Type ii bonding is also possible via space. As the Hg atom in HgSe is partially electropositive it can form an electrostatic interaction with the negatively charged –SH group of GSH. This is in agreement with the presence of an unbound S (2p) peak in the XPS (Figure 5.3b) and reminiscence of the organic moiety in the FTIR spectrum of Species C and D (Figure 5.5) when taken only after filtration and dried and not washed with water. Type iii bonding (S-Se-Hg covalent bonding) was proposed by Gailer et al. (*13*) based on EXAFS analysis of Species A. Although this is possible (see Reactions 3a,b), the resulting compound would be prone to hydrolysis, as the Se-S bond can be easily broken down under the present reaction conditions (*39*) and subsequently form HgSe, which would not explain the reversibility of Reaction 2b. Gailer et al. (*13*) indeed acknowledged that the EXAFS data were not conclusive and did not rule out the possibility of S-Hg-Se bonding.

Implications in the Hg-Se Antagonism in Biological Systems

One of the major puzzles in the Hg-Se bioantagonism is that the occurrence of HgSe(s) granules so far has only been reported in the liver and kidneys of animals. Given the strong affinity of Hg(II) to Se(-II), one would expect HgSe(s) be formed at any body tissues where both reactants are present. Suzuki et al. (*9-11*) explained the lack of HgSe(s) in plasma by proposing the presence of a soluble $(HgSe)_n$-SelP complex. Gailer et al. (*13*) further proposed the bonding between SelP and $(HgSe)_n$ could be via replacement of GSH by SelP on the surface of the $(HgSe)_n$ core. Schemes 1 and 2 proposed in the present study suggest that SelP is not necessarily involved in solubilizing HgSe; the presence of free or bound GSH (or potentially other thiol-containing

biomolecules) may be sufficient. Furthermore, the lack of HgSe(s) in the blood plasma may be simply due to its pH. According to Reaction 2b, at the physiological pH of the blood (~7.4), HgSe nanoparticles are present as the water soluble GS-HgSe and thus do not form HgSe(s) granules. In the gastric fluid, where pH is much lower (2.0), GS-HgSe aggregates into insoluble HgSe nanoclusters due to interparticle interactions and may eventually result in HgSe(s) nanoparticles.

In addition to the pure HgSe(s) solid, Schemes 1 and 2 also explain the presence of mixed solid $HgSe_xS_{1-x}$ in biological systems as confirmed in the liver of striped dolphin (*3*) and blackfooted albatross (*4*). Furthermore, $HgSe_xS_{1-x}$ in the striped dolphin liver was found to be in the size range of 5-10 nm (*3*), which agrees very well with the size of nanoparticles C and D reported in this study.

Acknowledgement

Funding of this research was provided by the Natural Sciences and Engineering Council of Canada (NSERC). M.A.K.K. was supported by a NSERC Postgraduate Student – Doctoral Fellowship (PGS-D). The authors like to thank Nail Ball for assisting in the XRD analysis, Panseok Yang in the MSEM analysis, Sergei Rudenja and Michael Freund in the XPS and FTIR analysis, and John Van Dorp in the TEM analysis.

References

(1) Khan, M. A. K. and Wang, F. (2009) Mercury-selenium compounds and their toxicological significance: toward a molecular understanding of the mercury-selenium antagonism. *Environ. Toxicol. Chem. 28*, 1567-1577.

(2) Khan, M. A. K., Asaduzzaman, A. M., Schreckenbach, G. and F., W. (2009) Synthesis, characterization and structures of methylmercury complexes with selenoamino acids. *Dalton Trans.* 5766-5772.

(3) Ng, P. S., Li, H., Matsumoto, K., Yamazaki, S., Kogure, T., Tagai, T. and Nagasawa, H. (2001) Striped dolphin detoxificates mercury as insoluble Hg(S, Se) in the liver. *Proc. Japan. Acad. 77*, 178-183.

(4) Arai, T., Ikemoto, T., Hokura, A., Terada, Y., Kunito, T., Tanabe, S. and Nakai, I. (2004) Chemical forms of mercury and cadmium accumulated in marine mammals and seabirds as determined by XAFS analysis *Environ. Sci. Technol. 38*, 6468-6474.

(5) Kim, E. Y., Murakami, T., Saeki, K. and Tatsukawa, R. (1996) Mercury levels and its chemical form in tissues and organs of seabirds. *Arch. Environ. Contam. Toxicol. 30*, 259-266.

(6) Kim, J. H., Birks, E. and Heisinger, J. F. (1977) Protective action of selenium against mercury in Northern Creek chubs. *Bull. Environ. Contam. Toxicol. 17*, 132-136.

(7) Nigro, M. and Leonzio, C. (1996) Intracellular storage of mercury and selenium in different marine vertebrates. *Mar. Ecol. Prog. Ser. 135*, 137-143.

(8) Palmisano, F., Cardellicchio, N. and Zambonin, P. G. (1995) Speciation of mercury in dolphin liver: a two-stage mechanism for the demethylation accumulation process and role of selenium. *Mar. Environ. Res. 40*, 109-121.

(9) Suzuki, K. T., Sasakura, C. and Yoneda, S. (1998) Binding sites for the (Hg-Se) complex on selenoprotein P. *Biochim. Biophys. Acta 1429*, 102-112.

(10) Yoneda, S. and Suzuki, K. T. (1997) Detoxification of mercury by selenium by binding of equimolar Hg-Se complex to a specific plasma protein. *Toxicol. Appl. Pharmacol. 143*, 274-280.

(11) Yoneda, S. and Suzuki, K. T. (1997) Equimolar Hg-Se complex binds to selenoprotein P. *Biochem. Biophys. Res. Commun. 231*, 7-11.

(12) Naganuma, A., Tabata, J. and Imura, N. (1982) A reaction product from mercuric mercury, selenite and reduced glutathione. *Res. Comm. Chem. Pathol. Pharmacol. 38*, 291-299.

(13) Gailer, J., George, G. N., Pickering, I. J., Madden, S., Prince, R. C., Yu, E. Y., Denton, M. B., Younis, H. S. and Aposhian, H. V. (2000) Structure basis of the antagonism between inorganic mercury and selenium in mammals. *Chem. Res. Toxicol. 13*, 1135-1142.

(14) Turner, E. A., Rösner, H., Huang, Y. and Corrigan, J. F. (2007) Accessing $HgSe_xS_{1-x}$ nanoparticles using the single-source reagent $Me_3Si\text{-}SeS\text{-}SiMe_3$. *J. Clust. Sci. 18*, 764-771.

(15) Kuno, M., Higginson, K. A., Qadri, S. B., Yousuf, M., Lee, S. H., Davis, B. L. and Mattoussi, H. (2003) Molecular clusters of binary and ternary mercury

chalcogenides: Colloidal synthesis, characterization, and optical spectra *J. Phys. Chem. B. 107*, 5758-5767.

(16) Liu, Y., Cao, J., Wang, Y., Zeng, J., Li, C. and Qian, Y. (2002) Aqueous solution route to nanocrystalline HgE (E=S, Se, Te). *J. Mater. Sci. Lett. 21*, 1657-1659.

(17) Bonnissel-Gissinger, P., Alnot, M., Ehrhardt, J. J. and Behra, P. (1999) Modeling the adsorption of mercury(II) on (Hydr)oxides II. .alpha.-FeOOH (goethite) and amorphous silica. *J. Colloid Interface Sci. 215*, 313.

(18) Ding, T., Zhang, J.-R., Hong, J.-M., Zhu, J.-J. and Chen, H.-Y. (2004) Sonochemical synthesis of taper shaped HgSe nanorods in polyol solvent. *J. Cryst. Growth 260*, 527-531.

(19) Wang, H., Xu, S., Zhao, X.-N., Zhu, J.-J. and Xin, X.-Q. (2002) Sonochemical synthesis of size-controlled mercury selenide nanoparticles. *96*, 60-64.

(20) Kedarnath, G., Kumbhare, L. B., Jain, V. K., Phadnis, P. P. and Nethaji, M. (2006) Group 12 metal monoselenocarboxylates: synthesis, characterization, structure and their transformation to metal selenide (MSe; M = Zn, Cd, Hg) nanoparticles. *Dalton Trans.*, 2714-2718.

(21) Singh, N., Patil, K. R. and Khanna, P. K. (2007) Nano-sized HgSe powder: Single-step preparation and characterization. *Mater. Sci. Eng. B 142*, 31-36.

(22) Ehrhardt, J.-J., Behra, P., Bonnissel-Gissinger, P. and Alnot, M. (2000) XPS study of the sorption of Hg(II) onto pyrite FeS_2. *Surf. Interface Anal. 30*, 269-272.

(23) Behra, P., Bonnissel-Gissinger, P., Alnot, M., Revel, R. and Ehrhardt, J. J. (2001) XPS and XAS Study of the Sorption of Hg(II) onto Pyrite. *Langmuir 17*, 3970-3979.

(24) Sudeep, P. K., Joseph, S. T. S. and Thomas, K. G. (2005) Selective detection of cysteine and glutathione using gold nanorods. *J. Am. Chem. Soc. 127*, 6516-6517.

(25) Basu, S. and Pal, T. (2007) Glutathione-induced aggregation of gold nanoparticles: electromagnetic interactions in a closely packed assembly *J. Nanosci. Nanotechnol. 7*, 1904-1910.

(26) Lim, I.-I., S., Mott, D., Ip, W., Njoki, P. N., Pan, Y., Zhou, S. and Zhong, C.-J. (2008) Interparticle interactions in glutathione mediated assembly of gold nanoparticles. *Langmuir 24*, 8857-8863.

(27) Cui, S.-Y., Jin, H., Kim, S.-J., Kumar, A. P. and Lee, Y.-I. (2008) Interaction of glutathione and sodium selenite in vitro investigated by electrospray ionization tandem mass spectrometry. *J. Biochem. 143*, 685-693.

(28) Tsen, C. C. and Tappel, A. L. (1958) Catalytic oxidation of glutathione and other sulfhydryl compounds by selenite. *J. Biol. Chem. 233*, 1230-1232.

(29) Mas, A. and Sarkar, B. (1989) Role of glutathione in selenite binding by human plasma. *Biol. Trace Elem. Res. 20*, 95-104.

(30) Patterson, K. G., Trivedi, N. and Stadtman, T. C. (2005) Methanococcus vannielii selenium-binding protein (SeBP):chemical reactivity of recombinant SeBP produced in Escherichia coli. *Proc. Nat. Aca. Sci. 102*, 12029-12034.

(31) Ganther, H. E. (1968) Selenotrisulfides. Formation by the reaction of thiols with selenious acid. *Biochemistry 7*, 2898-2905.

(32) Aruga, M., Awazu, S. and Hanano, M. (1978) Kinetic studies on decomposition of glutathione. I. Decomposition in solid state. *Chem. Pharm. Bull. 26*, 2081-2091.

(33) Aruga, M., Awazu, S. and Hanano, M. (1980) Kinetic studies on decomposition of glutathione. II. Anaerobic decomposition in aqueous solution. *Chem. Pharm. Bull. 28*, 514-520.

(34) Aruga, M., Awazu, S. and Hanano, M. (1980) Kinetic studies on decomposition of glutathione. III. Peptide bond cleavage and desulfurization in aqueous solution *Chem. Pharm. Bull. 28*, 521-528.

(35) Cuesta, J., Arsequell, G., Valencia, G. and González, A. (1999) Photochemical desulfurization of thiols and disulfides. *Tetrahedron:Asymmetry 10*, 2643-2646.

(36) González, A. and Valencia, G. (1998) Photochemical desulfurization of L-cysteine derivatives. *Tetrahedron:Asymmetry 9*, 2761-2764.

(37) Bieri, M. and Bürgi, T. (2005) l-Glutathione Chemisorption on Gold and Acid/Base Induced Structural Changes: A PM-IRRAS and Time-Resolved in Situ ATR-IR Spectroscopic Study. *Langmuir 21*, 1354-1363.

(38) Chen, W. J., Boehlert, C. C., Rider, K. and Armstrong, R. N. (1985) Synthesis and characterization of the oxygen and desthio analogues of glutathione as dead-end inhibitors of glutathione S-transferase. *Biochem. Biophys. Res. Commun. 128*, 233-240.

(39) Hodes, G. (2003) *Chemical solution deposition of semiconductor films*, 1st ed., Marcel Dekker Inc., New York.

Chapter 6: Conclusion

6.1. Summary of Findings

This research was inspired by some of the major knowledge gaps in understanding the Hg-Se antagonism. For example, even though MeHg was thought to bind strongly with all selenoamino acids present in biological systems, only one MeHg selenoamino acid (SeAA) compound was synthesized and characterized. Whether this single complex can represent the properties and functions of possible complexes that could be formed between MeHg and other selenoamino acids was unknown. Another major data gap was that although HgSe(s) is analytically detected as the final metabolic product for the Hg-Se antagonism in many biota, the pathway(s) leading to its formation has not been established. Therefore, as discussed in Chapter 1, this thesis research was initiated with the following specific goals:

(a) To synthesize and characterize MeHg complexes with several important Se-containing biomolecules and to compare their properties with their sulfur analogs.
(b) To investigate the mechanisms of the interaction between Se and inorganic Hg leading to the formation of HgSe(s); and,
(c) To investigate the mechanisms of the interaction between Se and MeHg leading to the formation of HgSe(s).

We addressed the first objective by synthesizing four MeHgSeAA complexes and characterized them by using different spectroscopic methods and quantum chemical calculations. The results showed that chemically and structurally all four MeHgSeAA are similar to their sulphur counterparts with the exception of the bond length which may

play a role in the bioantagonism. The bond length of Hg-Se is marginally shorter than the sum of their covalent radii which implies that this bond is stronger compared to Hg-S bond (Hg-S bond is also slightly shorter than the sum of their covalent radii but in the case of Hg-Se, it is much shorter when compared with the covalent radii of sulphur and selenium). This was supported by the $J_{199Hg-1H}$ values of the complexes which range from 191 Hz to 232 Hz and are lower than those of the similar sulphur complexes (for example, MeHg complex with selenomethionine has a $J_{199Hg-1H}$ value of 213 Hz while that with sulphurmethionine is 217.4 Hz (*1*)). Quantum chemical calculations further supported these findings.

The remaining two objectives of this research were addressed by studying the demethylation of MeHgSeAA complexes and the interaction of inorganic Hg with selenite in the presence of glutathione (GSH), respectively. The major technique used included ^{1}H and ^{199}Hg nmr, XRD and other spectroscopic and non-spectroscopic techniques. Both reactions were found to lead to the formation of HgSe(s) as the end product, but with different mechanisms.

In the case of MeHg, it initially forms a complex with one selenoamino acid which will then interact with another molecule of MeHg selenoamino acid complex to form bis(methylmercury)selenide (BMSe). BMSe is not a stable molecule under physiological conditions and will degrade to dimethylmercury (DMHg) and HgSe(s). The formed DMHg could be decomposed further to CH_3Hg^+. So the net reaction is MeHg selenoamino acid complexes degrade to HgSe(s) as end product through a Se aided demethylation.

Inorganic Hg also forms HgSe(s) as end product but via a completely different mechanism. Inorganic Hg interacts with SeO_3^{2-} in the presence of GSH and the reaction is sensitive to pH. At physiological pH, the reaction results in the formation of $HgSe_xS_{1-x}$ ($0<x<1$) as end product which was characterized by XRD. The particle size is calculated to be ~ 9 nm. It is assumed that desulfurization of GSH forms an inorganic sulfide HS^- which together with –SeH, in the absence of excess GSH, reacts rapidly with Hg(II) to form insoluble $HgSe_xS_{1-x}$(s). However, in the presence of an excess amount of GSH, the $HgSe_xS_{1-x}$ species formed is immediately bonded to GSH to form the soluble GS-$HgSe_xS_{1-x}$ species. Upon acidification, the carboxylic acid groups of GSH get protonated and form hydrogen bonding with other GS-$HgSe_xS_{1-x}$ resulting in $(GS\text{-}HgSe_xS_{1-x})_n$ nanoclusters. The chemical composition (molar fraction) of the solid, the ratio of HgSe and HgS, was estimated to be 0.7:0.3 which is in excellent agreement with the size of the mixed solid $HgSe_xS_{1-x}$ in the striped dolphin liver which is in the size range of 5-10 nm and with the same composition.

These findings improve our understanding of the Hg-Se antagonism in at least the following ways:

1. The synthesis and characterization methods for the four new MeHg selenoamino acids complexes make it possible to further study these complexes as well as other similar complexes with respect to both their chemical properties and toxicological significance.
2. The finding that selenoamino acids can readily demethylate MeHg makes it the second characterized chemical demethylation pathway for MeHg under physiological or environmental conditions. Prior to this study, the only other

chemical demethylation pathway for MeHg in nature is via the reaction of sulfide. Other than that, MeHg demethylation was thought to occur via photolysis or microbial processes. The new chemical demethylation pathway opens a new opportunity to revisit MeHg cycling in extra- and intra-cellular environments.

3. The pH-reversible dissolution-precipitation of glutathione-bound $HgSe_xS_{1-x}$ provides a new pathway for the formation and tissue distribution of $HgSe_xS_{1-x}$ in biological systems; it may also offer a simple technique for synthesizing $HgSe_xS_{1-x}$ nanoparticles.
4. Although $HgSe_{1-x}S_x$ granules have been analytically detected in the liver and kidneys of several species, it was thought to be produced from inorganic Hg. This research is the first to demonstrate that $HgSe_{1-x}S_x$ granules found in biological systems could result from the metabolism of both inorganic Hg and MeHg.

6.2. Future Perspectives

This research deals with the complexes formed between MeHg and "free" selenoamino acids. It should be realized that selenoamino acids in biological systems are normally attached to or part of proteins or enzymes. It is possible that selenoamino acids embedded in biomolecules may behave differently as folding or misfolding of proteins could change the bioavailability, and inter-molecular interactions may change the reactivity of the selenoamino acids. It was reported that coordination of Hg^{2+} to the donor atoms (N and O) of the amino acid residues in human serum alnumin may destabilize the hydrogen bonds between the carbonyl and amide in α-helix structure, but somewhat promote the hydrogen bonds contributing to the β-turn arrangement. However, binding with $MeHg^+$, $EtHg^+$, and $PhHg^+$ does not produce appreciable changes even

when the mercurial species are in large excess (*2*). This raises the question as what structural or conformational or spatial changes at the molecular level are actually responsible for the Hg induced toxicity. Therefore, a future direction of this research could be the study of the interactions of Hg and MeHg with Se-containing proteins and enzymes. Synchrotron-based X-ray absorption spectrometric methods (e.g., EXAFS, XANES), electrochemical techniques, fluorescence correlation spectroscopy might be useful tools for this research.

It is also of great interest to provide analytical evidences (or lack thereof) of Hg (organic and inorganic)-SeAA complexes in biological systems. As the mobility and distribution of Hg is highly dependent on the complex formation and so is the Hg-Se antagonism, a speciation technique is crucial for the understanding of the bioavailability and toxicity of Hg. Recently, Lemes and Wang(*3*) reported a HPLC-ICP-MS speciation method for detecting MeHg complexes with sulphur-amino acids in fish muscle. It would be neat to see whether such a technique can be applied or developed for identifying MeHg complexes with selenoamino acids as well.

A third direction could be the study of the thermodynamic stability and formation constants of the complexes formed between Hg and Se embedded in biomolecules. For example, the formation constant of MeHgSeGlu has not been reported to date, even though MeHg complexes with GSH and selenoglutathione (GSeH) are perhaps the most important in controlling the mobility of Hg and the bioantagonism of Se against Hg in biological systems. MeHg distribution inside the organs is caused by the formation of the MeHgGlu (*4*). Its seleno-counterpart, MeHgSeGlu, acts as a potential oxidative stress reducer to protect the cell against oxidative damage caused by MeHg (*5*). An in situ study

with GSeH and MeHg hydroxide with consecutive ^{1}H and ^{199}Hg nmr measurements with mathematical expressions developed may help to determine the formation constants of these important complexes.

6.3. Reference

(1) Sugiura, Y., Tamai, Y. and Tanaka, H. (1978) Selenium protection against mercury toxicity: High binding affinity of methylmercury by selenium-containing ligands in comparision with sulphur-contaning ligands. *Bioinorg. Chem. 9*, 167-180.

(2) Li, Y., Yan, X.-P., Chen, Xia, Y.-L. and Jiang, Y. (2007) Human serum albumin−mercurial species interactions. *J. Proteome Res. 6*, 2277-2286.

(3) Lemes, M. and Wang, F. (2009) Methylmercury speciation in fish muscle by HPLC-ICP-MS following enzymatic hydrolysis. *J. Anal. At. Spectrom. 24*, 663-668.

(4) Kerper, L. E., Ballatori, N. and Clarkson, T. W. (1992) Methylmercury transport across the blood-brain barrier by an amino acid carrier. *Am. J. Physiol. 262*, R761-R765.

(5) Olin, K. L., Walter, R. M. and Keen, C. L. (1994) Copper deficiency affects selenoglutathione peroxidase and selenodeiodinase activities and antioxidant defense in weanling rats. *Am. J. Clin. Nutr. 59*, 654-658.

Appendix A

Crystallographic details and Crystal structure of Complex 4 (MeHg-$_L$-selenomethioninate complex via Hg-N bonding)

1. Crystallographic details about Complex 4

Table A1. Crystallographic details about Complex **4**

Wavelength	0.71073 Å
Crystal system	Monoclinic
Space group	P21 (No. 2)
Unit cell dimensions:	
a, Å	6.8723 (5)
b, Å	5.8351 (4)
c, Å	13.3288 (10)
α, deg	90.000 (1)
β, deg	90.410 (1)
γ, deg	90.000 (1)
V, Å3	534.48 (11)
D_{calc}, g/m^3	0.773
crystal size, mm^3	7×80×200
Maximum θ for data collection	30°
GOF (F2)	1.290
R1[a] [I > 2σ (I)]	0.054
wR2[b] (all data)	0.117

[a] $R1 = [\sum||F_o| - |F_c||]/[\sum|F_o|]$ for $[I > 2\sigma(I)]$.

[b] $wR2 = \{[\sum w(F_o^2 - F_c^2)^2]/[\sum w(F_o^2)^2]\}^{1/2}$ for all data.

2. Crystal structure of Complex 4

Although the structure of Complex **4** refined to an acceptable geometry and R values, the relatively large and very anisotropic displacement parameters for the Se atom (U_{11} 0.192(2); U_{22} 0.126(3); U_{33} 0.061(1)) and the carbons connected to it suggested the presence of some kind of disorder. Accordingly, a model was constructed in which the atoms of the MeSe group were split, and constraints were applied to keep corresponding C-Se distances as well as displacement parameters equal. The resulting disorder model refined to occupancies of 0.88/0.11 for the two sets of positions and produced a slight decrease in the R values (R1 = 5.26% for 2732 |Fo| > 4σ(Fo), R1 = 6.07% and wR2 = 11.17% for all 3080 data for the disorder model, as compared to R1 = 5.31% for |Fo| > 4σ(Fo), R1 = 6.11% and wR2 = 11.26% for all data for the original unsplit model). However, the displacement parameters of the disorder model were not much better than for the original model, so we do not believe this adequately explains the problem. Therefore, we report in the paper the results from the original, ordered model. It seems clear that the distances resulting from this structure determination should be treated with caution. Figure S1 shows the two models side by side.

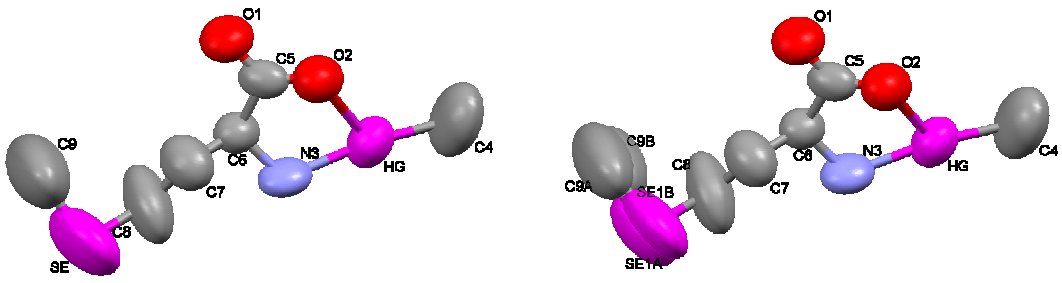

Figure A1. Ordered (left) and disorder (right) models for Complex **4**.

Appendix B

^{1}H NMR spectra of Complexes 1 (Methylmercury-$_{D,L}$-selenopenicillaminate) (A), 2 (Methylmercury-$_{L}$-selenoglutathionate) (B), and 3 (MeHg-$_{L}$-selenomethioninate; Hg-Se bonding) (C) and 4 (MeHg-$_{L}$-selenomethioninate; Hg-N bonding) (D)

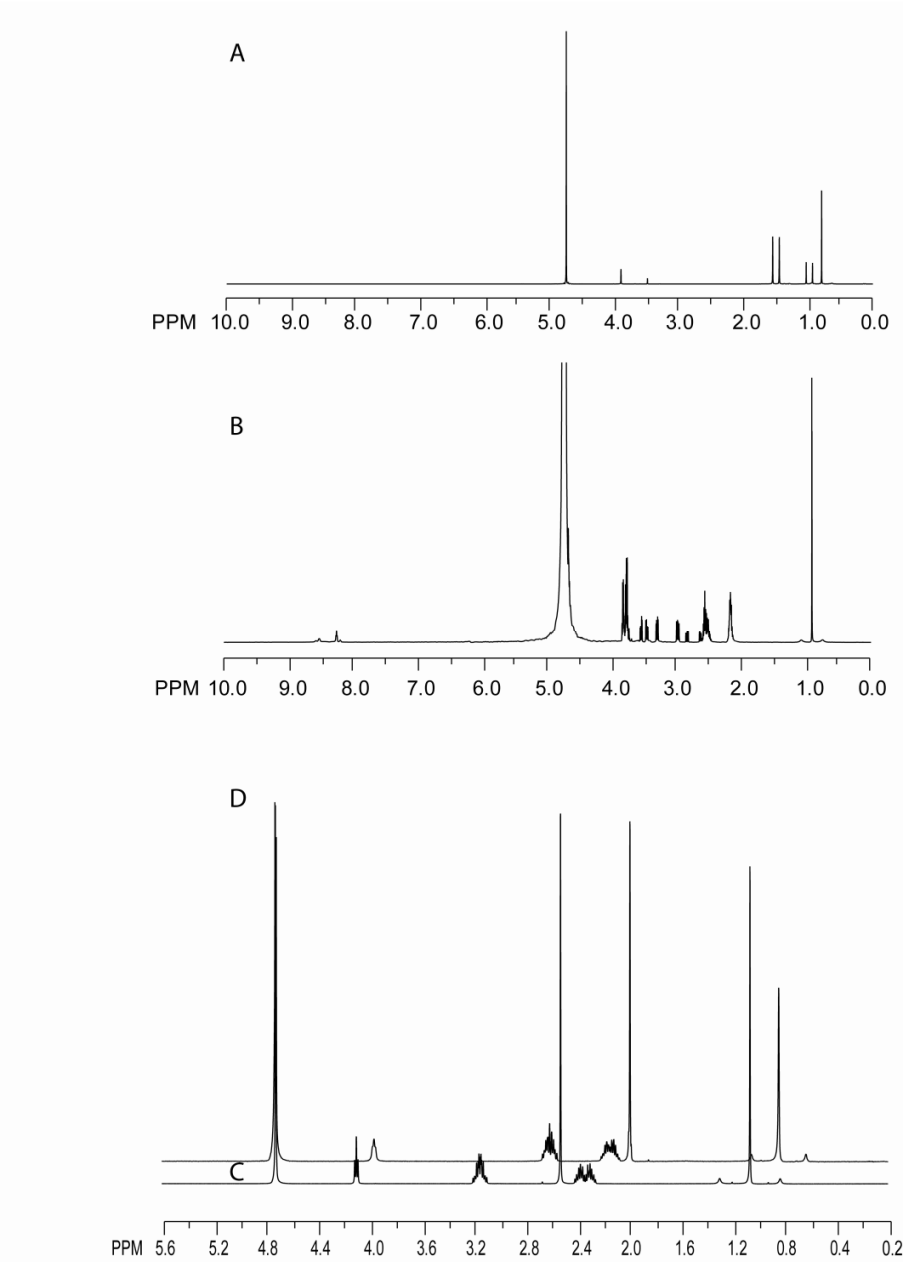

Figure B1. ^{1}H NMR spectra of Complexes **1** (A) , **2** (B), and **3** (C) and **4** (D)

Appendix C

Optimized coordinates of MeHg amino and selenoamino acids

1. Methylmercury-$_L$-cysteinate

Atomic Number	Coordinates (Angstroms) X	Y	Z
6	-1.795655	-1.359604	0.544367
1	-2.341709	-2.294074	0.674998
1	-1.447512	-1.035735	1.525991
6	-2.768832	-0.336796	-0.035740
1	-3.079866	-0.655606	-1.032404
6	-2.147837	1.050773	-0.158339
8	-1.252401	1.496136	0.525357
8	-2.784173	1.802077	-1.082972
1	-2.387924	2.686578	-1.052956
7	-3.972300	-0.271067	0.810648
1	-4.678359	0.320747	0.384636
1	-3.746474	0.125156	1.718886
16	-0.359076	-1.759017	-0.549159
80	1.232774	-0.059606	-0.009480
6	2.713764	1.377953	0.420958
1	2.255861	2.194261	0.980180
1	3.508654	0.926243	1.014885
1	3.130657	1.763027	-0.510385

2. Methylmercury -$_L$-selenocysteinate

Atomic Number	Coordinates (Angstroms) X	Y	Z
6	-1.881223	-1.006193	0.790115
1	-2.460296	-1.884541	1.071300
1	-1.472085	-0.556779	1.693894
6	-2.808460	-0.032647	0.073312
1	-3.143779	-0.469278	-0.869322
6	-2.125494	1.295100	-0.240432
8	-1.196847	1.782486	0.364227
8	-2.751026	1.948714	-1.243980
1	-2.314133	2.809065	-1.338215
7	-4.003326	0.205949	0.903065
1	-4.680119	0.770958	0.399602
1	-3.751927	0.710152	1.748976
34	-0.382806	-1.700436	-0.331355
80	1.315925	0.108063	0.031548
6	2.811952	1.578490	0.318709
1	2.325661	2.531046	0.529157

1	3.447282	1.294613	1.157814
1	3.416375	1.664797	-0.584654

3. Methylmercury -$_{D,L}$-penicillaminate

Atomic Number	Coordinates (Angstroms) X	Y	Z
6	2.557318	0.384952	-0.117058
6	1.925537	-0.923260	0.434000
16	0.473791	-1.525873	-0.600371
1	3.512221	0.515820	0.409313
7	2.868927	0.273540	-1.544340
1	2.014633	0.076963	-2.065054
1	3.283745	1.134670	-1.892353
6	1.770505	1.674578	0.147111
8	0.572426	1.827084	0.308964
8	2.604146	2.742070	0.104787
1	2.042820	3.536101	0.199029
6	2.978322	-2.043140	0.300850
1	3.861136	-1.798878	0.907239
1	2.568068	-2.991642	0.658998
1	3.299196	-2.161155	-0.735960
6	1.546127	-0.764284	1.914245
1	1.175361	-1.714479	2.309285
1	2.429077	-0.474318	2.502237
1	0.774222	-0.005318	2.065101
80	-1.414794	-0.119942	-0.078330
6	-3.179713	0.985900	0.304795
1	-2.899670	1.998005	0.607413
1	-3.791097	1.030523	-0.600215
1	-3.750486	0.506505	1.104024

4. Methylmercury -$_{D,L}$-selenopenicillaminate (Compound 1)

Atomic Number	Coordinates (Angstroms) X	Y	Z
6	2.396491	0.841208	-0.450393
6	2.148848	-0.413088	0.449292
34	0.582550	-1.543891	-0.186562
1	3.381643	1.224336	-0.154023
7	2.460202	0.482858	-1.858328
1	1.570079	0.076086	-2.143674
1	2.631131	1.305304	-2.432990
6	1.408122	1.974981	-0.162249
8	0.290185	2.089421	-0.633862
8	1.921285	2.904709	0.673763

1	1.228760	3.583746	0.795396
6	3.362597	-1.348284	0.309683
1	4.257717	-0.852102	0.709952
1	3.205390	-2.271476	0.875914
1	3.549179	-1.596824	-0.736924
6	1.956770	-0.023731	1.919591
1	1.864748	-0.922106	2.536219
1	2.819988	0.554757	2.277920
1	1.058284	0.580431	2.080721
80	-1.466490	-0.099437	0.015289
6	-3.296884	0.966201	0.170442
1	-3.112045	2.015594	-0.071258
1	-4.022445	0.550372	-0.533553
1	-3.688728	0.882367	1.187207

5. Methylmercury -$_{L}$-glutathionate

Atomic Number	Coordinates (Angstroms) X	Y	Z
6	4.986567	-0.166894	0.653381
8	5.090344	-0.443177	1.827093
8	6.016162	-0.160865	-0.213897
1	6.809874	-0.427726	0.288054
6	3.686534	0.193805	-0.043192
1	3.853810	1.113564	-0.617315
1	3.460116	-0.609071	-0.759367
7	2.651406	0.334481	0.958991
1	2.904495	-0.031887	1.873170
6	1.311656	0.520228	0.785730
8	0.528261	0.316568	1.714597
6	0.767695	1.111891	-0.537013
1	-0.309554	1.108278	-0.379478
6	1.024984	0.301409	-1.821242
1	0.339243	0.670494	-2.589422
1	2.039188	0.464966	-2.197281
7	1.195356	2.503258	-0.676628
1	2.190121	2.699024	-0.663068
6	0.438976	3.653423	-0.578968
8	0.979951	4.750442	-0.541518
6	-1.077599	3.496195	-0.545672
1	-1.493554	4.455790	-0.862314
1	-1.402592	2.730334	-1.255945
6	-1.616952	3.128835	0.855484
1	-1.064353	2.287551	1.284170
1	-1.501500	3.976543	1.535895
7	-3.032870	2.777701	0.822017
1	-3.731526	3.426085	1.154206
6	-3.456438	1.622661	0.260953
8	-2.732684	0.773442	-0.251346
8	-4.808320	1.501812	0.323582

1	-5.016004	0.654390	-0.106569
16	0.842663	-1.529660	-1.640509
80	-0.996396	-1.898838	-0.089530
6	-2.528428	-2.471823	1.249512
1	-2.643603	-1.674220	1.986189
1	-3.460930	-2.611207	0.697599
1	-2.253065	-3.403581	1.749471

6. Methylmercury -$_L$-selenoglutathionate (Compound 2)

Atomic Number	Coordinates (Angstroms) X	Y	Z
6	4.901971	0.214733	0.876121
8	4.977586	0.010595	2.066751
8	5.957864	0.203093	0.040878
1	6.742653	-0.009394	0.581340
6	3.614222	0.491191	0.121601
1	3.771622	1.377026	-0.505951
1	3.429754	-0.364145	-0.545520
7	2.546075	0.663638	1.083636
1	2.784278	0.362173	2.025259
6	1.204951	0.783829	0.865223
8	0.406119	0.608974	1.786806
6	0.671870	1.283896	-0.499309
1	-0.407515	1.205802	-0.381673
6	1.036305	0.469089	-1.748997
1	0.363941	0.763087	-2.557615
1	2.057191	0.665659	-2.084100
7	1.004121	2.700068	-0.662752
1	1.981713	2.966331	-0.616405
6	0.164787	3.794975	-0.616095
8	0.624957	4.928386	-0.586247
6	-1.337101	3.530305	-0.626976
1	-1.809144	4.449352	-0.982956
1	-1.583915	2.725571	-1.325818
6	-1.893553	3.160654	0.767118
1	-1.296342	2.371964	1.234094
1	-1.859171	4.031327	1.427236
7	-3.279683	2.708869	0.702316
1	-4.032971	3.320733	0.980067
6	-3.603441	1.508621	0.170648
8	-2.806170	0.692816	-0.283718
8	-4.945633	1.297852	0.190778
1	-5.079815	0.423756	-0.214487
34	0.928468	-1.509427	-1.515099
80	-0.971056	-1.841188	0.132918
6	-2.484001	-2.365929	1.522126
1	-2.624104	-1.518762	2.196628
1	-3.412455	-2.577579	0.986613

1	-2.176589	-3.247287	2.090069

7. Methylmercury -$_L$-methioninate(via Hg-S bonding)

Atomic Number	Coordinates (Angstroms) X	Y	Z
80	1.733987	-0.216484	0.036053
16	-0.281082	1.313959	-0.597410
6	-1.407924	1.422380	0.881223
1	-1.267750	2.426617	1.288127
1	-1.070855	0.710582	1.637117
6	3.395792	-1.457933	0.473817
1	3.008085	-2.470380	0.591987
1	4.073872	-1.374067	-0.376475
1	3.841024	-1.076323	1.393227
6	-2.903489	1.227059	0.534811
1	-3.476707	1.836767	1.245346
1	-3.115655	1.620171	-0.467245
6	-3.423807	-0.223979	0.657967
1	-3.287848	-0.582898	1.684431
6	-2.729038	-1.233818	-0.266082
8	-1.532882	-1.388742	-0.247156
8	-3.604649	-1.891799	-1.034287
1	-3.153288	-2.554954	-1.599648
7	-4.932386	-0.245420	0.418544
1	-5.429725	0.352691	1.092904
1	-5.176814	0.079406	-0.527331
1	-5.314379	-1.198259	0.501587
6	0.419873	3.012080	-0.670830
1	1.128756	3.021341	-1.502947
1	-0.389028	3.713318	-0.888520
1	0.927204	3.278868	0.258085

8. Methylmercury -$_L$-selenomethioninate (via Hg-Se bonding) (Compound 3)

Atomic Number	Coordinates (Angstroms) X	Y	Z
80	1.830401	-0.363344	0.074141
34	-0.246223	1.241428	-0.556639
6	-1.453333	1.189638	1.049393
1	-1.292621	2.149560	1.543790
1	-1.102113	0.402090	1.717316
6	3.489255	-1.623680	0.488537
1	3.522806	-2.367522	-0.308574
1	4.373784	-0.985454	0.489637

1	3.311795	-2.076478	1.464726
6	-2.952990	1.039971	0.704119
1	-3.509367	1.599003	1.468386
1	-3.178855	1.513915	-0.259437
6	-3.492917	-0.407950	0.720285
1	-3.306498	-0.866196	1.698642
6	-2.872759	-1.334788	-0.334608
8	-1.677885	-1.441750	-0.460509
8	-3.806827	-1.990307	-1.033187
1	-3.399577	-2.606768	-1.679262
7	-5.013499	-0.389537	0.569917
1	-5.463059	0.118675	1.343993
1	-5.309326	0.057632	-0.309054
1	-5.399772	-1.344266	0.550408
6	0.549316	3.036274	-0.289183
1	1.303537	3.158333	-1.069858
1	-0.241536	3.775717	-0.426391
1	1.003046	3.117104	0.698998

9. Methylmercury -$_{L}$-methioninate(via Hg-N bonding)

Atomic Number	Coordinates (Angstroms) X	Y	Z
6	-2.082675	-0.167882	-0.565242
1	-1.731087	-1.193494	-0.741895
1	-2.336471	0.257792	-1.546044
6	-0.889926	0.616328	0.032162
1	-0.713773	0.243265	1.049370
6	-1.227896	2.122249	0.197814
8	-2.094167	2.533922	0.942087
8	-0.468212	2.924566	-0.557479
7	0.319231	0.484508	-0.806708
1	0.170809	2.290868	-0.996153
6	-3.335236	-0.211275	0.315513
1	-3.087880	-0.606037	1.308601
1	-3.753204	0.789582	0.444601
6	-5.981129	-1.025427	0.684121
1	-6.819942	-1.626039	0.321129
1	-5.728318	-1.350578	1.698612
1	-6.279537	0.027676	0.697743
16	-4.591987	-1.300638	-0.465954
1	0.088416	0.042022	-1.694869
80	2.086321	-0.297695	-0.020968
6	3.907819	-0.993830	0.752212
1	4.281964	-1.809082	0.126729
1	4.637799	-0.179752	0.764370
1	3.756026	-1.360838	1.771120

10. Methylmercury -$_L$-selenomethioninate (via Hg-N bonding) (Compound 4)

Atomic Number	Coordinates (Angstroms) X	Y	Z
6	-1.619333	0.067679	-0.481907
1	-1.344592	-0.986563	-0.624368
1	-1.866387	0.471833	-1.473760
6	-0.355269	0.788025	0.051663
1	-0.184504	0.452730	1.082807
6	-0.579395	2.320852	0.146772
8	-1.399309	2.831350	0.882269
8	0.221555	3.027247	-0.660151
7	0.820808	0.524419	-0.802515
1	0.802710	2.328123	-1.078885
6	-2.842654	0.154089	0.432231
1	-2.613515	-0.241439	1.426955
1	-3.187296	1.183270	0.537781
6	-5.694898	-0.401352	0.988721
1	-6.617832	-0.914930	0.708494
1	-5.396495	-0.712193	1.992685
1	-5.854523	0.678786	0.955714
34	-4.326373	-0.926374	-0.327979
1	0.536674	0.059047	-1.663070
80	2.540508	-0.352708	-0.012586
6	4.319714	-1.144706	0.766807
1	4.678380	-1.946526	0.115381
1	5.077259	-0.358443	0.827067
1	4.133545	-1.547552	1.766255